2010

Exosporium Morphogenesis in Bacillus Cereus and Bacillus Anthracis

Monica Maria Fazzini Bellinzona

EXOSPORIUM MORPHOGENESIS

IN

BACILLUS CEREUS AND *BACILLUS ANTHRACIS*

A Thesis Presented to the Faculty of

The Rockefeller University

in Partial Fulfillment of the Requirements for

the degree of Doctor of Philosophy

by

Monica Maria Fazzini Bellinzona

June 2010

EXOSPORIUM MORPHOGENESIS IN *BACILLUS CEREUS* AND *BACILLUS ANTHRACIS*

Monica Maria Fazzini Bellinzona, Ph.D.

The Rockefeller University 2010

Bacillus cereus is a Gram-positive spore-forming bacteria that can cause food poisoning and its close relative, *Bacillus anthracis* is the etiological agent of anthrax. In both cases, the spore, a differentiated cell type in a dormant state, starts the infection process. Thus, the exosporium, which constitutes the surface of the spore, plays an important role during natural infection of both *B. cereus* and *B. anthracis*. Proteins from the exosporium of *B. cereus* ATCC 4342, a *B. anthracis*-like strain, were extracted with 2% β-mercaptoethanol under alkaline conditions and identified by liquid chromatography coupled with tandem mass spectrometry. A novel cell surface protein, reticulocyte binding protein (Rbp), was identified in this sample. Inactivation of *rbp* by insertional mutagenesis resulted in spores devoid of the hair-like nap typical of the exosporium, which suggests that Rbp could be a new component of the exosporium nap or could have a role in its assembly. GerQ, a protein that is crosslinked by transglutaminase in the spore coat of *Bacillus subtilis*, was also identified in the *B. cereus* ATCC 4342 exosporium. Absence of GerQ during sporulation resulted in a brittle exosporium in both *B. cereus* ATCC 4342 and *B. anthracis* ΔSterne spores. This suggests that transglutaminase participates in exosporium assembly and maturation by crosslinking small proteins and processed peptides, providing structural stability and resistance to degradation to the spore surface.

In addition, a novel exosporium protein, ExsM, was characterized in this study. Subcellular localization of an ExsM-GFP fusion protein revealed a dynamic pattern of fluorescence that follows the site of formation of the exosporium around the forespore. Under scanning electron microscopy, *exsM* null mutants presented a tightly wrapped exosporium resulting in smaller and rounder spores than wild-type spores that have an extended exosporium. Thin-section electron microscopy revealed that *exsM* spores were encased by a double layer exosporium, both of which were composed of a basal layer and a hair-like nap. Compared to wild-type spores, *exsM* spores were more resistant to lysozyme treatment, germinated with a higher efficiency, and had a delay in outgrowth. Insertional mutagenesis of *exsM* in *B. anthracis* ΔSterne rendered spores with a partial second exosporium that were also smaller in size. These findings suggest that ExsM plays a critical role in the formation of the exosporium.

B.cereus, but not *B. anthracis,* spores possess long appendages projecting from their surface. *B. cereus* ATCC 14579 appendages were isolated from spores by extraction with 2% β-mercaptoethanol under alkaline conditions, followed by CsCl gradient ultracentrifugation. Mass spectrometry analysis revealed that camelysin (CalY) and spore coat-associated protein N (CotN) were associated with the appendages sample. Both proteins are homologous to TasA, the main component of *B. subtilis* biofim extracellular matrix. TasA forms amyloids fibrils that hold the cells together and provide structure to the extracellular matrix. Therefore, spore appendages may have a role in biofilm formation, acting like a scaffold for the biofilm matrix and holding the spores together.

To my parents

To my husband Peter

Acknowledgments

First of all, I would like to thank my advisor Dr. Vince Fischetti, who always offered invaluable assistance, support and guidance. His cool temperament is a standard that I aspire to (but will probably never achieve!). I would also like to acknowledge the support of Dr. Raymond Schuch. He supported me immensely, giving encouragement, constructive critique and friendship. In addition, this work would have been impossible without the help, advice and emotional support from all present and past members of the Fischetti Lab. You are all my family away from home.

I would like to thanks the members of my faculty advisor committee: Dr. Alex Tomasz and Dr. Erec Stebbins, without their advice and insightful discussions, this work would not have been successful. I am also appreciative of Dr. Richard Calendar who was kind enough to join the committee as the external member.

My sincere thanks also goes to the laboratories of Dr. Maria Karayiourgo and Dr. Robert Darnell where I carried out my laboratory rotations and lead me to work on diverse exciting projects.

I wish to thank Eleana Sphicas at the Electron Microscopy Resource Center and Joe Fernandez at the Proteomic Resource Center for their technical expertise. Both were helpful in numerous ways.

I am grateful to Kristen Cullen, Marta Delgado, Cristian Rosario, Michelle Sherman, Sue Ann Chong and Marnel Herbert for their assistance and support. I would also like to thank Maritza Victoria for her genuine warmth and care.

I owe my most sincere gratitude to all my professors at Facultad de Ciencias Exactas y Naturales, Universidad de Buenos Aires, who formed me as a scientist.

A special thank you to my friends Dr. Yun Hsu and Dr. Martin Kampmann, who helped me through all my years at Rockefeller University. I would also like to thanks my Argentinean friends who no matter how far away they were, always gave me their support and advice: Dr. Isabel Garcia Tornadu, Mariana Graciarena, Dr. Ana Ortalli, Dr. Mariana Fiori, Geraldine Sacca, Daniela Converso and Diego DeGennaro.

My deepest gratitude goes to my parents who supported me in this journey, even though it meant that I would be away from them. Their belief that one should always follow what they love, allowed me the freedom to pursue my science studies. Also, I thank my sisters, their husbands and my nieces for their love and support.

Last but not least, I thank my husband Peter who stood beside me at every step of this journey and encouraged me constantly.

Table of Contents

List of Figures

List of Tables

Introduction

The *Bacillus cereus* group

The *Bacillus cereus* group also known as *Bacillus cereus* "sensu lato" is a non-taxonomical division which is comprised of six closely related Bacillus species: *Bacillus cereus* "sensu stricto" (called *B. cereus* in this work), *Bacillus anthracis*, *Bacillus thuringiensis*, *Bacillus mycoides*, *Bacillus pseudomycoides* and *Bacillus weihenstephanensis* (Rasko et al., 2005). All the members of this group have different phenotypic characteristics that are used to define the different species division. In brief, *B. cereus* is mainly non-pathogenic, but certain strains are known to cause food poisoning, *B. anthracis* is the etiological agent of anthrax, *B. thuringiensis* is an insect pathogen, *B. weihensephanenesis* is non-pathogenic with psycotrophic physiology and *B. mycoides* and *B. pseudomyc*oides produce rhizoid colonies on agar.

Although members of the *Bacillus cereus* group present different phenotypes, they are all very similar genetically. Comparison of the chromosomes of *B. anthracis*, *B. cereus* and *B. thuringiensis* showed that these genomes were highly similar in both gene content and their order in the chromosome (Anderson *et al.*, 2005; Ivanova *et al.*, 2003; Rasko *et al.*, 2004). Analysis of 16S rRNA sequences shows that they are 99% similar (Ash *et al.*, 1991) between several members of the *B. cereus* group, which is above the threshold established for species differentiation (Cohan, 2002); and in fact, the presence of large conserved regions of 16S RNA makes *B. cereus*, *B. anthracis* and B.

thuringiensis indistinguishable from one another through this technique (Porwal *et al.*, 2009). Other genotyping techniques, such as multilocus enzyme electrophoresis (MLEE), fluorescence amplified fragment length polymorphism (AFLP) and multilocus sequence taping (MLST) also concur with the conclusions obtained from analysis of 16S rRNA sequence (Helgason *et al.*, 2000b; Helgason *et al.*, 2004; Hill *et al.*, 2004) These techniques also show that while *B. anthracis* is a monophyletic group, *B. cereus* and *B. thuringiensis* are intermixed across the *B. cereus* group phylogenetic tree. MLST analysis reveals three clades or lines of descent, not matching the typical species division (Fig. 1). Clade I is composed of *B. anthracis* and *B. cereus* strains with a few *B. thuringiensis* strains (Didelot *et al.*, 2009; Kolsto *et al.*, 2009; Priest *et al.*, 2004). Interestingly, most of *B. cereus* and *B. thuringiensis* strains found in clade I are clinical isolates. Clade II contains mostly *B. thuringiensis* with some *B. cereus* strains intermingled, and finally, clade III comprises *B. cereus*, *B. mycoides* and *B. weienstephanensis*. Two more distant clusters include *B. pseudomycoides* in one, and the thermophilic members of the *B. cereus* group in the other.

The phenotypic determinant of pathogenicity of *B. thuringiensis* and *B. anthracis* are encoded mainly in plasmids. *B. thuringiensis* Cry and Cyt insecticidal proteins are encoded on large plasmids. When these plasmids are lost, *B. thuringiensis* becomes undistinguishable from *B. cereus*, with some strains even causing food poisoning or becoming opportunistic pathogens (Damgaard, 1995; Ghelardi *et al.*, 2007; Jackson *et al.*, 1995; McIntyre *et al.*, 2008). *B. anthracis*, plasmids pX01 and pX02 contains the genes for production of the anthrax toxins and the capsule, respectively. Unlike *B.*

thuringiensis, *B. anthracis* does not become *B. cereus* with the loss of these plasmids because many of the phenotypic characteristics that differentiate *B. anthracis* from *B. cereus* arise not from differences in gene content but in gene expression (Agaisse *et al.*, 1999; Slamti *et al.*, 2004). Mainly, *B. anthracis* lacks a functional PlcR protein, a pleitropic transcriptional regulator that drives the expression of *B. cereus* secreted and membrane proteins. On the contrary, certain *B. cereus* strains that carry a plasmid with high similarity to pX01 are known to cause disease with symptoms similar to inhalational anthrax, (Hoffmaster *et al.*, 2004; Hoffmaster *et al.*, 2006).

As a result of the highly conserved genetic information and the presence of differential traits in plasmids, the taxonomical status of the *B. cereus* group, and particularly of *B. cereus*, *B. thuringiensis* and *B. anthracis*, remains controversial. However, the traditional species division remains due to their medical (in case of *B. anthracis*) and economic importance (as with *B. thuringiensis*).

Fig. 1: Phylogenetic relationships within *Bacillus cereus* group bacteria. In A, The tree shown is a subtree extracted from the MLST supertree available in the SuperCAT database (Kolsto *et al.*, 2009). Roman numerals (I, II, III) indicate the three main phylogenetic clusters of the *B. cereus* group population. In B, the relationship among *B. anthracis* isolates and close relatives is shown. The three main evolutionary branches (A, B and C) within *B. anthracis* are indicated. The scale bars are in average numbers of nucleotide substitutions per site. Reprinted from Kolstø et al, 2009. Copyright 2009, with permission from Annual Reviews.

Fig. 1A

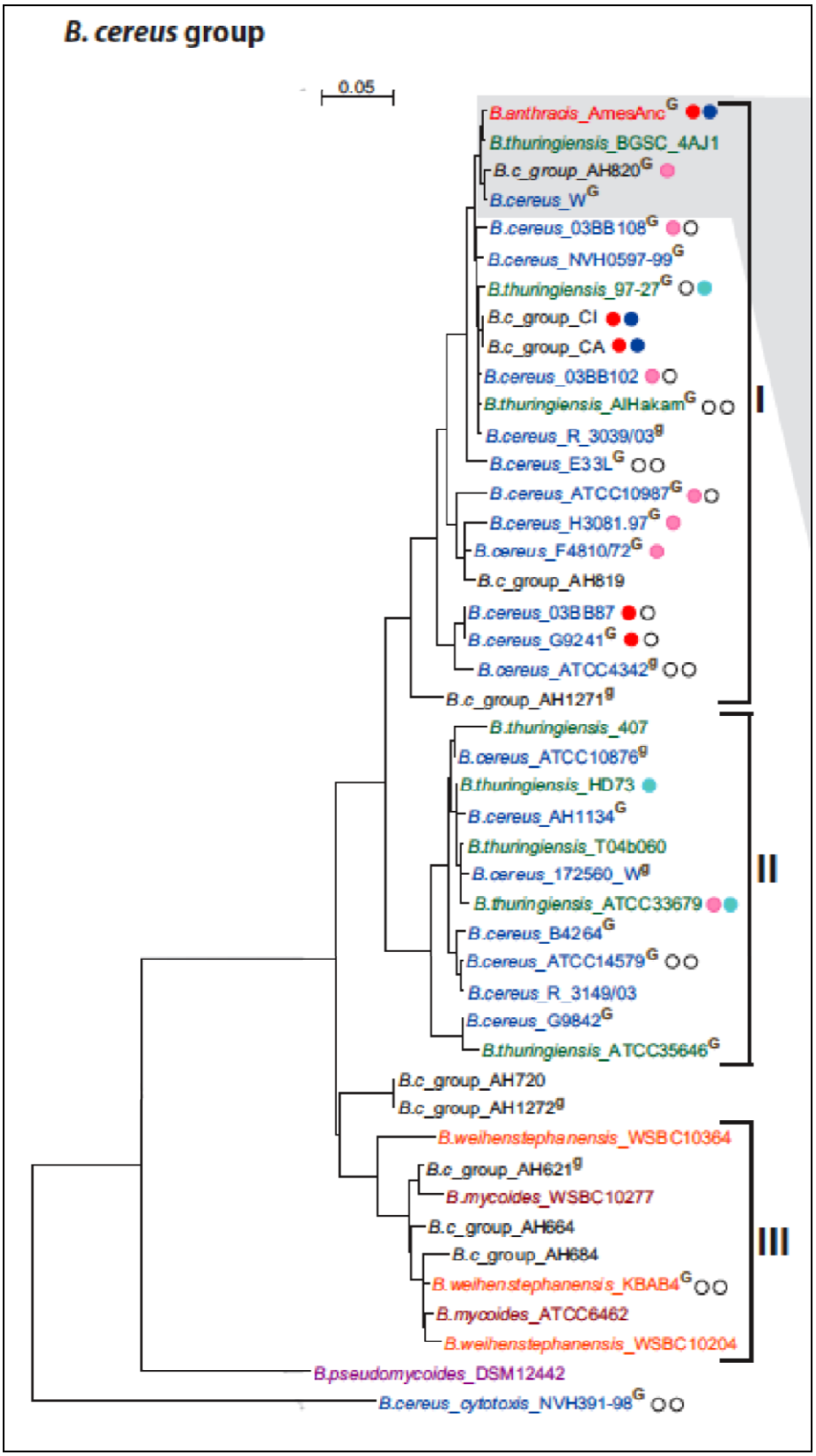
B. cereus group
0.05
B.anthracis_AmesAnc^G
B.thuringiensis_BGSC_4AJ1
B.c_group_AH820^G
B.cereus_W^G
B.cereus_03BB108^G
B.cereus_NVH0597-99^G
B.thuringiensis_97-27^G
B.c_group_CI
B.c_group_CA
B.cereus_03BB102
B.thuringiensis_AlHakam^G
B.cereus_R_3039/03^g
B.cereus_E33L^G
B.cereus_ATCC10987^G
B.cereus_H3081.97^G
B.cereus_F4810/72^G
B.c_group_AH819
B.cereus_03BB87
B.cereus_G9241^G
B.cereus_ATCC4342^g
B.c_group_AH1271^g
B.thuringiensis_407
B.cereus_ATCC10876^g
B.thuringiensis_HD73
B.cereus_AH1134^G
B.thuringiensis_T04b060
B.cereus_172560_W^g
B.thuringiensis_ATCC33679
B.cereus_B4264^G
B.cereus_ATCC14579^G
B.cereus_R_3149/03
B.cereus_G9842^G
B.thuringiensis_ATCC35646^G
B.c_group_AH720
B.c_group_AH1272^g
B.weihenstephanensis_WSBC10364
B.c_group_AH621^g
B.mycoides_WSBC10277
B.c_group_AH664
B.c_group_AH684
B.weihenstephanensis_KBAB4^G
B.mycoides_ATCC6462
B.weihenstephanensis_WSBC10204
B.pseudomycoides_DSM12442
B.cereus_cytotoxis_NVH391-98^G
I
II
III

Fig. 1B

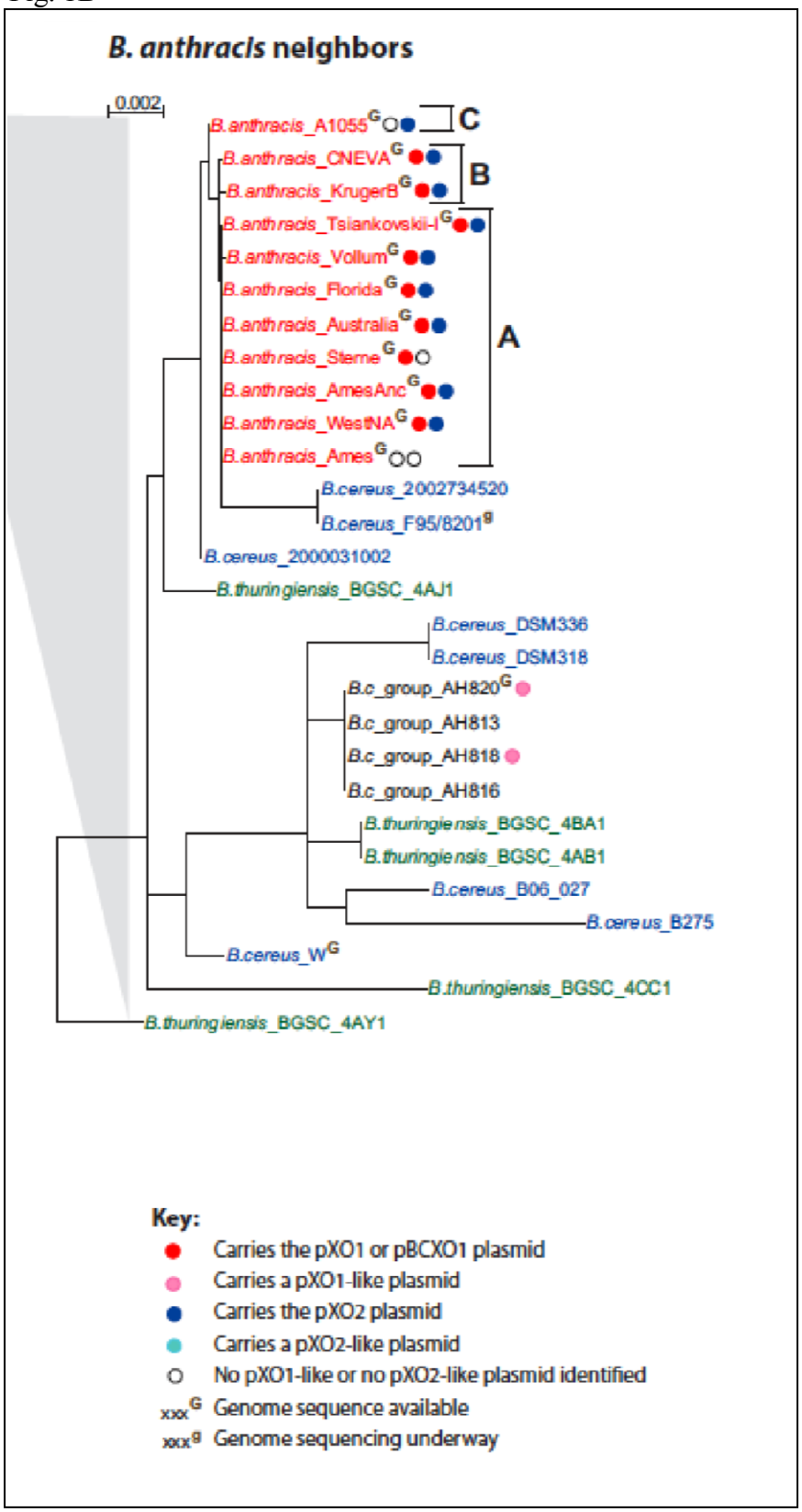
B. anthracis neighbors
0.002
B.anthracis_A1055G
B.anthracis_CNEVAG
B.anthracis_KrugerBG
B.anthracis_TsiankovskiiIG
B.anthracis_VollumG
B.anthracis_FloridaG
B.anthracis_AustraliaG
B.anthracis_SterneG
B.anthracis_AmesAncG
B.anthracis_WestNAG
B.anthracis_AmesG
C
B
A
B.cereus_2002734520
B.cereus_F95/8201g
B.cereus_2000031002
B.thuringiensis_BGSC_4AJ1
B.cereus_DSM336
B.cereus_DSM318
B.c_group_AH820G
B.c_group_AH813
B.c_group_AH818
B.c_group_AH816
B.thuringiensis_BGSC_4BA1
B.thuringiensis_BGSC_4AB1
B.cereus_B06_027
B.cereus_B275
B.cereus_WG
B.thuringiensis_BGSC_4CC1
B.thuringiensis_BGSC_4AY1
Key:
Carries the pXO1 or pBCXO1 plasmid
Carries a pXO1-like plasmid
Carries the pXO2 plasmid
Carries a pXO2-like plasmid
No pXO1-like or no pXO2-like plasmid identified
xxxG Genome sequence available
xxxg Genome sequencing underway

Bacillus cereus

B. cereus is an endospore-forming Gram-positive organism. While mainly aerobic, *B. cereus* can grow well in the absence of oxygen. Some of its most distinguishable biochemical features are motility, beta-hemolysis on blood agar, production of a very active lecithinase and the inability to ferment manitol (Johnson *et al.*, 1984). Another phenotypic characteristic of *B. cereus* is the presence of endospores that have a central or terminal location and do not swell the sporangia.

B. cereus is ubiquitous in the enviroment and it is usually considered a soil dweller, though it is most probable that the invertebrate gut is also an ecological niche (Jensen *et al.*, 2003). For example, *B. cereus* colonization of the gastrointestinal tract of termites, cockroaches and sow bugs has been observed (Feinberg *et al.*, 1999; Swiecicka and Mahillon, 2006; Wenzel *et al.*, 2002), during which *B. cereus* presents a filamentous growth phase, known as the Arthromitus stage (Margulis *et al.*, 1998).

Though mainly apathogenic, *B. cereus* can also behave as an opportunistic pathogen causing systemic or local infections, and certain strains are well-known food poisoning agents (Drobniewski, 1993). The extent of *B. cereus* food poisoning is usually underestimated since symptoms are mild and self-contained, and medical attention is rarely sought. Additionally, *B. cereus* food poisoning is often confused with *Clostridium perfringes* or *Staphyilococcus aureus* food contamination. In Norway, *B. cereus* was the most common bacteria isolated from food-borne illnesses in 1990 (Kotiranta *et al.*, 2000) and, it was in this country, that in 1950 *B. cereus* was first established as an agent of food

poisoning. It is estimated that *B. cereus* only represented 1% of total food poisoning in the United States between 2001 and 2005 (CDC, 2009a). Despite its low incidence in the United States, *B. cereus* contamination has resulted in a high economic cost for the food industry. In December of 2009, a recall for all canned Slim-Fast products was issued in relation to *B. cereus* contamination which affected 10 million units (FDA, 2009). Two years early, in December 2007, a recall was issued for all Metromint flavored bottled water, also due to *B. cereus* contamination (FDA, 2007).

B. cereus contamination of the food industry pipelines is difficult to avoid due to the ubiquity of this organism, its capability to form biofilms and the highly adhesive and resistant properties of its spores that can survive through routine cleaning and disinfection procedures (Andersson *et al.*, 1995). In addition, psychotolerant *B. cereus* strains can grow during refrigerated storage and distribution of perishable foods, like dairy products and prepared foods, which can result in changes of a product organoleptic characteristics or create direct spoilage, besides raising safety concerns (Guinebretiere *et al.*, 2008).

Food-poisoning disease

B. cereus can cause two different types of food poisoning: diarrheal disease or emetic syndrome. The diarrheal disease symptoms include abdominal pain, cramps and watery diarrhea that are evident after an incubation period of 8 to 16 hs (Granum, 1997). These symptoms are usually mild, rarely last more than 24 hs and are commonly confused with *Clostridium perfringes* food poisoning. Usually the diarrheal diseases is

associated with protein-rich foods such as meats, dairy products, soups and vegetables. The infective dose has been indicated to be 10^5 to 10^8 spores per gram of food, although presence of 10^4 spores per gram cannot be considered safe (Granum, 1997).

Diarrheal syndrome occurs when ingestion of spores that survived the cooking process germinate in the intestinal tract and start secreting enterotoxins. Although *B. cereus* vegetative cells can also be present in the food, they cannot survive passage through gastric fluids. Pre-made enterotoxins are also inactivated during gastric transit (Granum, 1997). Therefore, the long incubation period associated with the diarrheal syndrome reflects the time necessary for spore germination, outgrowth and production of enterotoxins. In this respect, it has been demonstrated that *B. cereus* spores can adhere to the colon cancer line Caco-2, germinate and produce non-hemolytic enterotoxin (Andersson *et al.*, 1998). The hydrophobic properties of the spore plus the presence of adherent appendages may contribute to attachment of the spore to the intestinal epithelial, avoiding expulsion by the peristaltic movement of the intestines (Stenfors Arnesen *et al.*, 2008).

Three major enterotoxins are associated with the diarrheal syndrome: Hbl (Beecher *et al.*, 1995), Nhe (Granum *et al.*, 1999) and CytK (Lund *et al.*, 2000), in addition to several other cytotoxins and degradative enzymes such as phospholipase C (PI-PLC, PC-PLC and sphingomyelinase), cereolysin O, InhA2 and hemolysin II and III. The most important virulence factor seems to be Nhe, as cytotoxicity correlates well with the amount of production of this protein but not with Hbl (Moravek *et al.*, 2006).

However, the enterotoxin contributing the most to virulence may vary depending on the specific *B. cereus* strains in a given study (Lindback *et al.*, 1999). Furthermore, different subsets of these toxins may act synergistically to cause gastroenteritis. All of the enterotoxins are chromosomally encoded; and while all known strains carry the *nhe* operon; *hbl* and *cytK* genes are only present in 50% of a random sample *B. cereus* strains (Ehling-Schulz *et al.*, 2006; Moravek *et al.*, 2006).

Both Hbl and Nhe are tripartite toxins (Beecher and Macmillan, 1991; Granum *et al.*, 1999), and are composed of three different but homologous peptides. Binding component B (35 kDa) and lytic component L1 and L2 (36 and 45 kDa) form Hbl (Beecher and Macmillan, 1991), and Nhe consists of NheA, NheB and NheC (Granum *et al.*, 1999). Hbl is a dermonecrotizing, cytotoxic and hemolytic protein. It exerts its toxic effect by forming a transmembrane pore that disrupts the osmotic equilibrium of the cell, inducing its lysis (Beecher and Wong, 1997). Nhe, which was at first described as a non-hemolytic toxin, was recently shown to have hemolytic activity, although its relative activity levels with respect to Hbl hemolysis were not studied (Fagerlund *et al.*, 2008). Nhe has a similar mode of action to Hbl and thus, it has been demonstrated that this protein can make pores on synthetic lipid bilayers (Fagerlund *et al.*, 2008). Both Hbl and Nhe are structurally related to the cytolysin A (ClyA) family composed of pore-forming enterotoxins expressed by enteropathogenic *Escherichia coli*, *Shigella flexneri* and *Salmonella enterica* serovars Typhi and Paratypi A. They all share an alpha-helix bundle and unique hydrophobic beta-hairpin subdomain that may be involved in membrane interaction (Fagerlund *et al.*, 2008; Wallace *et al.*, 2000). CytK is a dermonecrotic,

cytotoxic and hemolytic protein that was isolated from a *B. cereus* strain involved in a severe food poisoning outbreak in which several people presented bloody diarrhea (Lund *et al.*, 2000). This 34 kDa toxin also disrupts the osmotic balance by forming pores on the planar lipid bilayer through oligomerization (Lund *et al.*, 2000). CytK is a putative member of the beta-barrel pore-forming toxins and it has sequence similarity with *Clostridium perfringes* beta-toxin and *Staphylococcus aureus* alpha-hemolysin.

The potential for virulence of *B. cereus* does not depend on the presence of genetic information for any of the enterotoxins, but rather in their level of expression; hence, immunological techniques to detect secretion of enterotoxin are preferred when studying the pathogenic potential of the different strains of *B. cereus*. The expression of all these proteins is under control of the pleiotropic regulator PlcR that activates the transcription of secreted and cell wall bounded proteins involved in virulence and host adaptation. Deletion on the PlcR in *B. cereus* decreases 10 to 50 times the expression of Hbl, Nhe and cytK cytotoxins (Gohar *et al.*, 2008). In addition, the expression of these toxins is controlled in response to environmental conditions (pH, temperature, oxygen tension), nutrient availability and metabolic state of the cell (Stenfors Arnesen *et al.*, 2008).

B. cereus can also cause an emetic food-borne syndrome that features many differences with respect to the diarrheal syndrome. Its main symptoms are nausea and vomiting that commence between 30 min to 6 hs after consumption of contaminated food, lasting approximately from 4 to 12 hs. Although it is usually confused with *S.*

aureus intoxication, the emesis is rarely accompanied by diarrhea. This kind of food poisoning is associated with farinaceous food, especially rice and pasta. In Asian-style restaurants, rice is traditionally cooked and allowed to cool slowly and stored at room temperature, in order to avoid clumping that occurs at lower (refrigerated) temperatures. During this period, *B. cereus* spores germinate and produce the emetic toxin, cereulide. Consumption of this pre-made toxin causes the rapid onset of the emetic syndrome (Drobniewski, 1993), presumably by stimulation of the vagus afferent through its 5-HT3 serotonin receptors (Agata *et al.*, 1995). The minimal emesis-causing dose calculated from animal models is 8-10 μg per kg of body weight (Stenfors Arnesen *et al.*, 2008). Cereulide can also act as an ionophore and inhibit mitochondrial activity resulting in hepatocyte damage (Mikkola *et al.*, 1999), and even fulminant liver failure (Dierick *et al.*, 2005; Mahler *et al.*, 1997).

Cereulide is a 1.2 kDa cyclic dodecadepsipeptide with structure [D-O-Leu-D-Ala-D-O-Val-D-Val]$_3$ (Agata *et al.*, 1994). Its unusual structure confers resistance to heat, extremes in pH (pH2- pH11) and protease digestion (Shinagawa *et al.*, 1996); and consequently, it can tolerate re-heating of the food products and gastric passage. Cereulide is not gene encoded; instead, it is synthetized by a multidomain protein complex generically known as non-ribosomal peptide synthetase (NRPS) (Ehling-Schulz *et al.*, 2005b). The 24 kb cereulide synthetase (*ces*) gene cluster is encoded in plasmid pBCE4810 (also called pCER 270) which has homology to *B. anthracis* pathogenic plasmid, pX01 (Ehling-Schulz *et al.*, 2006). Cereulide production is restricted to two clonal cluster of *B. cereus* strains (Ehling-Schulz *et al.*, 2005a; Vassileva *et al.*, 2007),

and as a result, specific primers for *ces* genes have been designed in order to identify potential emetic strains in the environment (Ehling-Schulz *et al.*, 2005a) or in food products (Fricker *et al.*, 2007).

Cereulide is principally produced during the early stationary phase, and rice and pasta support the highest level of its production (Ehling-Schulz *et al.*, 2004). Temperature, pH, aeration and presence of specific aminoacids influence the amount of cereulide produced, though the specific mechanisms of regulation are unknown. In order to avoid contamination with cereulide, prepared pasta and noodles should be cooled quickly and refrigerated, or should be maintain at 55°C as toxin production only occurs at temperatures between 10°C and 40°C (Ehling-Schulz *et al.*, 2004).

Non-gastrointestinal infections

B. cereus non-gastrointestinal infections mainly affect immunocompromised individuals, neonates, intravenous drug users and patients with traumatic or surgical wounds. Systemic infections are uncommon and are usually associated with contaminated intravenous catheters or cerebral fluid shunts. Bacteremia is usually transient and mild; however, central nervous system infections have a high mortality risk and may require aggressive antibiotic therapy and removal of the shunt (Drobniewski, 1993).

B. cereus local infections usually occur in post-traumatic or post-surgical wounds and burns. In addition, *B. cereus* can cause severe ocular infections that usually ends with loss of vision in less than 48 hs post-infection, which is only second in occurrence to *Staphylococcus epidermis* endolphthalmitis (Drobniewski, 1993). The bacteria can infect the eye after a traumatic injury with a contaminated object, or from a distant site of infection through the blood stream, which is usually the case with intravenous drug users. *B. cereus* is able to migrate throughout the eye within 12 hs post-infection, which contributes to the severity and negative outcome of the infection (Callegan *et al.*, 2003). Although antibiotic therapy can readily clear *B. cereus*, the toxins already produced continue to damage eye tissues resulting in irreversible damage (Callegan *et al.*, 2006). The specific toxins involved in tissue damage have not been identified but several secreted proteins under PlcR regulation may act synergistically. Other toxins not belonging to the PlcR regulon may also contribute to virulence as *plcR* null *B. cereus* still causes fulminant endophthalmitis. However, in this case, the course of the disease is slower (Callegan *et al.*, 2003).

B. cereus has also been isolated from marginal and apical periodontitis . The periodontal isolates belong to a single phylogenetic linage, and they all carry a 300 kb plasmid that may harbor virulence determinants for periodontal disease (Helgason *et al.*, 2000a). In addition, the production of collagenases by two of the oral isolates, Soc67 and Ply19, likely contributes to its periodontal pathogenesis (Soderling and Paunio, 1981).

As an opportunistic pathogen, *B. cereus* can cause pulmonary infections in immunosuppressed individuals or patients with underlying conditions. However, certain atypical virulent strains have been associated with life-threatening pulmonary infections

with anthrax-like symptoms in healthy individuals. These isolates, G9241, 03BB87 and 03BB102, are classified as *B. cereus* because of their phenotypical traits associated with a functional PlcR; however, phylogenetically, they are closer to *B. anthracis* than *B. cereus*. Also, India ink staining showed that these strains possess a polysaccharide capsule that may protect the bacteria from the host immune system (Hoffmaster *et al.*, 2004; Hoffmaster *et al.*, 2006). The atypical virulence traits expressed by these strains are encoded in plasmids. *B. cereus* G9241 plasmid, pBCX01, is 99.6% homolog to *B. anthracis* pX01 and contains the genes for anthrax toxins and their transcriptional regulator, and plasmid pBC218, encodes for a novel polysaccharide capsule biosynthetic gene cluster (Hoffmaster *et al.*, 2004). There has been no characterization of the plasmids carried by strains 03BB87 and 03BB102, but homologous gene for *B. anthracis* protective antigen has been found in both strains. *B. cereus* 03BB87 also possesses orthologs for some of the *B. anthracis* capsule genes, *cap A*, *B* and *C* (Hoffmaster *et al.*, 2006).

Bacillus cereus as a probiotic

Probiotics are "live microbial feed supplements that can benefit the host by improving its intestinal balance" (Fuller, 1989). Probiotics are usually taken as food supplements for prevention of mild gastrointestinal disorders, and they are also used as growth enhancers for farm animals instead of antibiotics. Although *B. cereus* is not a true commensal, it is able to persist temporally in the gastrointestinal tract (GIT) of animals, which makes it a candidate for use as a probiotic (Duc le *et al.*, 2004). *B. cereus*

has the advantage that its spores can survive in a desiccated state, at room temperature for prolonged periods of time, facilitating its storage and distribution. However, *B. cereus* strains should be considered potentially pathogenic; therefore, enterotoxin production should be extensively tested as well as checked for the ability to transfer antibiotic resistance to the GIT microbiota, before being considered safe to use as a probiotic (Hong *et al.*, 2004). *B. cereus* var toyoi has been deemed safe for animal feed and it is commercialized as Toyocerin in Japan with license in the European Union. Piglets fed *B. cereus* var toyoi show a reduced incidence and severity of post-weaning diarrhea syndrome, increasing their weight gain (Kyriakis *et al.*, 1999; Taras *et al.*, 2005).

Bacillus anthracis

B. anthracis differs from *B. cereus* and the rest of the members of the *Bacillus cereus* group by the severe pathology that results from its infection, named anthrax. This distinctive phenotype derives from its two principal virulence factors: anthrax toxin and polyglutamate capsule, which are encoded in two plasmids: pX01 and pX02. Plasmid pX01 carries the anthrax toxin structural genes: *pagA*, *lef* and *cya,* which encode the protective antigen, lethal factor and edema factor, respectively. These elements are contained in a 44.2 kb pathogenicity island, which also includes the toxin transcriptional activator *atxA* and repressor *pagR* (Kolsto *et al.*, 2009; Mock and Fouet, 2001). The capsule synthesis operon (*capBCAED*) and its transcriptional activators *acpA* and *acpB*, which act downstream of AtxA, are all encoded in the 35 Kb pathogenecity island of pX02 plasmid.

B. anthracis carries a non-sense mutation in the *plcR* gene that results in a truncated and inactive PlcR (Agaisse *et al.*, 1999). Fixation of this mutation appears to be a consequence of an incompatibility between the PlcR and AtxA regulons that results in an impairment of sporulation when both are active (Mignot *et al.*, 2001). Absence of an active PlcR results in some of the typical phenotypic traits of *B. anthracis*, such as lack of motility, absence of beta-hemolysis on 5% sheep blood agar plates, lack of production of phospolipases C and susceptibility to penicillin (Drobniewski, 1993). Besides the presence of a capsule and production of the anthrax toxin, these biochemical characteristics plus sensitivity to gamma phage have been traditionally used to distinguish *B. anthracis* strains. However, these phenotypic traits are not universal or exclusive to *B. anthracis*. Molecular genotyping methods have been developed so that *B. anthracis* strains can be rapidly and reliably identified when used in combination with biochemical techniques; such methods are especially helpful with environmental isolates that may have lost one or both plasmid (Marston *et al.*, 2006). Moreover, Multiple Locus VNTR Analysis (MLVA) is powerful enough to differentiate between the different strains of the highly monoclonal *B. anthracis*, allowing epidemiology studies (Beyer and Turnbull, 2009).

Until now, *B. anthracis* was considered to be an obligate pathogen whose lifecycle only occurred in its mammalian host. *B. anthracis* spores remain dormant in the soil and germinate only inside its host, where the vegetative cell would multiply until death of the animal. Once the carcass was opened by scavengers, the vegetative cells

would sporulate and remain in a dormant state until the next mammalian infection (Mock and Fouet, 2001). However, new insights have revealed that *B. anthracis* has a vegetative lifecycle outside the mammalian host, as it can germinate and survive as a saprophyte in the rhizosphera (Saile and Koehler, 2006). Moreover, the whole *B. anthracis* lifecycle, germination- vegetative growth- sporulation, can take place inside the worm gastrointestinal track (Schuch and Fischetti, 2009).

Anthrax

Anthrax was the leading cause of death of domestic livestock in the 19th century. During this time, the study of anthrax led to the elucidation of "Koch's postulates" and the birth of modern microbiology when it was proved that anthrax was caused by infection with a particular microbe, *B. anthracis* (Schwartz, 2009). In addition, anthrax was one of the first diseases that Louis Pasteur successfully developed a live vaccine against. While anthrax continues to be endemic in certain areas of Sub-Sahara Africa and East and Central Asia, it was an almost forgotten disease in the United States thanks to the application of prophylaxis measures such as the use of the animal vaccine and proper disposal of diseased carcasses. However, the terrorist mail attacks in December of 2001 brought attention back to this disease, and now *B. anthracis* is considered a potential bioterrorist agent (Schwartz, 2009).

All mammals are susceptible to infection with *B. anthracis*; however, grazing herbivores are particularly sensitive to contracting the infection (Mock and Fouet, 2001).

Carnivores and especially scavengers have a high level of resistance to anthrax probably through adaptation, as they have usually fed on diseased carcasses. Humans can also contract anthrax when they are exposed to contaminated animal products, meat or directly to anthrax spores in the case of a bioterrorism attack.

In humans, anthrax can have different manifestations depending on the route of entry of the anthrax spores. Cutaneous anthrax occurs when *B. anthracis* spores access subcutaneous tissues through a cut or abrasion, where they germinate and produce the anthrax toxins in a localized manner. The infection manifests as a painless necrotic black eschar surrounded by an edema that develops after 2-3 days at the site of the initial lesion. Cutaneous anthrax accounts for approximately 95% of cases, and it usually has good prognosis. It is treatable with antibiotic therapy and usually resolves without complication, although 20% of untreatable cases can result in death (Turnbull, 2002).

Inhalational anthrax occurs when airborne spores reach the pulmonary alveoli and are engulfed by the macrophages. The spores germinate inside the phagolysosome in transit to the regional lymph nodes, where the vegetative cells first multiply (Guidi-Rontani, 2002). From the lymph node, the vegetative cells spill into the bloodstream causing a systemic infection (Hanna and Ireland, 1999). Initial symptoms are flu-like during the first days, soon progressing to severe breathing problems and shock (CDC, 2009b). Inhalational anthrax is usually fatal unless it is treated during the first hours with aggressive antimicrobial therapy.

Gastrointestinal anthrax is uncommon and oropharyngeal anthrax is even rarer, occurring when meat contaminated with anthrax spores is consumed. It is characterized by acute inflammation of the intestinal tract, with ulceration, edema and mucosal necrosis at the site of infection (Dutz and Kohout-Dutz, 1981). Its prognosis is poor, but its fatality rate is not known due to a lack of data. It is estimated by the CDC to be between 25-60% (CDC, 2009b).

Anthrax meningitis is a rare but can occur as a fatal complication derived from cutaneous anthrax, or in the case of inhalational or gastrointestinal anthrax. It is currently not clear if the bacteria reach the meninges through the lymphatic system or the bloodstream. Death occurs 1 to 6 days after the onset of the illness (Dixon *et al.*, 1999).

Anthrax toxin and its role in pathogenesis

Anthrax toxin is composed of protective antigen (PA), lethal factor (LF) and edema factor (EF) and is an important virulence determinant of *B. anthracis*. Actually, many of the characteristic symptoms of anthrax infection are the result of the action of the anthrax toxin. Inability to produce any of the tripartite components of the anthrax toxin causes a decrease in virulence of *B. anthracis* (Pezard *et al.*, 1991; Pezard *et al.*, 1993). Furthermore, *B. anthracis* strains unable to produce either lethal factor or edema factor are greatly attenuated, indicating a synergism of these two proteins during infection (Pezard *et al.*, 1991).

Anthrax toxin is an A-B type toxin with PA as a common cell binding component of both toxins, and LF or EF displaying both the toxic and enzymatic activities. PA, LF and EF are encoded by *pga*, *cya* and *lef* genes localized in pX01 plasmid. Their transcription is driven by AtxA (Dai *et al.*, 1995), a master regulator of *B. anthracis* virulence, which is also encoded by pX01. These genes achieve maximum expression at 37°C under 5% CO_2 atmosphere, all conditions found inside the mammalian host (Bartkus and Leppla, 1989; Cataldi *et al.*, 1992; Sirard *et al.*, 1994).

Delivery of the anthrax toxins into the cytoplasm of the host cell requires a series of coordinated steps. The first step is the binding of PA to the surface cell receptors ANTRX1/TEM-8 or ANTRX2/CMG-2, which are present on the surface of many cell types. On the cell surface, PA gets cleaved through action of furin–like proteases, liberating a 20 kDa N-terminal domain. The remaining 63 kDa PA (PA63) self-associates to form an heptameric prepore complex that binds to three molecules of lethal factor, edema factor or a combination of both. The whole complex is then internalized by raft-dependent, clathrin-mediated endocytosis. The acidic environment of the early endosomes induces a conformational change of PA63, leading to the formation of a transmembrane pore onto the intraluminal vesicles, into where the lethal factor and the edema factor are translocated. These intraluminal vesicles are transported to the late endosome, where they fuse to the endosome membrane and liberate the lethal and edema factor to the perinuclear cytoplasm (Abrami *et al.*, 2005) (Fig. 2).

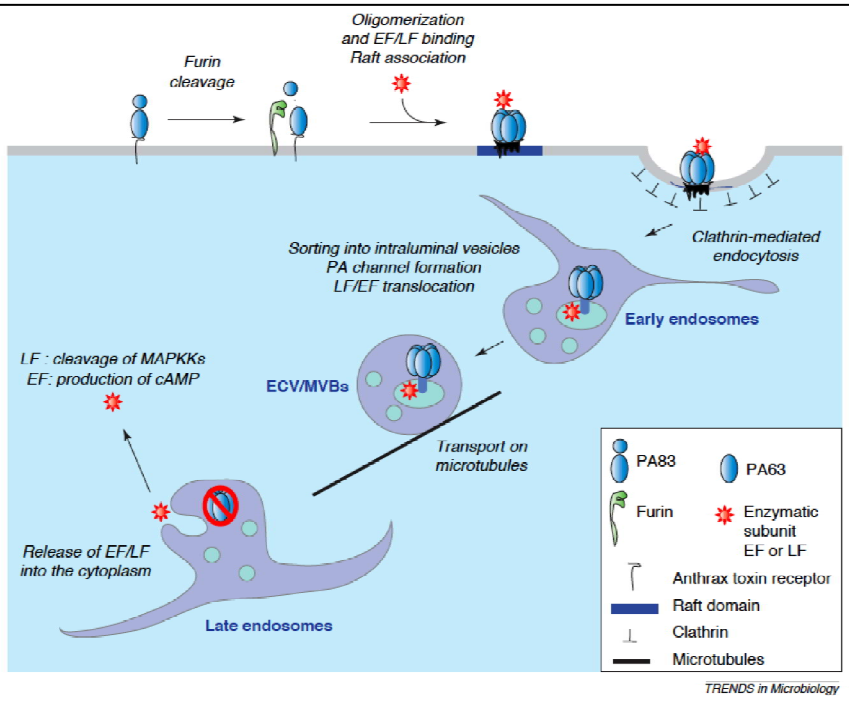

Fig. 2: Anthrax toxin and the endocytic pathway of the mammalian cell. Reprinted from Abrami et al., 2005. Copyright 2005, with permission from Elsevier.

Once in the cytoplasm, the lethal and edema factor gain access to their substrates. Lethal factor is a metalloprotease that cleaves mitogen-activated protein kinase kinase or MAPKK (Duesbery *et al.*, 1998), disrupting the signaling cascade involved in a long range of cellular processes, such as inflammation, proliferation, differentiation and cell survival. The edema factor has adenylate cyclase activity dependent on calmodulin (Leppla, 1982, 1984) that elevates the level of intracellular cAMP, a second messenger that also affects diverse cellular responses. Although anthrax toxin can affect any cell in the body, it is believed that its target is directed to disrupt the host immune response.

The mechanism of *B. anthracis* infection has been best studied in the case of inhalational anthrax. The infective particle is the spore, a dormant and highly resistant cell form that is able to survive the initial encounter with the host immune system and use

the macrophages as a "Trojan horse" to surpass the epithelial barrier of the host and access the lymph nodes (Guidi-Rontani *et al.*, 1999b; Guidi-Rontani, 2002). After being phagocytosed by alveolar macrophages and dendritic cells (DC), the anthrax spores germinate inside the phagolysosome (Cleret *et al.*, 2007; Guidi-Rontani *et al.*, 1999b) and start producing the components of the anthrax toxin: PA, LF and EF, immediately after germination (Banks *et al.*, 2005). LF alters macrophage function, inhibiting its bactericidal activity. Both, LF and EF inhibit the secretion of pro-inflammatory cytokines preventing the recruitment and differentiation of monocytes that could potentially halt the early stages of *B. anthracis* infection (Tournier *et al.*, 2007). The germinating spores inside the macrophages and DC, reach the regional lymph nodes where they multiply in the extracellular space. It is not clear how the new vegetative cells escape the antigen presenting cells (macrophages and DCs). In the lymph node, anthrax toxins inhibit the adaptative immune response by altering the function of all the key players: DC, T-helper cells and B cells. LF and EF impair DC maturation, and LF blocks the expression of co-stimulatory molecules necessary for antigen presentation to T cells (Agrawal *et al.*, 2003; Cleret *et al.*, 2006). LF also inhibits B cell proliferation and antibody (IgM) production (Cleret *et al.*, 2006). LF and EF prevent T cell chemotaxis and activation of both naïve and effector T cells (Tournier *et al.*, 2009). However, EF favors Th2 differentiation (Tournier *et al.*, 2005) and enhances the humoral response when administered subcutaneously (Duverger *et al.*, 2006), which correlates with the strong antibody response seen in the resolution of cutaneous anthrax infection (Quinn *et al.*, 2004).

During the terminal phase of the infection, *B. anthracis* proliferate in the bloodstream where LF and EF induce vascular leakage. While the effect of EF on endothelial tissues is not completely understood, LF induces apoptosis of endothelial cells (Kirby et al., 2004) and disruption of the endothelial barrier (Warfel *et al.*, 2005). In addition, EF and LF inhibit platelet aggregation affecting coagulation (Alam *et al.*, 2006; Kau *et al.*, 2005). Disregulation on the vascular system may be the main mechanism leading to host death.

Capsule

The *B. anthracis* vegetative cell is covered by a poly-γ- D-glutamic acid capsule. The operon for capsule biosynthesis is encoded by plasmid pX02, and it contains the genes necessary for synthesis and attachment of the glutamic acid polymer to the cell wall. The expression of the capsule operon is under the transcriptional activators AcpA and AcpB, which are also encoded by pX02 genes. Transcription of *acpA* and *acpB* is activated by both bicarbonate/CO_2 and AtxA (Vietri *et al.*, 1995), suggesting that the expression of anthrax toxins and capsules are coordinated.

B. anthracis strains that lack pX02 as well as strains that carry a deletion of the capsule biosynthetic operon are less virulent when compared to isogenic capsulated strains (Drysdale *et al.*, 2005; Welkos, 1991). The anthrax capsule is antiphagocytic (Makino *et al.*, 2002; Preisz, 1909) and non-immunogenic as it covers surface antigens (Schneerson *et al.*, 2003). Therefore, the capsule also enables the bacterium to avoid the host immune response complementing the actions of the anthrax toxins.

The *Bacillus* Spore

Bacillus vegetative cells start a developmental program called sporulation when faced with starvation. Through this process, which is controlled by the sequential and spatial activation of a series of sigma factors, the vegetative cell differentiates into a spore. The spore architecture confers its typical properties of dormancy, resistance and germination. Sporulation has been best studied in *Bacillus subtilis*, the model organism for Gram-positive bacteria, and most of the processes detailed herein are based on this organism.

Initiation of Sporulation

B. subtilis can adapt to an environment poor in nutrients by inducing motility and chemotaxis, hydrolytic enzymes secretion, competence, production of antibiotics to suppress competitors, and even cannibalism (Errington, 2003). Thus, commitment to sporulation is the bacteria last resort after all available alternatives to scavenge nutrients have been exhausted. In order to ensure that sporulation only occurs under the right conditions, the bacteria integrates environmental and metabolic cues into a phosphorelay system that induces sporulation.

The sporulation phosphorelay system is a complex variation of the 'two component' signal transduction system in bacteria. The two 'component system' is composed of a sensor protein histidine kinase that perceives the stimulus and

autophosphorylates a conserved histidine residue. The phosphoryl moietiy is then transferred to an aspartate residue on the response regulator, inducing a conformational change that activates the response regulator latent function. Response regulators are usually (but not always) transcription factors that can activate or repress gene expression (Stock *et al.*, 2000).

The sporulation phosphorelay is composed of sensors, regulator proteins and phosphotransferases intermediaries that allow the input of both positive and negative signals at different levels of the transduction cascade (Fig. 3). A series of histidine kinases respond to external or internal signals, feeding phosphoryl groups from their histidine residue to the aspartate residue of SpoF. Phosphorylated SpoF then passes the phosphoryl group to a histidine side chain on SpoB, which in turn, phosphorylates an aspartate residue on SpoA. Phosphorylated SpoA (SpoA~P) then activates or represses gene transcription (Burbulys *et al.*, 1991). Five sensor histidine kinases have been described in *B. subtilis*; yet, the identities of the signals that stimulate them remain unknown (Jiang *et al.*, 2000).

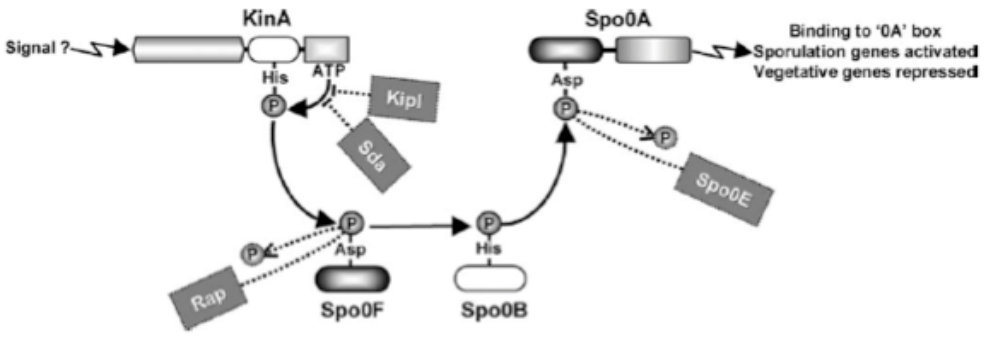

Fig. 3: The *Bacillus subtilis* sporulation phosphorelay. Reprint from Sephenson and Lewis, 2005. Copyright 2005, with permission from Elsevier.

The phosphorelay is also subject to negative regulation at different levels. Rap and SpoE are two families of aspartatyl phosphate phosphatases that specifically desphosphorylate SpoF~P and SpoA~P, respectively (Perego *et al.*, 1994; Perego, 2001). At the same time, Rap proteins are inhibited by specific pentapeptides in a quorum sensing mechanism that ensures that sporulation happens in high cell-density conditions (Perego and Brannigan, 2001). Pentapeptides derive from a Phr precursor that is processed during the export-import pathway. Other negative regulators of the sporulation phosphorelay include KipI that inhibits the sensor histidine kinase KinA, and it is antagonized by KipA (Wang *et al.*, 1997).

Expression of SpoA is also tightly regulated. Transcription of *spoA* is repressed by CodY, SinR and Soj (Sonenshein, 2000). CodY is a global repressor of early stationary phase and its repression activity is released when levels of intracellular GTP fall in response to nutrient starvation. SinR is counteracted by SinI (Bai *et al.*, 1993); and Soj is antagonized by SpoOJ (Quisel *et al.*, 1999). Soj and SpoOJ are required for proper chromosome portioning during cell division, and their modulation of SpoA expression couples sporulation initiation to chromosome segregation (Sonenshein, 2000).

The balance of positive and negative inputs into the sporulation phosphorelay determines the intracellular levels of SpoA~P, which affects the transcription levels of almost 600 genes (Fawcett *et al.*, 2000). SpoA~P activates the expression of genes involved in adaptation to low nutrient conditions directly or through inhibition of the transition state regulator, AbrB. Further activation of the sporulation phosphorelay results

in higher levels of SpoA~P that are necessary to activate the transcription of sporulation essential genes such as *spoIIA*, *spoIIE*, *spoIIG (Baldus et al., 1994)*. Thus, initiation of sporulation then depends on high levels of active histidine kinases, increased synthesis of SpoA and neutralization of several of the inhibitors of the phosphorelay.

The genomes of *B. anthracis* and *B. cereus* contain all the components of the sporulation phosphorelay. Analysis of the genome of *B. anthracis* Ames revealed the presence of 9 putative sensor histidine kinases. Five of the putative sensor proteins are active in sporulation. However, deletion of any of these does not result in impairment of sporulation, indicating that the initiation of sporulation in *B. anthracis* might result from diverse activation signals (Brunsing *et al.*, 2005). The rest of the putative sensor kinases are truncated by frameshift mutations, or are under the control of inactive or poorly active promoters. While SpoA~P is necessary to inhibit AbrA and increase the expression levels of anthrax toxin and capsule, high levels of SpoA~P can trigger sporulation during infection. Therefore, the level of intracellular SpoA~P needs to be tightly controlled. *B anthracis* pX01 and pX02 carry the kinase inhibitors, pX01-118 and pX02-61, which are highly homologous to the sensor domain of BA2291, a sensor histidine kinase (White *et al.*, 2006). When the inhibitors interact with BA2291, the latter begins functioning as a phosphatase, abolishing sporulation. In addition, pX01 encodes for a Rap phosphatase (Bongiorni *et al.*, 2006).

Analysis of *B. cereus* ATCC 14576 genomic sequence reveals the presence of 11 putative sensor histidine kinases; yet, no functional studies have been done on any of

these genes. The variety of sensor kinases suggests that a larger range of signals than in *B. subtilis* and *B. anthracis* are necessary to trigger sporulation in *B. cereus* (Stephenson and Lewis, 2005).

Regulation of Spore Morphogenesis

The first major morphological event during sporulation is an assymetric division that results in two compartments of different size and fate: a bigger mother cell and a smaller forespore. During normal vegetative growth, a tubulin-like protein, FtsZ, forms the Z-ring (cytokinetic ring) in the middle of the mother cell, marking the site of cell division (Margolin, 2002), but during this assymetric division, Ftsz assembles in two Z-rings near the cell poles instead of the cell mid-point. Relocation of the Z-ring occurs through a helical FtsZ intermediate, which is preceded by a sudden increase of expression of FtsZ by σ^H (Ben-Yehuda and Losick, 2002). Formation of the spiral intermediate also depends on interaction between SpoIIE and FtsZ. Interesting, only one of the Z-rings will lead to the formation of the septum, regulated by an unknown mechanism. It has been suggested that the sub-polar Z-rings are not equivalent and their development occurs at different rates (Pogliano *et al.*, 1999).

Concomitant to relocation of the Z-ring, the nucleoids rearrange into an elongated structure that extends from pole to pole of the cell, termed the 'axial filament.' In this case, the oriC of each chromosome is anchored to the cell pole through RacA, a protein that interacts with both DNA and the polar division protein, DivIVA (Ben-Yehuda *et al.*,

2003). Formation of the 'axial filament' also requires the involvement of the Soj-SpoOJ system, suggesting that this system mediates a checkpoint between DNA replication and initiation of sporulation, as noted previously (Wu and Errington, 2003).

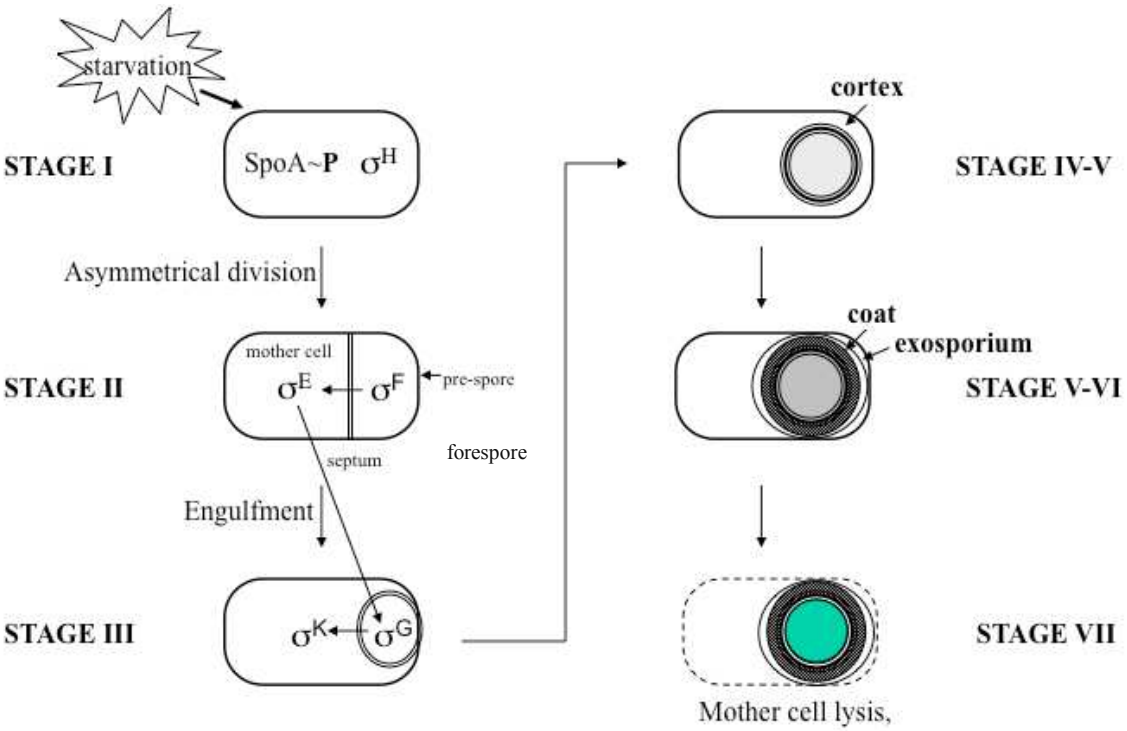

Fig. 4: Morphological stages of sporulation. Stages of sporulation are indicated by roman numerals.

After septum formation, only one third of the chromosome is present in the forespore compartment. The remainder of the forespore chromosome is actively translocated through the septum by SpoIIIE that localizes at the newly formed septum (Pogliano *et al.*, 1999; Wu and Errington, 1997). While translocation is fast and it is

completed in approximately 15 minutes (Pogliano *et al.*, 1999), this transient genetic asymmetry between the forespore and the mother cell is important for the forespore-specific activation of σ^F.

Expression of σ^F depends on σ^H and SpoA~P, and occurs prior to septum formation. Still, σ^F remains inactive in the predivisional cell and in the mother cell, through its association with the anti-sigma factor SpoIIAB that prevents the interaction between σ^F and RNA polymerase (Duncan and Losick, 1993). Furthermore, SpoIIAB phosphorylates and inactivates SpoIIAA (Min *et al.*, 1993), a protein able to reverse the inhibition of σ^F (Alper *et al.*, 1994; Diederich *et al.*, 1994). Therefore, activation of σ^F requires the generation of a high concentration of unphosphorylated SpoIIAA, which is in part achieved by the phosphatase activity of SpoIIE (Arigoni *et al.*, 1996). Although SpoIIE is present in both the forespore and the mother cell, dephosphorylated SpoIIAA only crosses a critical threshold concentration in the forespore (Carniol *et al.*, 2004), which is 8 times smaller than the mother cell. In addition, the levels of SpoIIAB in the forespore may drop slightly immediately following septation; as this protein is susceptible to proteolysis and its gene locus is located in the terminal region of the chromosome excluded from the forespore (Dworkin and Losick, 2001). These two mechanisms, desphophorylation of SpoIIAA by SpoIIE and *spoIIAB* chromosome positioning, contributes to activation of σ^F exclusively in the forespore.

Genes controlled under σ^F can be divided into two classes, origin proximal genes that can be expressed right after septum formation such as *spoIIR* and *spoIIQ*, and origin

distal-genes that are expressed after DNA translocation is completed, such as *sigG*. The σ^F regulon also includes genes involved in DNA binding and repair, cortex formation, detoxification and germination (Wang *et al.*, 2006).

After activation of σ^F, σ^E becomes active in the mother cell. This sigma factor is synthetized as an inactive precursor, pro-sigmaE (Trempy *et al.*, 1985), whose amino-terminal domain holds the protein at the septum membrane (Fujita and Losick, 2002; Ju *et al.*, 1997). Activation of pro-sigmaE involves proteolysis of the amino-terminal domain probably by SpoIIGA (LaBell *et al.*, 1987; Stragier *et al.*, 1988), a putative serine protease that also localizes at the sporulation septum. SpoIIGA activation is triggered by the secreted forespore protein SpoIIR, (Hofmeister, 1998; Karow *et al.*, 1995), coupling the activation of σ^E in the mother cell with the activation of σ^F in the forespore. Another mechanism that contributes to the compartmentalization of σ^E activation is the preferential expression of the *spoIIG* operon (spoIIGA-sigE) in the mother cell. Transcription of *spoIIG* is activated by SpoA~P, which becomes a mother cell-specific transcription factor after assymetric division (Fujita and Losick, 2003). In addition, pro-σ^E may be selectively degraded in the forespore by a hypothetical σ^F-dependent protease (Pogliano *et al.*, 1997). After activation of σ^E, two transcriptional regulators are expressed: GerE and SpoIIID. While GerE appears to act as a transcriptional repressor with σ^E (Eichenberger *et al.*, 2004), SpoIIID can act both as an activator and a repressor (Kroos *et al.*, 1989) and has a larger influence in the expression of the σ^E regulon. The σ^E regulon is the largest of the sporulation regulons and encompasses 272 genes that are involved in engulfment, formation of the spore cortex and coat and metabolism.

Activation of σ^E is followed by the engulfment of the forespore. This process, which is similar to cell phagocytosis, results in the release of the forespore in the cytoplasm of the mother cell. SpoVG and SpoIIB, which are expressed in the predivisional cell, participate in the initiation of the engulfment process, although their function is dispensable (Margolis *et al.*, 1993; Matsuno and Sonenshein, 1999; Perez *et al.*, 2000). On the contrary, SpoIID, SpoIIM and SpoIIP are all essential for this process (Frandsen and Stragier, 1995). Expression of SpoIID and SpoIIM are dependent of σ^E, while SpoIIP expression is under the control of σ^F and σ^E. These proteins may participate in hydrolyzing the cell wall material in the septum, but only SpoIID cell wall hydrolytic activity has been demonstrated *in vitro* (Abanes-De Mello *et al.*, 2002). Degradation of the cell wall may be necessary to allow the migration of the septal membranes around the forespore. SpoIID, SpoIIM and SpoIIP initially localize at the center of the septum, but later concentrate at the leading edge of the engulfing membrane (Abanes-De Mello *et al.*, 2002); therefore, they may act as a motor of the migrating membrane, dragging it as they degrade peptidoglycan. The final step of engulfment requires SpoIIIE to fusion the migrating membranes (Sharp and Pogliano, 1999). SpoIIIE has a dual role in sporulation, and after DNA translocation, it relocates from the septum to the opposite pole by moving along with the engulfing membranes. Ultimately, the forespore is separated from the mother cell cytoplasm by two cell membranes of different topology.

After engulfment, σ^G becomes active in the forespore. Activity of σ^G depends on the expression in the mother cell of eight proteins (SpoIIIAA-SpoIIIAH) encoded by the σ^E controlled *spoIIIA* operon (Illing and Errington, 1991), and the expression of SpoIIQ

controlled by σ^F in the forespore (Londono-Vallejo *et al.*, 1997; Sun *et al.*, 2000). These proteins interact in the space between the inner and outer forespore membranes, forming a channel that interconnects the mother cell and the forespore (Camp and Losick, 2008; Meisner *et al.*, 2008). It has been proposed that the metabolic capacity of the forespore diminishes after engulfment, as the result of its isolation from the external environment and/or preparation for dormancy. Therefore, this channel acts like a 'feeding tube' that provides small molecules such as ATP and/or amino acids to the forespore and allows general macromolecules synthesis (Camp and Losick, 2009). Interestingly, the channel does not introduce a specific regulator of σ^G. Interaction of SpoIIIA and SpoIIQ proteins fails if engulfment is compromised, coupling activation of σ^G with completion of engulfment (Doan *et al.*, 2009). Other mechanisms that may be involved in regulation of σ^G activation are: delay in the transcription if *sigG* by σ^F (Evans *et al.*, 2004; Partridge and Errington, 1993), presence of a saturable inhibitor that prevents early activation of σ^G (Karmazyn-Campelli *et al.*, 2008) and competition of σ^G with σ^F for binding to core RNA polymerase (Chary *et al.*, 2006). The σ^G regulon includes 95 genes and shows significant overlap with σ^F regulon (Wang *et al*., 2006). It includes genes involved in DNA repair and protection, such as the *ssp* genes that encode the small acid soluble proteins (SASP). The σ^G regulon also includes *spoVT* (Bagyan *et al.*, 1996), a transcriptional regulator that represses early σ^G genes and activates transcription of late σ^G genes (Wang *et al*., 2006).

In *B. subtilis*, but not in the *B. cereus* group, *sigK* is disrupted by *skin,* a prophage-like element (Stragier *et al.*, 1989). Reconstitution of *sigK* requires the SpoIIID and σ^E dependent expression of SpoIVCA, a DNA recombinase encoded in *skin* (Kunkel *et al.*, 1990). Expression of *sigK,* which is also positively regulated by σ^E and SpoIIID, results in pro-sigmaK, an inactive precursor. The amino-terminal domain of pro-sigmaK attaches the protein to the forespore external membrane and prevents σ^K to interact with the core RNA polymerase (Zhang *et al.*, 1998). Pro-sigmaK is probably processed by SpoIVFB (Rudner *et al.*, 1999), which is held inactive in a complex with both SpoIVFA and BofA also located at the forespore external membrane (Cutting *et al.*, 1990a; Ricca *et al.*, 1992). SpoIVFA anchors the complex to its proper localization and BofA directly inhibits SpoVIB proteases activity. After engulfment, SpoIVB whose expression is σ^G dependent, is liberated in the space between the inner and outer membrane, and promotes the release of SpoIVFB from the complex, triggering the processing of prosigmaK (Cutting *et al.*, 1991; Gomez *et al.*, 1995). Therefore, activation of σ^K only occurs after activation of σ^G. The σ^K regulon includes spore coat genes and the spoVF operon, which is involved in the synthesis of dipicolinic acid (DPA), a major component of the spore core (Eichenberger *et al.*, 2004). Further regulation of the σ^K regulon is achieved through GerE, a transcriptional regulator that is involved in transcription of the last genes to be expressed during the sporulation (Zheng and Losick, 1990).

The sequential and compartment-dependent activation of the sporulation-specific sigma factors leads to a coordinated pattern of gene expression in the forespore and in the mother cell that is necessary for the morphogenesis of the spores layers: core, cortex and

coat (Fig. 4). Finally, sporulation culminates with the lysis of the mother cell and the release of the mature spore into the environment.

Spore Structure

The spore architecture has no resemblance to the structure of the vegetative cell and it is the basis of the spore dormancy and its resistance to environmental insults (Fig. 5). While *B. subtilis* spores are composed of the core, the inner membrane, the cortex, the outer membrane and the coat, *B. cereus* group spores have an additional outer layer, the exosporium, which will be described in the next chapter of this work.

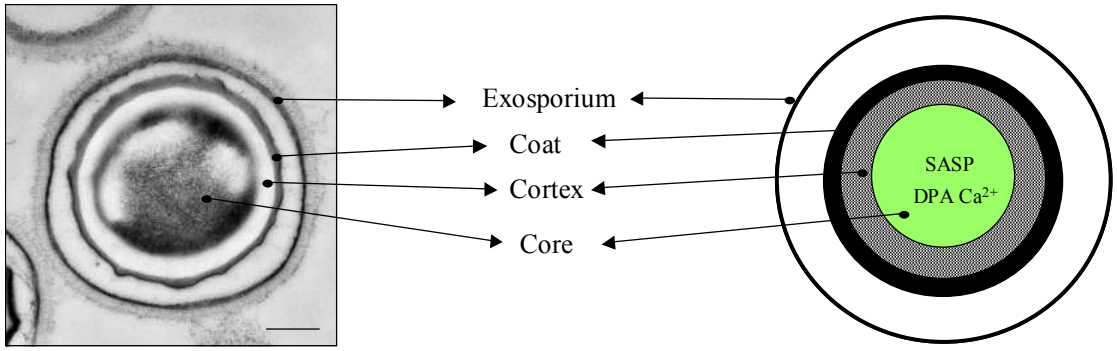

Fig. 5: Spore structure. Transmission electron micrograph of *B. anthracis* spore and representative scheme showing the spore layers. Scale bar, 500 nm.

The Core

The innermost layer of the spore, the core, contains the genetic material, ribosomes and most enzymes. While the concentration of high-energy compounds is low in the core, it contains large amounts of 3-phosphogliceric acid (3-PGA) and the enzymes for catabolism of this compound (Setlow, 1995). However, the core is metabolically inactive due to its low water content, which prevents enzymatic reactions. Compared to the vegetative cell whose water content is 80% of wet weight, the spore water content is only 25-50% (Gerhardt, 1989). The core dehydrated state plays an important role in wet heat resistance, probably because protein thermal stability is increased under a low hydratation state (Nicholson *et al.*, 2000). The pH of the core (pH 6.3-6.5) is also 1 pH unit lower than the growing cell pH (Magill *et al.*, 1994). The low pH may not contribute to any of the resistance properties of the spore, but it may have a role in dormancy, and contributes to the accumulation of 3-PGA during sporulation (Magill *et al.*, 1996).

The core also contains large amounts of dipicolinic acid (DPA) chelated 1:1 with divalent cations (mainly Ca^{2+}), which constitutes almost 10% of the dry weight of the spore and 25% of the spore core (Gerhardt, 1989). DPA promotes low water content in the core, and ergo, it contributes to spore stability and wet heat resistance. In addition, DPA plays a role in protecting DNA against dry heat and desiccation by a yet unknown mechanism (Setlow *et al.*, 2006).

While the low water content of the spore promotes dormancy and wet heat resistance, DNA protection is mainly provided by its association with α/β small acid soluble proteins (SASP). SASP are expressed under the control of σ^G and they make up 20% of the total spore protein (Setlow and Waites, 1976). Spores lacking 85% of α / β SASP ($\alpha^- \beta^-$ spores) present an increase in DNA damage, and hence, sensitivity to wet and dry heat, desiccation, hydrogen peroxide and formaldehyde treatments (Setlow, 2007). SASP also contribute to UV resistance and are associated with a change in the UV photochemistry of DNA. UV irradiation of spore DNA results in the formation of the spore photoproduct (SP), an intra-stand thyminyl-thymine product that is different from the photoproducts usually observed in vegetative cells DNA after UV treatment. An SP-repair system already present in the spore repairs SP during the first minutes of spore germination (Setlow, 1995). SASP binding stiffens the DNA backbone and eliminates sequence-dependent bends (Griffith *et al.*, 1994). This change in DNA topology may be one of the mechanisms through which SASP protect the spores DNA.

The Inner Membrane

The inner membrane surrounds the core and constitutes a major permeability barrier, providing resistance against DNA-damaging chemicals, such as formaldehyde, nitrous acid and hydrogen peroxide (Cortezzo *et al.*, 2004). The lipid composition of the inner membrane mimics the composition of the vegetative cell membrane, and therefore the restriction on the passage of small hydrophobic molecules may be associated with its lack of fluidity. Furthermore, lipid immobility may be related to the "compressed" state

of the inner membrane (Cowan *et al.*, 2004), which allows the membrane to rapidly expand during outgrowth.

The Cortex and Germ Cell Wall

The cortex is a thick layer of peptidoglycan (PG) located between the inner and outer spore membrane. It constitutes 80% of the spore PG (the other 20% forms the germ wall) and it is synthesized in the mother cell. Cortex synthesis depends on σ^K activation, which is necessary for accumulation of the PG (Vasudevan *et al.*, 2007). Cortex PG has a unique structure with 50% of the muramic acid modified to δ-lactam muramic acid, which carries no peptide side chain (Foster, 2002). The level of PG cross-linking is several degrees lower than the cell wall peptidoglycan, and it depends on the action of 2 DD-carboxypeptidases, PBP5 and DacF. Interestingly, the level of cross-linking is not homogeneous, showing gradient variation in which the innermost layers of the cortex are more loosely cross-linked than the outermost (Meador-Parton and Popham, 2000). The cortex promotes the high level of core dehydration and maintenance of the integrity of the inner membrane, and therefore, contributes to spore dormancy and resistance to wet-heat and damaging chemical compounds (Setlow, 2007).

Underlying the cortex, the germ cell wall or primordial cell wall has the same basic structure of vegetative cell PG (Tipper and Linnett, 1976), and it forms the initial cell wall of the newly vegetative cell upon germination (Atrih *et al.*, 1998). The germ

wall PG is synthesized before the cortex by enzymes expressed in the forespore (McPherson *et al.*, 2001).

The Outer Membrane

The outer membrane lies on top of the cortex. This membrane has an opposite polarity resulting from the engulfing process. While the outer membrane plays an important role during spore morphogenesis, it may not impose a permeability barrier in the mature spore (Setlow, 2007). In fact, the integrity of the *B. subtilis* spore outer membrane is in doubt, as it can be barely seen as a bilayer structure under electron microscopy (Tipper, 1972).

The Coat

The coat is a proteinaceous multilayer shell that surrounds the cortex. In *B. subtilis*, the coat is organized into two major layers, the inner and outer coat, which can be distinguished by differential staining under thin-section electron microscopy. While the lightly stained inner coat is finely striated and it is about 75 nm wide, the darkly stained outer coat is thicker (200 nm wide) and has a coarse layered appearance (Driks, 1999). *B. anthracis* and *B. cereus* spores possess a compact and thinner coat than *B. subtilis*; yet, it can still be differentiated in two distinct layers (Aronson and Fitz-James, 1976). Atomic force microscopy analysis of the coat showed the presence of ridges running along the long axis of the spore (Chada *et al.*, 2003). This coat surface topology

is not random and it seems to be species specific, as the ridge patterns on the coats of *B. anthracis* and *B. cereus* are different from those seen on *B. subtilis* coats (Chada *et al.*, 2003). The ridges may play a role in the flexibility of the coat, which allows the spore to respond to changes in the environment humidity and also during germination (Chada *et al.*, 2003).

The coat is composed of over 50 proteins that are often highly crosslinked (Kim *et al.*, 2006). Coat proteins make 30% of the total protein of the spore and their amino acid composition is unusually rich in cysteine and tyrosine (Driks, 1999). *B. anthracis* coat contains a similar number of coat proteins to the number present in *B. subtilis* (Lai *et al.*, 2003). Yet, whereas the majority of the early assembly coat proteins in *B. subtilis* have *B. cereus* and *B. anthracis* homologs, this is true only for a small fraction of late assembled proteins. Thus, most of the variation in composition between spores of different species occurs at the outer coat layer, which could reflect adaptations to different ecological niches (Driks, 2002; Henriques and Moran, 2007).

Coat proteins are synthesized in the mother cell and layered onto the spore surface during development. The timing of expression of the coat genes is likely crucial for the proper formation of the coat (Driks, 1999). Expression of the coat proteins that participate in early stages of coat assembly are under the control of σ^E, while the rest of the coat components are regulated by σ^E, σ^K, and GerE.

A small group of proteins, called morphogenetic proteins, direct the assembly of the coat by guiding deposition of other pre-made coat proteins. Coat synthesis starts with the deposition of SpoVIA onto the forespore outer membrane through interaction with SpoVM. In the absence of SpoVIA, the coat and also the cortex fail to properly assemble, suggesting that this protein coordinates the formation these two spore structures. SpoVIA then promotes the assembly of the first coat proteins and other morphogenetic proteins such as SpoVID and SafA, which are both necessary for the proper attachment of the coat to the cortex. Next, CotE localizes 75nm from the outer membrane, forming a shell around the forespore. The region underneath the CotE shell constitutes the matrix or pre-coat, which will mature into the inner coat. CotE plays a critical role in the outer coat assembly and directs the deposition of 40% of the coat proteins known to date. However, it has little effect on the assembly of the inner coat. CotG, CotH and CotO are all intermediate morphogenetic proteins that promote the assembly of late-synthesized outer coat proteins. Besides the role played by morphogenetic proteins, deposition of the coat also depends on low-affinity, low-specific interaction between a large subset of morphogenetic independent proteins. During the maturation phase of coat formation, coat proteins are processed, modified and crosslinked. Crosslinking results in insolubilization of 30% of the coat proteins and involves the formation of disulfide bonds as well as O-O' dityrosine bonds and glutamyl-lysine bonds which are enzymatically facilitated (Driks, 1999; Henriques and Moran, 2007; Lai *et al.*, 2003).

While the morphogenetic proteins, SpoIVA, CotE and CotH are conserved in the *B. cereus* group; coat assembly differs between *B. subtilis* and *B. anthracis*. SpoVIA

maintains its initial role in coat and cortex formation (Giorno *et al.*, 2007), but ExsA appeared to have a more critical role in *B. anthracis* coat assembly than its ortholog SafA in *B. subtilis* (Bailey-Smith et al., 2005). On the contrary, CotE has a modest role in coat deposition, and it only directs the assembly of very few of the orthologues and paralogues of *B. subtilis* CotE-dependent proteins (Giorno *et al.*, 2007). Different from *B. subtilis*, deposition of CotH in *B. anthracis* coat is independent of CotE, but it still directs assembly of a subset of protein like in *B. subtilis* (Giorno *et al.*, 2007). A novel morphogenetic protein belonging to the *B. cereus* group, Cot-α, participates in outer coat assembly (Kim *et al.*, 2004). Although, its localization is likely independent of CotE or CotH, Cot-α role in CotH deposition cannot be discarded (Giorno *et al.*, 2007).

The coat provides the mechanical and chemical resistance properties of the spore. It mainly acts as a permeability barrier to organic solvents (chloroform, phenol, octanol and others), and also to lysozyme, a peptidoglycan hydrolytic enzyme (Driks, 1999). The resistance to lysozyme likely contributes to the spore resistance to predation by unicellular organisms, such as *Tetrahymena thermophila* (Klobutcher *et al.*, 2006). The coat is also an important protective factor during passage through the mammalian gastrointestinal tract, as it is associated with resistance to bile salts and other gastric conditions (Barbosa *et al.*, 2005). In addition, the coat protects against oxidizing agents (chlorine, dioxide hypochlorite and hydrogen peroxide) by detoxifying these chemicals. CotA laccase has a role in protection against hydrogen peroxide, and other putative enzymes have been proposed to also have a role in detoxifying oxidizing compounds such as the superoxide dismutase SodA, two pseudocatalases, CotJC and YjqC, and

OxdD, an oxalate decarboxylase (Henriques and Moran, 2007). CotA is also involved in synthesis of a melanin-like brown pigment, which may provide protection against UV light (Martins *et al.*, 2002).

Besides the morphogenetic proteins, deletion of most coat proteins has subtle effects on the coat phenotype, with no alteration on spore resistance or germination. This observation can be interpreted in two ways: the durability of the coat does not result from a single protein, but rather is an emergent property of the interaction of several proteins, or the coat has alternative roles from the protective ones assigned historically (Driks, 2002).

Germination

While spores can remain in a dormant state for many years, they are able to resume vegetative growth once encountered with favorable conditions through the process of germination and outgrowth (Fig. 6). Spores are able to sense the presence of certain compounds, termed germinants, which likely signal availability of nutrients in the environment. Germinants can be single amino acids, sugars or purine ribonucleosides. *B. subtilis* spores also respond to a combination of aspargine, glucose, fructose and potassium salt (AGFK) (Paidhungat, 2002). Before adding the germinants, spores can be activated usually with a sublethal heat shock. Activation is reversible, and it primes and synchronizes spore germination; however, this mechanism is not well understood (Keynan, 1969).

Germination is initiated when germinants bind to receptors located in the spore inner membrane. These receptors are composed of three proteins encoded in tricistronic operons that are expressed in the forespore, under the control of σ^G (Moir *et al.*, 2002). *B. subtilis* spores respond to L-alanine via the GerA receptor, while the GerB and GerK receptors are required for AGFK induced germination (Paidhungat, 2002). The *B. anthracis* genome carries 7 putative germination receptors operons, although two of them, *gerA* and *gerY*, contain a frameshift mutation (Fisher and Hanna, 2005). Initiation of germination usually requires the cooperation of at least two different receptors, indicating that *B. anthracis* need multiple signals to break dormancy, preferably inside the host. For example, GerL and GerK cooperate when germination is induced with L-alanine, and germination with L-alanine and inosine requires cooperation of GerL, GerS and GerH/GerK. GerH and GerS participate in germination induced by both aromatic aminoacids and inosine. Cooperation of GerH, GerS and GerL is required when L-alanine and aromatic aminoacids are used as co-germinants (Fisher and Hanna, 2005). In addition, GerX, whose loci is located in pX01 plasmid, plays a role in germination inside macrophages and hence, virulence (Guidi-Rontani *et al.*, 1999a). *B. cereus* has some divergence in the response to germinants with respect to *B. anthracis*, which reflects differences in their ecology (Hornstra *et al.*, 2006). *B. cereus* requires GerQ or GerL to germinate with L-alanine as a germinant, and both GerI and GerQ for germination in the presence of inosine (Barlass *et al.*, 2002; Hornstra *et al.*, 2006). In addition, germination in contact with Caco-2 cells, an intestinal cell line, requires GerI and GerL (Hornstra *et al.*, 2009).

Spores respond to the presence of germinants by releasing H^+, monovalent cations and Zn^{2+} from the spore core. Secretion of H^+ results in alkalinization of the core, which is necessary for posterior activation of the core enzymes. Next, DPA-$Ca2^+$ is also released and replaced by water, resulting in partial hydration of the spore core. While the core water content at this moment is not sufficient for enzyme activity, it decreases the spore wet-heat resistance. The mechanisms involved in ion movement and water uptake are unknown (Paidhungat, 2002). *B. cereus* GerN, an Na^+/H^+K^+ antiporter, is required for inosine germination via GerI activation; however, its specific role as a ion transporter during germination is unclear (Southworth *et al.*, 2001).

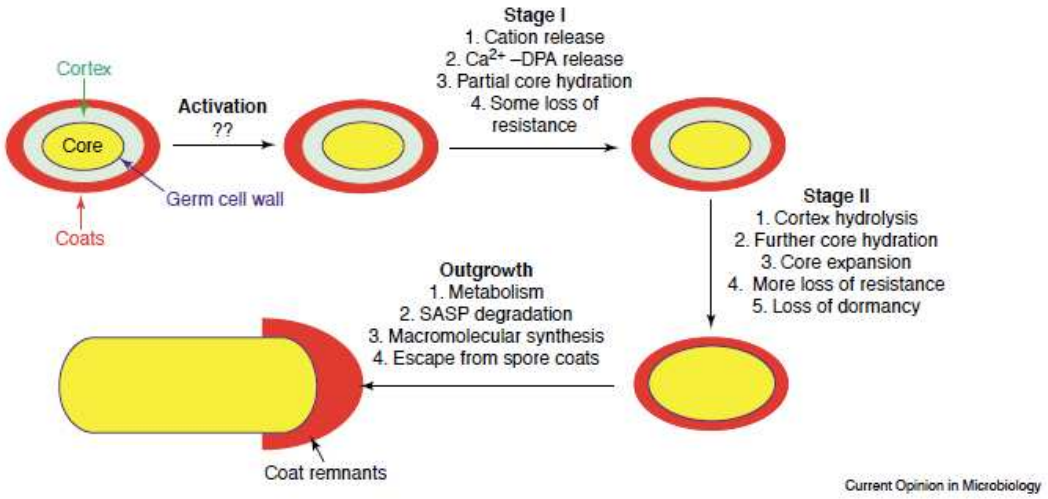

Fig. 6: Events in spore germination. Reprinted from Setlow, 2003. Copyright 2003, with permission from Elsevier.

To complete core hydration, cortex hydrolysis is necessary. In *B. subtilis*, two enzymes, CwlJ and SleB, participate in cortex degradation. Orthologs of these cortex hydrolytic enzymes are also present in *B. anthracis* and *B. cereus* (Heffron *et al.*, 2009).

CwlJ is located in the spore coat and SleB is likely situated between the cortex and the coat and it may also be associated with the inner membrane (Chirakkal *et al.*, 2002). CwlJ and SleB only degrade the cortex, as they require muramic δ-lactam for their activity (Atrih and Foster, 2001). The germ cell wall does not contain this modification, and therefore, it is not degraded during germination. While CwlJ is activated by $Ca2^{+}$-DPA (Paidhungat *et al.*, 2001), the mechanism that regulates activity of SleB is not known.

Degradation of the cortex allows the core to fully hydrate. The core swelling requires the rapid expansion of the 'compressed' inner membrane, the germ cell wall and the coat, which loses its ridges during this process (Paidhungat, 2002). In the core, SASP are hydrolyzed by a specific protease, GPR, which provides amino acids for new protein synthesis and energy production during outgrowth (Nessi *et al.*, 1998).

All the events that constitute the process of germination occur without energy metabolism. Resumption of metabolism after core hydratation, marks the beginning of the outgrowth process that ends with the first division of the new vegetative cell. Energy needs in the initial moments of outgrowth is met by catabolism of compounds stored in the cores, such as 3-PGA by phosphoglycerate mutase, PGM. Amino acids derived from degradation of SASP are also catabolized by a variety of enzymes already present in the core. Repair of DNA damage accumulated during dormancy also occurs at this time. Synthesis of macromolecules is reinitiated, starting first with RNA synthesis and then with protein and cell-wall synthesis (Paidhungat, 2002).

Bacillus cereus and *Bacillus anthracis* spore surface

The Exosporium

Spores of *B. cereus*, *B. anthracis* and other members of the *Bacillus cereus* group are encased by a loose fitting, bag-like layer, known as the exosporium. The exosporium is also present on spores outside the *Bacillus cereus* group such as *Bacillus megaterium*, *Bacillus sphaericus*, *Bacillus pumilis, Bacillus clausii* and some clostridia (Barbosa *et al.*, 2005; Beaman *et al.*, 1972; Holt *et al.*, 1975; Panessa-Warren *et al.*, 1997). *B. subtilis* spores do not possess a conspicuous exosporium, although the external glycosylated layer of the spore coat may constitute a rudimentary exosporium (Waller *et al.*, 2004).

The exosporium comprises a paracrystalline basal layer and a glycosylate hair-like nap on top (Fig. 7). The basal layer has a hexagonal crystal structure (Gerhardt and Ribi, 1964) with 23 to 34 Armstrong pores that would allow the unrestricted passage of small molecules, like germinants (Ball *et al.*, 2008). The hair-like nap length is strain-specific and varies from 20 nm to 60 nm (Plomp *et al.*, 2005a, b). The exosporium is separated from the rest of the spore by an interspace, with no evident connection between these two structures as seen under electron microscopy. This interspace appears to have a spring-like quality, although its composition has not yet been described (Giorno *et al.*, 2007).

The exosporium is composed of at least 20 proteins and glycoproteins in both a tight and loose association with each other. Some proteins, ExsA, CotE, ExsB, ExsY, CotY, CotB, ExsK, are orthologs and paralogs of *B. subtilis* morphogenetic and outer-coat proteins, while others are unique and have no homologs outside the *B. cereus* group such as BxpA, BclA, ExsFA, ExsFB, BxpC, ExsC, ExsD, ExsG, ExsJ/ExsH (Lai *et al.*, 2003; Redmond *et al.*, 2004; Steichen *et al.*, 2003; Todd *et al.*, 2003). The exosporium also contains the enzymes: alanine racemase (Alr), inosine hydrolase (Iunh) and superoxide dismutase. Interestingly, composition of the exosporium is not homogenous, as Alr is excluded from an exosporium substructure, known as the cap (Steichen *et al.*, 2007).

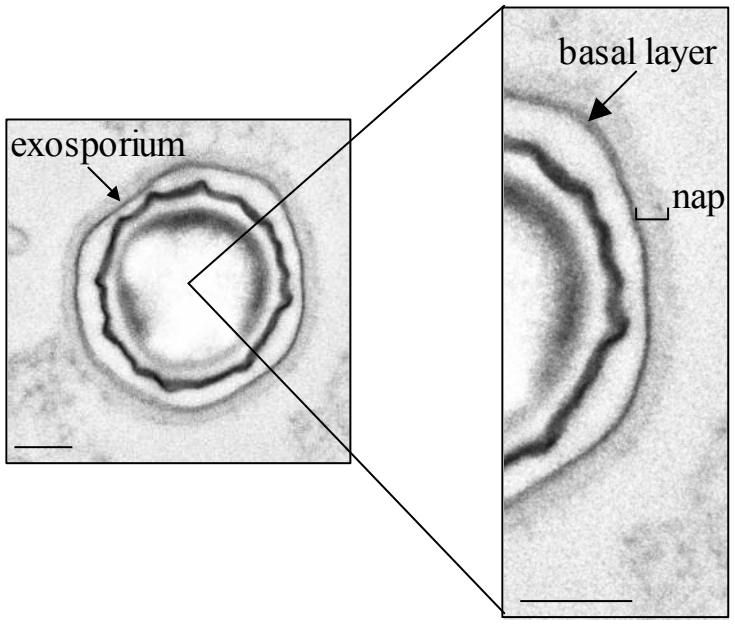

Fig.7: Exosporium structure. Transmission electron micrograph of a *B. anthracis* spore. Detail shows the basal layer and the hair-like nap of the exosporium. Scale bar, 250 nm.

Exosporium Assembly

Exosporium assembly is concomitant but independent from coat and cortex formation. Assembly always begins on the mother-side pole of the forespore and extends laterally until both ends meet and fuse at the forespore opposite pole (Ohye and Murrell, 1973). SpoIVA and ExsA promote attachment of the exosporium, as well as the coat, to the rest of the spore (Bailey-Smith *et al.*, 2005; Giorno *et al.*, 2007). While CotE has no role in exosporium synthesis, it participates in the proper attachment of this layer to the spore (Giorno *et al.*, 2007). In this respect, purified exosporium fractions do not contain CotE, suggesting that it localizes in interspace and acts as a bridge between both layers.

Assembly of the exosporium is discontinous and non-homogenous and it starts with cap formation on the mother-cell facing pole (Boydston *et al.*, 2006; Steichen *et al.*, 2007). The cap is a substructure whose requirement for assembly differs from the rest of the exosporium. Cap assembly is independent of ExsY, which is required for the lateral expansion of the exosporium (Boydston *et al.*, 2006). Ergo, there is a clear switch in the mode of assembly after cap formation, which may point to a possible checkpoint during exosporium synthesis (Steichen *et al.*, 2007). CotY, paralogue of ExsY, has no dramatic effect during the assembly phase, but deletion of both *exsY* and *cotY* genes results in spores with no cap and major defects in the coat, suggesting that ExsY and CotY also participate in coat formation (Johnson *et al.*, 2006).

The nap is composed mainly of BclA, a glycosilated protein that contains a collagen like region consisting in GXX triplets repeats, with a large portion being GPT

triplets (Sylvestre *et al.*, 2002). The number of repeats varies between strains and determines the length of the filaments that composes the nap (Sylvestre *et al.*, 2003). BclA is glycosilated with a disaccharide comprised of a rhamnose and a 3-O-methyl-rhamonse, and a tetrasacharide composed of three rhamnose and a novel sugar anthrose, only present in *B. anthracis* strains (Daubenspeck *et al.*, 2004). The sugar composition of BclA in *B. cereus* has not been studied thus far. Attachment of BclA to the basal layer and formation of the hair-like nap requires ExsFA/BxpB (Steichen *et al.*, 2005). While BclA can assemble at the cap in an ExsA/BxpB independent manner, this assembly is unstable (Giorno *et al.*, 2009). BclB/ExsJ is also a collagen-like glycoprotein that localizes on the surface of the spore and possibly forms part of the hair-like nap (Thompson *et al.*, 2007). Correct localization of both BclA and BclB depends first on the association to the basal layer through their N-terminal domain, and secondly, on attachment following a proteolytic event that liberates the N-terminal domain (Thompson and Stewart, 2008).

BclA, ExsY, CotY and ExsK form a high molecular mass complex (>250 KDa) (Redmond *et al.*, 2004; Severson *et al.*, 2009), which indicates that the exosporium goes through a maturation phase after assembly. Exosporium maturation involves the processing and cross-linking of proteins by YabG and Tgl (Moody *et al.*).

Roles of the Exosporium

The exosporium constitutes the first barrier between the spore and the environment. While the exosporium is a semipermeable layer, its pores are sufficiently small to avoid the passage of large macromolecules (Ball *et al.*, 2008). Thus, it may contribute to protection against damaging macromolecules such as hydrolytic enzymes and antibodies. An increased sensitivity to lysozyme treatment has been observed in *exsY* null spores that do not possess a complete exosporium. Unlike the coat, the exosporium does not provide resistance to organic compounds (chloroform, methanol and phenol) (Boydston *et al.*, 2006; Johnson *et al.*, 2006; Steichen *et al.*, 2005; Thompson *et al.*, 2007).

Being the outermost layer, the exosporium confers particular adherence and hydrophobic properties to the spore (Bowen *et al.*, 2002; Koshikawa *et al.*, 1989). BclA inhibits the interaction of *B. anthracis* spores with bronchial epithelial cells, thus, promoting uptake of the spore by the macrophages (Bozue *et al.*, 2007b). Furthermore, recognition of BclA rhamnose residues by CD14 enhances Mac-1 dependent phagocytosis of *B. anthracis* spores (Oliva *et al.*, 2009). As noted before, spore phagocytosis by pulmonary macrophages is essential for the establishment of anthrax infection (Guidi-Rontani, 2002). Also, BclA interacts with SP-C, a component of pulmonary surfactant, suggesting that BclA plays a role in host recognition (Rety *et al.*, 2005). The *B. cereus* spore surface contains a binding receptor for mammalian cell surface gC1qR/p33, promoting attachment to and colonization of the intestinal epithelial cells (Ghebrehiwet *et al.*, 2007; Peerschke and Ghebrehiwet, 2007). Moreover,

gC1qR/p33 and SP-C are both receptors of C1q (first complement protein), whose 3-D structure is similar to the BclA structure (Peerschke and Ghebrehiwet, 2007; Rety *et al.*, 2005). In addition, BclA is the major immunogenic protein of the *B. anthracis* spores, and it actually forms a shield around the spore that may limit access of antibodies to spore antigens located in the basal layer of the exosporium (Basu *et al.*, 2007; Boydston *et al.*, 2005). In *B. cereus*, InhA, a major component of the exosporium, promotes virulence by inducing escape from the macrophages (Ramarao and Lereclus, 2005).

The exosporium also provides resistance to oxidative stress generated by macrophages (Cybulski *et al.*, 2009; Weaver *et al.*, 2007). This protection involves the detoxifying activity of arginase and superoxide dismutase (SOD15, SODA1) present on the exosporium. Interestingly, the exosporium does not contribute to virulence during *B. anthracis* infection in several small animal models. In these cases, both exosporium-less and nap-less spores from fully virulent Ames strains are as pathogenic as wild-type (Bozue *et al.*, 2007a; Giorno *et al.*, 2007; Giorno *et al.*, 2009; Sylvestre *et al.*, 2003). However, the exosporium may contribute to pathogenesis and virulence during natural infection of the host, which usually occurs with a lower infection dose by increasing interaction with and survival to macrophages (Bozue *et al.*, 2007b; Cybulski *et al.*, 2009; Weaver *et al.*, 2007).

The exosporium contains two enzymes, Alr and Iunh that inactivate two main germinants, L-alanine and inosine, respectively (Chesnokova *et al.*, 2009; Liang *et al.*, 2008; Yan *et al.*, 2007). These enzymes likely suppress germination when the amount of

nutrients available cannot support vegetative growth. Moreover, Alr suppresses premature germination of the spore during mother cell lysis (Chesnokova *et al.*, 2009). ExsK inhibits germination as well by an unknown mechanism that may be related to the assembly of Alr or Iunh on the exosporium (Severson *et al.*, 2009). At the same time, a functional exosporium is necessary for promoting germination, as exosporium-less *cotE* mutants have lower rates of germination in rich media and also inside macrophages (Giorno *et al.*, 2007). Finally, the exosporium may oppose a physical barrier to the process of outgrowth, during which the new vegetative cells escape the spore shell (Steichen *et al.*, 2007). Outgrowth always occurs through the cap (the exosporium substructure), which may constitute a weakened spot to facilitate this process.

Spore Appendages

Spores of *B.cereus* and *B. thuringiensis*, but not *B. anthracis*, have long surface appendages that can be seen under scanning electron microscopy (SEM) (Hachisuka and Kozuka, 1981; Hachisuka *et al.*, 1984) (Fig. 8). These projections also have been reported for spores of the genus *Clostridium*. *B. cereus* appendages are pilus-like structures that can reach 3.8 μm length (Ankolekar and Labbe), but their origin remains uncertain (Kozuka and Tochikubo, 1985). While the appendages appear to emanate from the exosporium, they could also be connected to the coat. The appendage distribution around the spore is random and the number and length of appendages varies between *B. cereus* strains (Ankolekar and Labbe, ; Tauveron *et al.*, 2006).

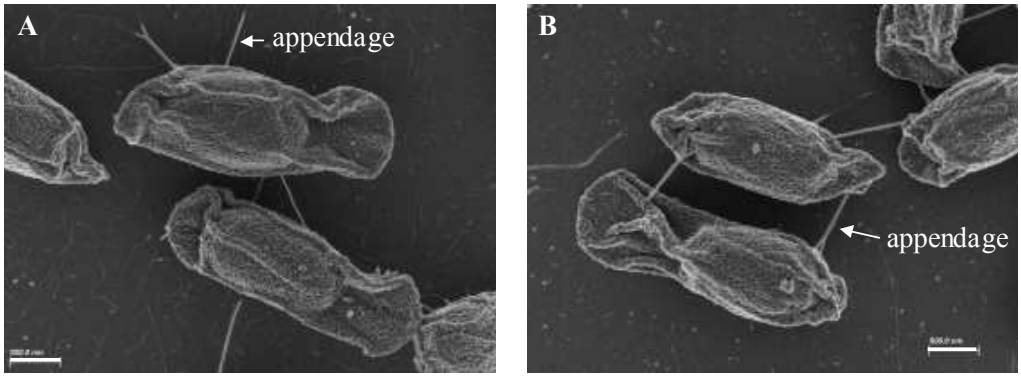

Fig. 8: *B. cereus* spore appendages. Scanning electron micrographs of *B. cereus* ATCC 14579 (A) and *B. cereus* ATCC 4342 (B) spores. Scale bar, 500nm.

The nature of these appendages is obscure. However, it has been demonstrated that they consist primarily of protein (DesRosier and Lara, 1981; Kozuka and Tochikubo, 1985). Appendages are highly insoluble and are resistant to extreme pH, organic solvents, detergents and protease digestion. The appendages role is likely to promote adhesion and attachment to abiotic surfaces and host cells by initiating contact with these surfaces. In this regard, a comparison of spores from several *B.cereus* strains have shown that spores surrounded by long appendages have a higher ability to adhere to stainless steel (Tauveron *et al.*, 2006). In addition, during the arthropod gut stage of *B. cereus*, spores attach to the host wall via their appendages (Margulis *et al.*, 1998). The fact that *B. anthracis* spores do not possess appendages could represent an adaptation to different lifestyles and pathogenesis.

Objective of study

The exosporium constitutes the surface of the spores. While it does not contribute to dormancy or any of the resistant properties usually associated with the spore (Boydston *et al.*, 2006; Johnson *et al.*, 2006; Steichen *et al.*, 2005; Thompson *et al.*, 2007), it provides the spore with its adhesion attributes (Bowen *et al.*, 2002; Koshikawa *et al.*, 1989). *B. cereus* spores present in contaminated food need to interact with the intestinal epithelial layer to initiate infection (Granum, 1997). Moreover, food contamination with *B. cereus* begins within the industry pipelines where the spores strongly adhere and survive cleaning procedures. *B. anthracis* spores are also the infective agent in anthrax. The *B. anthracis* exosporium surface reduces interaction with the epithelial cells (Bozue *et al.*, 2007b), and induces phagocytosis by pulmonary macrophages (Oliva *et al.*, 2009), which is necessary for the establishment of infection. Therefore, the exosporium plays an important role during natural infection of both *B. cereus* and *B. anthracis* and thus, the study of the proteins that compose the exosporium will facilitate a better understanding of this external layer and its role in spore adhesion, survival and germination.

The first aim of this thesis was to perform a survey of proteins comprising the exosporium of a *B. anthracis*-like *B. cereus* strain. Some of these proteins were inactivated in *B. cereus* and *B. anthracis*, and the effect on the spore structure was examined. One of these proteins, named ExsM, resulted in a novel phenotype, which

consisted of a double layer exosporium. We tested the effect of this double layer exosporium in survival to lysozyme treatment, germination and outgrowth.

The exosporium represents a high investment of energy during sporulation, which happens in low nutrition conditions, raising questions about the ecological advantage provided by this external layer. Results from the *exsM* mutant analysis provide insights into how the exosporium regulates germination and outgrowth, which are critical processes for the spore and its newly vegetative cell survival. Moreover, the double layer exosporium mutant will allow further testing of the role of the exosporium in spore survival in both the environment, and in the mammalian host during infection.

Materials and Methods

Bacteria Strains and Media

Escherichia coli DH5α Chemically Competent Cells (Subcloning efficiency) (Invitrogen, Carlsbad, CA) were used for routine cloning. *E. coli* INV110 Chemically Competent Cells (Invitrogen, Carlsbad, CA) were used for the growth of unmethylated plasmid DNA. *E. coli* DH5α and INV110 were grown in LB media (Sigma, St Louis, MO) at 37ºC.

B. cereus and *B. anthracis* strains used are described in table 1. *B. cereus and B. anthracis* strains were stored at -70ºC in LB media with 15% glycerol. Working strains were maintained at 4ºC on BHI agar (BD, Franklin Lakes, NJ), and were grown in BHI broth at 30ºC with or without antibiotics (depending the strain).

Antibiotic concentrations in the media were as follow: for *E. coli*, ampicillin 100 μg/ml and spectinomycin 100 μg/ml; for *B. cereus* and *B. anthracis*, spectinomycin 250 μg/ml; and for all strains, kanamycin 20 μg/ml.

Table 1: Bacteria strains used in this study.

Strain	Relevant genotype	Source
E. coli		
DH5α	cloning host	Invitrogen
INV 110	*dam*$^-$ *dcm*$^-$	Invitrogen
B. cereus		
ATCC 4342	wild-type	ATCC
MF15	*cotE*ΩpASD2-*cotE*	this study
MF18	*exsM*ΩpMFB4	this study
MF20	*becer0010_44320*ΩpMFB1	this study
MF22	*becer0010_22100*ΩpMFB2	this study
MF24	*becer0010_42210*ΩpMFB3	this study
MF26	*exsK*ΩpMFB7	this study
MF28	*becer0010_38120*ΩpMFB8	this study
MF30	*gerQ*ΩpMFB9	this study
MF33	*becer0010_29950*ΩpMFB12	this study
MF38	*rbp*ΩpMFB18	this study
MF65	*exsM*ΩpMFF3	this study
ATCC 14579	wild-type	ATCC
MF63	*exsM*ΩpMFB6	this study
MF82	*cotN*ΩpMFB24	this study
MF84	*calY*ΩpMFB25	this study
B. anthracis		
ΔSterne	wild-type pXO1$^-$ pXO2$^-$	J. Lederberg
MF43	*exsM*ΩpMFB10	this study
MF46	*BAS4323*ΩpMFB15	this study
MF57	*bxpC*ΩpMFB20	this study
MF59	*BAS2264*ΩpMFB5	this study
MF61	*gerQ*ΩpMFB14	this study

Spore preparation

B. cereus and *B. anthracis* spores were prepared by the nutrient exhaustation method (Nicholson and Setlow, 1990). *B. cereus* or *B. anthracis* stationary phase cultures were plated onto LD agar plates (Leighton and Doi, 1971), and incubated at 30°C for 3-5 days. The spores were harvested by centrifugation at 15,000 x *g* for 15 min at 4°C, and the spore pellets were washed in ice-cold distilled water 5-10 times by repeated centrifugation until the samples were >95% pure. The purity of the spore samples was checked by phase-contrast microscopy. Spores were counted with a Bright-Line hemacytometer (Hausser Sci, Horsham, PA) and stored at 4°C in buffer TE (50mM Tris-HCl pH 7.2, 10mM EDTA pH 8)

Exosporium extraction

Before protein extraction, spores were sequentially washed in 1M NaCl, 0.1% SDS/TE buffer and TE buffer to eliminate adsorbed proteins (Todd *et al.*, 2003). Later, washed spores (2. 10^9 spores/ml) were treated with 2% β-mercaptoethanol in 0.1 M buffer sodium carbonate pH 10 for 2 h at 37°C. The sample was centrifuged for 3 min at 15000 x *g*, and the supernatant was passed through a 0.22 μm filter to ensure that it was free of spores.

For exosporium extraction by sonication, washed spores ($2x10^9$ spores/ml) were sonicated with a W-380 Sonicator for 4 x 30 s at 50%. Between sonication bursts, the

sample was cooled for 1 min on ice. The exosporium was separated from the rest of the spore by centrifugation for 3 min at 15000 x *g*, and further purified by passage through a 0.22 μm membrane.

For comparison of the exosporium protein profiles between *B. cereus* strains and *B. anthracis* spores, and also between *B. cereus* wild-type and mutant spores, the same number of spores were extracted in each case.

Exosporium and Coat Extraction

Total separation of the exosporium from spores is not possible (Steichen *et al.*, 2007). Thus, to study the protein composition of the spore coat, it is necessary to extract both the coat and exosporium simultaneously. Two different extraction treatments were performed on the same number of *B. cereus* ATCC 4342 and *exsM* spores.

To extract exosporium and coat proteins, washed spores ($1x10^7$ spores/ml) were incubated in 50mM sodium carbonate buffer pH 9.8, 8M urea, 50mM DTT, 1% SDS for 2 h at 37°C (Aronson and Fitz-James, 1971; Cheng and Aronson, 1977). In addition, exosporium and coat proteins were extracted by boiling washed spores ($1x10^7$ spores/ml) in 125 mM Tris/HCl buffer pH 6.8, 4% SDS, 10% β-mercaptoethanol, 1mM DTT, 0.05% bromophenol blue, 10% glycerol (Henriques *et al.*, 1995). In both cases, the spores were removed by centrifugation and the supernatant was passaged through a 0.22 μm membrane.

Protein Electrophoresis

Spore proteins were separated by sodium dodecyl sulfate-polyacrylamide gel electrophoresis (SDS-PAGE). Samples were mixed with an equal volume of Laemmli buffer (125 mM Tris/HCl, pH 6.8, 20% glycerol, 4% SDS, 0.005% bromophenol blue and 5% β-mercaptoethanol) and boiled for 5 min. Next, the sample were held in ice for 2-10 min and centrifuged briefly (30 s at 15,000 x *g*) to remove any insoluble material. The samples were loaded onto a 4-16% or 4-20% Tris-HCl Ready Gel, (Bio-Rad, Hercules, CA). A molecular weight standard, Precision Plus Protein Standard (Bio-Rad, Hercules, CA) was included in all gels. Linear gradient gels were preferred as both exosporium and coat plus exosporium samples contained a wide range of molecular weights. Electrophoresis was performed in 1X Tris-glycine buffer (Bio-Rad, Hercules, CA), at 100V. For SDS-PAGE in non-reducing conditions, samples were boiled in Laemmli buffer without the addition of 5% β-mercaptoethanol.

To separate low-molecular weight mass proteins, samples were boiled in Tricine gel sample buffer (200 mM Tris/HCl pH 6.8, 40% glycerol, 2% SDS, Commassie blue G-250 0.04% and 2% β-mercaptoethanol) and separated on a 16% Tris-Tricine Ready Gel (Bio-Rad, Hercules, CA) at 75 V using 1X Tricine running buffer (100 mM Tris, 100 mM Tricine and 0.1% SDS). A polypeptide SDS-PAGE molecular weight standards ((Bio-Rad, Hercules, CA) was included in the gels.

Protein Staining

Coomassie Blue staining

Protein gels were soaked in stain solution (50% methanol, 10% acetic acid and 0.25 % Coommassie Blue R-250) on a table top shaker for 3-16 h. Then, the gels were destained by soaking in a solution of 50% methanol and 10% acetic acid. This destain solution was replaced periodically until desired destaining was achieved.

Colloidal Coomassie blue staining was performed with GelCode Blue Stain Reagent (Pierce, Rockford, IL). In this case, gels were prefixed with 50% methanol and 10% acetic acid for 15 min. After 3 x 15 min washes with water, the gels were soaked in GelCode Blue for 3-16 hs. Next, the gels were destained in water for 1-2 h.

Silver staining

Silver staining was performed according to a standard protocol (Blum et al., 1987). Gels were fixed for 2 h in 50% methanol and 10% acetic acid and then washed 3 times for 20 min each in 50% ethanol. The gels were soaked with gentle shaking in 0.2% sodium thiosulfate for 1 min, and then washed 2 times for 1 min in water. The gels were impregnated with 2% silver nitrate and 0.5% of 37% formaldehyde for 20 min. After rinsing the gels 3 times with water, the protein bands were developed with 6% sodium carbonate solution until desired intensity of staining was acquired. The staining was stopped with fixative solution (50% methanol and 10% acetic acid).

Sypro Ruby staining

Sypro Ruby (Bio-Rad, Hercules, CA) is a fluorescent protein stain that is capable of staining 2 ng of protein. Gels were first fixed in 10% methanol and 7% acetic acid for 15 min and then soaked in Sypro Ruby for 3-16 hs. Next, the gels were rinsed in 10% methanol and 7% acetic acid to decrease background fluorescence. The gels were visualized under UV light.

Glycoprotein staining

Gels were stained with GelCode Glycoprotein Staining Kit (Pierce, Rockford, IL) exactly as described by the manufacturer..

Mass spectrometry

Coomassie blue stained gels were serially divided into slices. Each gel slice was broken into pieces with a pipette tip and destained with 50% acetonitrile/50% ammonium bicarbonate. The gel slice was then reduced with 10 mM DTT in 50 mM ammonium bicarbonate, for 45 min at 56 ºC. Next, the proteins were alkylated with 100 mM iodoacetamide in 50 mM ammonium bicarbonate in the dark for 30 min. The gel slice was washed in 50% acetonitrile/50% ammonium bicarbonate, shrinked in 100% acetonitrile and dried down in a SpeedVac. The proteins were digested with 0.2 μg trypsin in 50 mM ammonium bicarbonate, at 37 ºC for 16 hs. The resulting peptides were

eluted from the gel with several changes of extraction buffer (50% acetonitrile/ 5%trifluoroacetic acid), and concentrated by evaporation. The samples were then diluted in water and placed into an LC packing vial (Fernandez J, 2009).

Peptides were analyzed by liquid chromatography coupled to tandem mass spectrometry (LC-MS/MS) on an Applied Biosystems Q-Star Mass Spectrometer equipped with an LC-Packing Ultimate nano-flow HPLC. Protein identification was performed with MASCOT search program (Matrix Science) using a database containing *B. cereus* and *B. anthracis* sequences. The mass spectrometry was performed at the Proteomics Resource Center of The Rockefeller University.

Construction of *B. cereus* and *B. anthracis* mutants

Mutagenesis was performed using shuttle plasmid pASD2 (Day *et al.*, 2007) (Fig.9) that harbors two origins of replication: ColE1 for replication in E. coli and pE194, a thermosensitive origin of replication active in *B. cereus* and *B. anthracis*. The plasmid also carries *aphA-3* and *add-9* genes encoding resistance to kanamycin and spectinomycin, respectively.

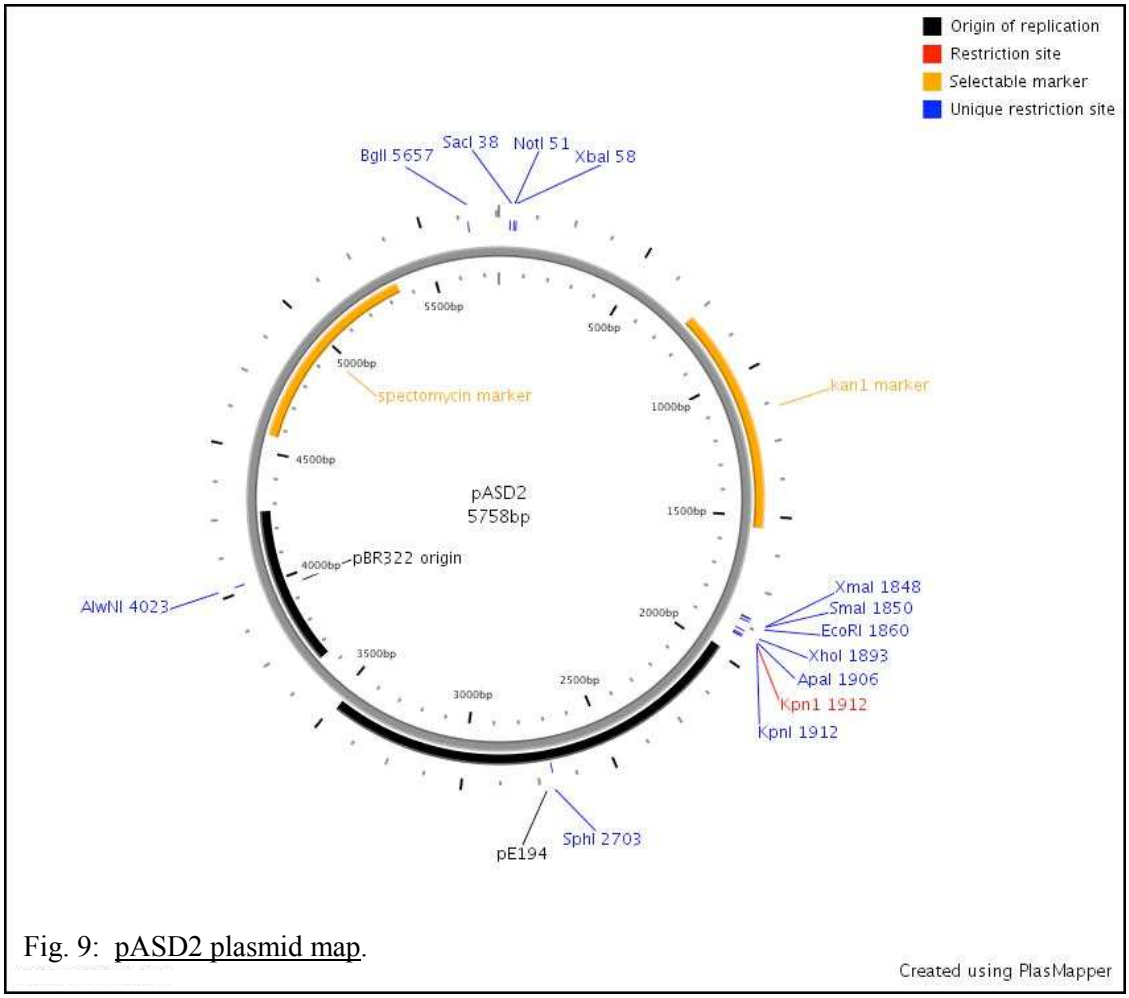

Fig. 9: pASD2 plasmid map.

An internal fragment (150-200 bp) towards the 5' end of each gene to be inactivated was amplified from chromosomal DNA of *B. cereus* ATCC 4342 using polymerase chain reaction (PCR) with appropriate primers containing a *Kpn*I recognition site. To amplify the *exsM* internal fragment, the following oligonucleotides were used: MF72 5'-ATGAGGTACCCAGAAGCTTATGGCGTAGCAGA-3' and MF73 5'-ATGAGGTACCCACCAGTCACGACTCCTTCA-3' (the *Kpn*I sites are underlined). The PCR was performed with a Taq PCR Master Kit (Qiagen, Germany) according to the manufacturer's protocol on an Eppendorf Mastercycler. The amplicon was separated on a 1.2% agarose (Seakem, Cambrex, Charles City, IA) gel in 0.5X Tris-acetate buffer (TAE,

Qiagen, CA) and then purified with QiaexII Gel Extraction Kit (Qiagen, Germany) according to the manufacturer's protocol. Next, the PCR product was digested with *Kpn*I (NEB, Ipswich, MA) for 3 hs at 37ºC, and purified from the digestion reaction with Nucleospin Extract II (MN, Germany) following the manufacturer's protocol. The *Kpn*I digested PCR product was then ligated into pASD2 (*Kpn*I digested and SAP (USB, Cleveland, OH) treated) with T_4 ligase (NEB, Ipswich, MA) for 16 h at 4ºC. The ligation reaction was then transformed into *E. coli* DH5α chemically competent cells according to the manufacture's protocols. Resulting transformants were screened for the presence of insert by colony PCR, and plasmid DNA was prepared with a QIAprep Spin Miniprep Kit (Qiagen, Germany) following the manufacturer's protocols. The resulting plasmid was sequenced to check for correct orientation and then, the plasmid was passed through *E. coli* INV110 to obtain unmethylated DNA suitable for transformation into *Bacillus cereus*. One *E.coli* INV110 transformant was picked randomly and grown in LB with antibiotics. The next day, plasmid DNA was prepared with a QIAfilter Plasmid Midi Kit (Qiagen, Germany), according to manufacturer's protocol. The resulting plasmid was checked again by *Kpn*I digestion and quantified using a Nanodrop ND-100. The plasmids used for all insertional mutagenesis are described in table 2.

Table 2: Plasmids used in this study.

Plasmids	Description	Source or Reference
pASD2	shuttle vector *E. coli*/*Bacillus*	(Day *et al.*, 2007)
pASD2-*cotE*	pASD2 + integral fragment of *cotE* (*B. cereus* ATCC 4342)	this study
pMFB1	pASD2 + internal fragment of *bcere0010_44320* (*B. cereus* ATCC 4342)	this study
pMFB2	pASD2 + internal fragment of *bcere0010_22100* (*B. cereus* ATCC 4342)	this study
pMFB3	pASD2 + internal fragment of *bcere0010_42210* (*B. cereus* ATCC 4342)	this study
pMFB4	pASD2 + internal fragment of *exsM* (*B. cereus* ATCC 4342)	this study
pMFB5	pASD2 + internal fragment of *BAS2264* (*B. anthracis*)	this study
pMFB6	pASD2 + internal fragment of *exsM* (*B. anthracis*)	this study
pMFB7	pASD2 + integral fragment of *exsK* (*B. cereus* ATCC 4342)	this study
pMFB8	pASD2 + internal fragment of *bcere0010_38120* (*B. cereus* ATCC 4342)	this study
pMFB9	pASD2 + integral fragment of *gerQ* (*B. cereus* ATCC 4342)	this study
pMFB10	pASD2 + internal fragment of *exsM* (*B. cereus* ATCC 14579)	this study
pMFB12	pASD2 + internal fragment of *bcere0010_29950* (*B. cereus* ATCC 4342)	this study
pMFB14	pASD2 + internal fragment of *BAS4323* (*B. anthracis*)	this study
pMFB15	pASD2 + internal fragment of *gerQ* (*B. anthracis*)	this study
pMFB18	pASD2 + integral fragment of *rbp* (*B. cereus* ATCC 4342)	this study
pMFB20	pASD2 + internal fragment of *bxpC* (*B. anthracis*)	this study
pMFB24	pASD2 + internal fragment of *cotN* (*B. cereus* ATCC 14579)	this study
pMFB25	pASD2 + internal fragment of *calY* (*B. cereus* ATCC 14579)	this study
pRS69	source of *gfpmut-2*	(Schuch *et al.*, 2002)
pMMF1	pASD2 + *gfpmut-2*	this study
pMMF3	pASD2 + *exsM-gfpmut-2*	this study

***B. cereus*/*B. anthracis* electroporation**

The unmethylated plasmid was introduced into *B. cereus* ATCC 4342 by electroporation following a previously described protocol (Turgeon *et al.*, 2006). Briefly, 100 ml of *B. cereus* culture was grown in BHI at 30º C to an optical density at 600 nm of 0.4. The cells were then harvested by centrifugation at 4000 x *g* for 10 min at 4 °C. All subsequent steps were done on ice. The cells were washed with 750µl ice-cold electroporation buffer (1 mM HEPES pH 6.8, 250 mM sucrose, 1mM magnesium chloride and 10% glycerol) five times and resuspended in 600 µl of the same buffer. Up to 1 µg of plasmid DNA (0.5-1 µl) in water was added to 50 µl of cells and pulsed (2.5 kV, 25 µF, 200 Ω) in a 0.1 cm gap electroporation cuvette. The cells were resuspended immediatly after the electric shock in 1 ml recuperation buffer (BHI additionated with 250 mM sucrose, 5 mM of magnesium chloride and 5 mM of magnesium sulfate), and incubated for 1.5 h at 30°C with aeration. Recovered cells were spread on BHI agar plates, containing kanamycin and spectinomycin. Colonies were visible after 20–24 h.

Selection of integrants

A culture from a single transformant grown overnight at 30°C in BHI with antibiotics was diluted 1/100 in fresh BHI medium without antibiotics and grown for 2 h at 30°C, and then for 6 h at 42°C to promote loss of the thermosensitive plasmid. The bacteria were then plated at 42°C on BHI agar supplemented with spectinomycin and kanamycin to promote the growth of recombinants. Since plasmid replication is inhibited at 42°C, only the cells that had undergone a Campbell-like integration event into the target gene were selected (Day *et al.*, 2007). Resulting colonies were screened by PCR

with primers external and internal to the pASD2 insertion site, to confirm that integration had occurred. The pASD2 primers used were: BD44 5'-GAAC CATTTGAGGTGATAGGTAAG-3'; BD45 5'- AAATCGGCTCCGTCGATACTATG-3'; BD55 5'-GAATTTAGGTGTCACAAGACACTC-3'. For the confirmation of *exsM* integrants, the primers used were: MF81 5'-CTTTGCGAGGTTAA CAGGTAAGAG-3' and MF82 5'-CCTTCAAACTCCTCCACATTGACT-3' (Fig. 10).

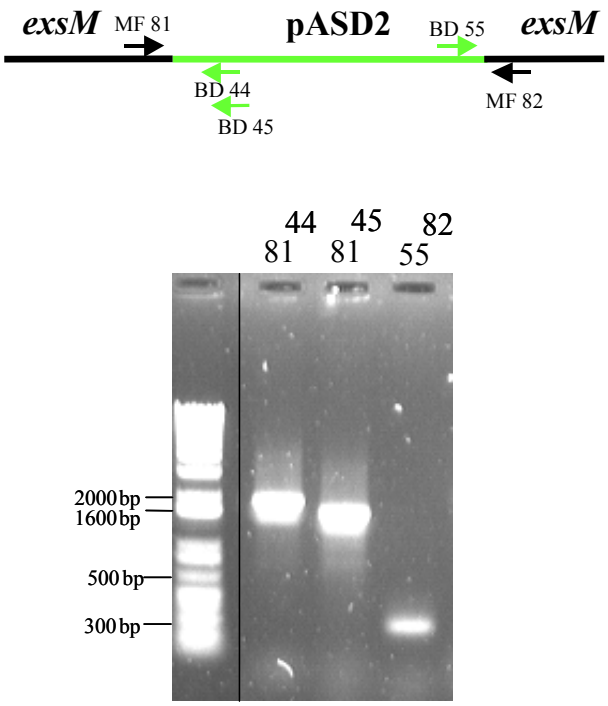

Fig. 10: *exsM* integrants confirmation. The scheme shows the position of the primers used for confimation that integration in the expected genomic locus had occurred (not to scale). The DNA agarose gel shows the PCR products obtained with the primers indicated on top. 1 kb DNA ladder (Invitrogen, Carlsbad, CA) with the molecular size of selected bands shown on the left.

B anthracis mutants were constructed following the same protocol, with the exception that internal gene fragments were amplified from the chromosomal DNA of *B. anthracis* ΔSterne. *B. cereus* ATCC 14579 mutants were also constructed with the same protocol, but in this case the target gene internal fragment was amplified from DNA of *B. cereus* ATCC 14579.

Construction of ExsM-GFP

To construct the ExsM-GFP expressing strain, *gfpmut2* gene was amplified from pRS69 with primers MF143: 5'-GATGGTACCGATCGAATTCATGAGTAAAGG AGAAGAACTTTTCAC-3' (*Kpn*I and *Eco*RI sequences are underlined), MF145 5'-CATGATATCTTATTTGTATAGTTCATCCATGCCATG–3' (*Eco*RV sequence is underlined). The PCR product was then digested with *Kpn*I and *Eco*RV (NEB, Ipswich, MA) and ligated into pADS2 digested with *Kpn*I and *Sma*I (NEB, Ipswich, MA) and SAP treated. Then, the last 200bp (lacking the stop codon) of *exsM* were amplified from *B. cereus* ATCC 4342 chromosomal DNA with primers MF146 5'-ATGAGGTACCGGAA GTATTACTGGTGTAGTGAATG-3' and MF174 5'-ATGAGAATTCCTTCTTTACTT TTCTAACTCGCCC-3' (*Kpn*I and *Eco*RI sequences are underlined). The amplicon was digested with *Kpn*I and *Eco*RI and ligated in frame to the 5' end of *gfpmut*2. The resulting plasmid (pMMF3) was then electroporated into *B. cereus* ATCC 4342. Transformants and recombinants were selected as already described for the insertion mutants.

Transmission electron microscopy

Spores were fixed in 2.5% glutaraldehyde–75 mM sodium cacodylate buffer pH 7.4 containing 0.15 % Alcian blue for 4 h (when indicated) at room temp. Spore pellets were then washed in cacodylate buffer pH 7.4, post-fixed for 1 h in 1% osmium tetraoxide–0.1 M sodium cacodylate buffer pH 7.4 on ice and with 1% uranyl acetate. Dehydratation involved the sequential treatment with a graded ethanol series. The samples were then embedded in LR white resin. Ultra-thin sections (70 nm) were cut on a Leica UltracutE and the sections were collected on uncoated 200-mesh grids and stained with 1% alcoholic uranyl acetate and Reynolds' lead citrate for 9 and 5 min, respectively. Grids were viewed with a TecnaSpiritBT Transmission Electron Microscope (FEI) at 80 kV and pictures were taken with Gatan 895 ULTRASCAN Digital Camera.

For negative staining transmission electron microscopy, 10 μl of properly diluted sample was spread on a glow discharged and carbon-coated copper grid for 1 min and the excess liquid was aspirated off with a filter paper. The samples were then stained with two drops of 2% phosphotungstate acid (PTA), pH 6.8 for 30 s and excess stain was removed by touching the edge of the grid with a tissue paper. The sample was washed with a drop of distilled water and again, dried with a tissue paper. Transmission electron microscopy (TEM) images were obtained as described before. TEM was performed at the Electron Microscopy Resource Center of The Rockefeller University.

Scanning electron microscopy

Spores were adhered to poly-L-lysine coated glass cover slips. After 4 h of fixation with 2.5% glutaraldehyde in 75 mM cacodylate buffer pH 7.4 with 0.15% Alcian blue, the spores were post-fixed for 1 h in 1% osmium tetraoxide–100 mM cacodylate buffer pH7.4. The samples were dehydrated through a graded ethanol series. The cover slips were then critical-point dried and sputter coated with gold-palladium particles in a Vacuum Desk-2 (Denton). Images were collected with a LEO 1550 Gemini Scanning Electron Microscope at 2 kV. Scanning electron microscopy (SEM) was performed at the Electron Microscopy Resource Center of The Rockefeller University.

Tranglutaminase Inhibition

Monodansylcadaverine (MDC, Sigma, St Louis IL), was diluted in water immediately before use. For 50 mM MDC treatment, 100 µl of 100 mM MDC was combined with 100 µl of PBS, spread onto LD sporulation plates and let to dry. For 25 µM MDC treatment, 50 µl of 100 MDC was mixed with 150 µl of PBS and for 12.5 mM treatment, 25 µl was diluted in 175 µl of PBS. Control plates were spread with 200 µl of PBS. Once dried, a *B. cereus* ATCC 4342 stationary phase culture was plated onto the supplemented LD plates and incubated for 3 days at 30 ºC. The spores were harvested, and exosporium protein were extracted as before described.

Biofilm formation

B. cereus cultured overnight at 30°C in BHI with aeration was diluted 1/100 in 5 ml of LD media contained in a 15 ml conical centrifuge tube. The culture was incubated without agitation at 30°C and checked daily for formation of a pellicle at the air/liquid interface.

Sporulation Rate

B. cereus or *B.anthracis* strains were grown overnight with aeration in BHI at 30ºC. Serial dilutions (10^{0}, 10^{-2}, 10^{-4}, 10^{-6}) in PBS of the stationary phase cultures were spotted (25 μl) onto an LD sporulation plates. The plates were incubated at 30ºC for 14 h, 18 h, 24 h and 48 h. At the indicated time points, the plates were exposed to chloroform vapors for 15 min, air dried for another 15 min and then returned to the 30ºC incubator for 24 h. The number of CFU obtained after 24 h incubation post-treatment represented the number of spores present at the time point of the chloroform treatment. This experiment was performed in duplicate and repeated 3 times.

Growth Rate

B. cereus wild-type and mutant strains grown overnight in BHI at 30ºC with aeration were diluted 1/100 in fresh BHI medium and incubated at 37ºC. Optical density at 600 nm (OD_{600}) was measured every 30 min for the first 6 h. The cultures OD_{600} was measured one more time after 16 h of incubation at 37ºC.

Spore size measurement

Length and width measurement of the wild-type and mutant spores were obtained from SEM photographs. *B. cereus* wild-type and *exsM* spore size were compared by Mann-Whitney *U* test, and *B. anthracis* wild-type and *exsM* spore size were analyzed by unpaired Student's *t* test.

Flourescence microscopy

Sporulation of MF65 carrying the ExsM-GPF fusion was induced by dilution 1/100 into LD liquid media. The culture growth was followed by measuring OD_{600} and the end of exponential growth was considered t_0 of sporulation. *B. cereus* sporangia bearing the ExsM-GFP fusion protein were stained with 1.5 μg/ml FM4-64 (Invitrogen), a cell membrane stain. Next, the cells were visualized with a Nikon Y-IM microscope equipped with a Qimaging charge-coupled device (CCD) camera. Images were obtained with Qimage program and processed with Adobe Photoshop 7.0 software.

Spore Resistance Assays

Assessment of spore resistance to organic solvents and lysozyme treatment was performed using the methods described by Nicholson and Setlow (Nicholson and Setlow, 1990).

Water-immiscible organic solvent resistance assay

50 µl of chloroform was added to 0.45 ml of spore suspension (10^6 spores/ml) in spore buffer (10 mM potassium phosphate buffer, pH 7.4, 50 mM potassium chloride and 1mM magnesium sulfate). The samples were shaken vigorously and incubated at room temperature for 10 min. Then, aliquots were removed, serially diluted in PBS, and plated on BHI plates for viable count determination. An aliquot without treatment was similarly plated on BHI and used to calculated the percentage of resistant spores. This experiment was performed in duplicate and repeated 3 times.

Water miscible organic solvent resistance assay

0.45 ml of methanol was added to 50 µl of spore suspension (10^6 spores/ml) in spore buffer. The samples were incubated at room temperature. Aliquots were removed after 10 min, serially diluted in PBS, and plated on BHI plates for viable count determination. An aliquot without treatment was similarly plated on BHI and used to calculated the percentage of resistant spores. This experiment was performed in duplicate and repeated 3 times

Organic acids resistance assay

50 µl of spore suspension (10^6 spores/ml) in spore buffer was added to 0.45 ml of ice-cold phenol. The samples were incubated at 4°C and treatment was stopped after 10 min by diluting the mixture 10-fold. The sample was then serially diluted in PBS, and plated on BHI plates for viable count determination. An aliquot without treatment was similarly plated on BHI and used to calculated the percentage of resistant spores. This experiment was performed in duplicate and repeated 3 times.

Lysozyme resistance assay

Spores were incubated with lysozyme (250 µg/ml in PBS) for 5, 10, 20 and 40 min at 37°C and the survivors were enumerated by dilution on BHI agar plate. An aliquot without treatment was similarly plated on BHI and used to calculated the percentage of survival after lysozyme treatment. This experiment was performed in duplicate with three different preparations of wild-type and mutant spores and statistical significance was analyzed using a paired Student's *t* st.

Germination assays

Spore germination was measured by assessing the loss of heat resistance or decrease in the optical density at 580 nm (OD_{580}). Loss of heat resistance was measured as described by Giebel et al., 2009 (Giebel *et al.*, 2009). Briefly, spores were diluted to $4x10^5$ spore/ml in water and heat treated at 65°C for 20 min to both activate spores and kill any remnant vegetative cell contaminating the spore sample. Samples were then

diluted 1/200 in germination buffer (10 mM Tris-HCl, pH 7.4, 10 mM NaCl) and germination was started with the addition of 50 mM L-alanine. Aliquots were removed at 2, 5, 10, 15, 20 and 30 min and incubated at 65°C for 20 min to kill germinated spores. ater, 50 µl of each aliquot was plated on BHI agar and incubated overnight. Also, an aliquot at time zero was plated without heat treatment. The fraction of germinated spores was calculated for each time point.

To measure the loss of OD_{580}, spores were first heat activated at 70°C for 30 min. After heat activation, spores were resuspended in ice-cold germination buffer to an OD_{580} of 0.5. The germinants used in this work were as follows: 50 mM L-alanine, 1 mM inosine, 1mM L-alanine and 1mM inosine, and 1 mM L-serine and 1 mM inosine. For germination in complete medium, spores were resuspended in 100 µl of germination buffer, and then 100 µl of BHI (0.5% final concentration) was added to initiate germination. After the addition of germinants, the OD_{580} of the spore suspension was measured in a Spectramax Plus Multi-Detection Reader (Molecular Devices) using 15 seconds interval for 60 min at 30°C. Before each time point, the plate was shaken 3 seconds to prevent spore settling. Spores were preincubated with 1mM D-cycloserine for 15 min at 30°C to inhibit Alr before the addition of germinants, when indicated. Spores were also observed under the phase-contrast microscope at different times during germination to control that germination was not blocked.

Outgrowth assays

The tetrazolium overlay assay was performed as previously described (Cutting *et al.*, 1990b; Giorno *et al.*, 2007). Briefly, *B cereus* wild-type and *exsM* were patched onto LD sporulation plates and incubated for 3 days at 30°C to allow sporulation to be completed. Next, the cells were transfered to a sterile filter paper. The filter was laid, colony side up, on a 3% agar plate with 0.1 g/l D-alanine (anti-germinant) and incubated in an oven at 65°C for 3 h to kill vegetative cells and to heat-activate the spores. After cooling, the filter was transfered to a tetrazolium (Tzm, Sigma, St Louis, MO) agar plate (0.167% L-alanine, 0.45 g/l L-asparagine, 1 g/l glucose, 1 g/l D-fructose, 0.33% casamino acids, 0.167% adenosine and 1 g/l Tzm), colony side up, and incubated at 37 °C for 1-2 h in the dark to allow the color reaction to develop.

Change in OD_{580} was also followed to quantify outgrowth in the wild-type and *exsM* samples. Spores were heat activated at 70°C for 30 min and then, diluted 50% in BHI, to an initial OD_{580} of 0.01 to allow bacteria growth. The OD_{580} was followed after dilution at 2.5 min intervals for 2 h at 30°C. Before each time point, the plate was shaken for 3 min to prevent spore settling. In addition, after 60 min, spores and outgrowth cells were counted under the phase contrast microscope. Sphere shaped cells were enumerated as spores and cylindrical shaped cells as nascent vegetative cells. At least 300 cells were counted for each sample.

Appendage purification

The appendage isolation procedure was adapted from DesRosier and Lara (DesRosier and Lara, 1981). Appendages were extracted from *B. cereus* ATCC 4342 and ATCC 14579 with 2% β-mercaptoethanol, as described in the exosporium extraction section, and then dialyzed against buffer TE (0.1 MTris/HCl pH 7.8 and 5.10^{-4} EDTA). Next, the sample was added to the top of a CsCl discontinous gradient. The CsCl discontinous gradient was prepared in a 12 ml Polyallomer centrifuge tube (Beckman) as follow: 1.5 ml of 1,4 g/l CsCl, 1.5 ml of 1.35 g/l CsCl, 2 ml of 1.3 g/l CsCl, 1.5 ml of 1.25 g/l CsCl and 1.5 ml of 1.2 g/l CsCl. The sample was ultracentrifuge in a Beckman SW 40 Ti rotor at 30000 rpm at 4ºC for 22 h. After centrifugation, the appendages were dialyzed against buffered TE and stored at 4ºC.

Results: Proteomic analysis of *Bacillus cereus* exosporium

Identification of exosporium proteins

Extraction of exosporium proteins by sonication

Exosporium was isolated from *B. cereus* ATCC 4342 spore preparations by four 30 s bursts of sonication at 50% power. The sample was then centrifuged to separate the exosporium fragments from the spores, and it was further purified by 0.22 μm filtration to remove any remaining spores. To assess the efficiency of the extraction, resulting spores were examined by scanning electron microscopy (SEM), and the exosporium fraction was studied by negative staining transmission electron microscopy (TEM) (Fig. 11). Sonication resulted in the separation of the exosporium, without further disruption of the spores. Analysis of the exosporium fraction showed that the exosporium fragments were intermixed with long spore appendages (Fig. 11A). SEM revealed that most of the spores lost their exosporium, as the spore coat ridges (usually covered by the exosporium) were evident (Chada *et al.*, 2003) (Fig. 11B and C). Few of the spores still maintained their exosporium, suggesting a strong connection between the exosporium and the spore (Steichen *et al.*, 2007).

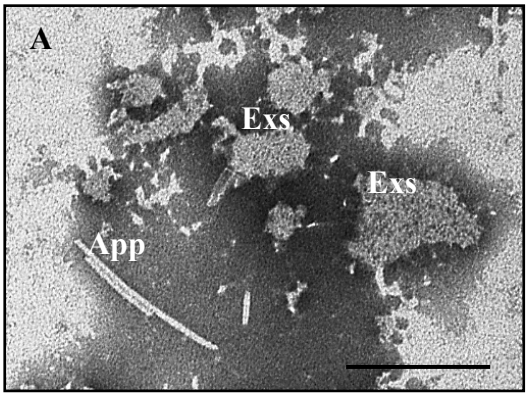

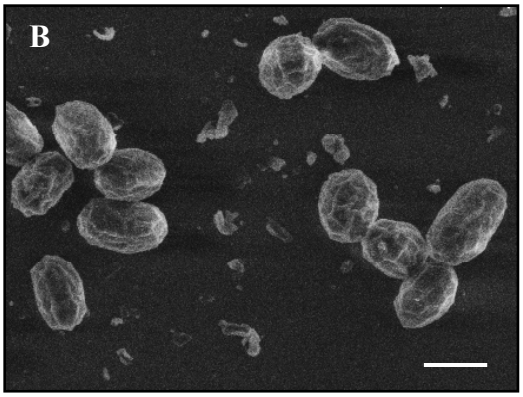

Fig. 11: Exosporium extraction by sonication. In A, negative staining electron micrographs showing the presence of spore appendages and exosporium fragments. App, appendages; Exs, exosporium fragments. Scale bar, 250 nm. In B, scanning electron micrograph of *B. cereus* ATCC 4342 sonicated spores. Scale bar, 1 μm.

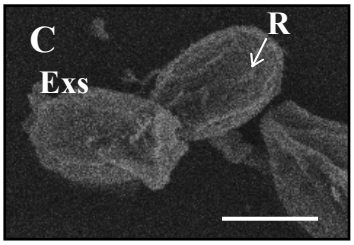

In C, scanning electron micrograph of a spore with exosporium (Exs) and a spore without exosporium, showing coat ridges (R). Scale bar, 1 μm.

Proteins in the exosporium sample were solubilized in Laemmli sample buffer (2% SDS and 0.5% β-mercaptoethanol), and then separated by 1-D SDS-PAGE (Fig. 12A), yielding a reproducible pattern. Then, proteins from highly stained bands were in-gel digested with trypsin, analyzed by liquid chromatography coupled with tandem mass spectrometry (LC-MS/MS), and identified with MASCOT search program. LC-MS/MS is a very sensitive technique that is appropriate for spore proteomics because it can identify individual proteins from a complex protein mixture, and can also detect hydrophobic proteins (Boydston *et al.*, 2005). The results obtained (Table 3) were similar to other proteomic studies performed on *B. cereus* and *B. anthracis* exosporium

preparations (Lai *et al.*, 2003; Redmond *et al.*, 2004; Steichen *et al.*, 2003; Todd *et al.*, 2003). Several components of the exosporium basal layer such as ExsY, CotY, ExsFA/BxpB and Alr were identified. Additionally, two hypothetical proteins identified (encoded in loci bcere0010_01680 and bcere0010_49400) had no homologs in the *B. subtilis* whose spores have no exosporium. Thus, these proteins were strong candidates to be putative exosporium proteins. Proteins identified as ribosomal proteins (ribosomal proteins: S10P, L7/L12, L15) were likely mother cell proteins adsorbed onto the exosporium, and therefore, did not represent true integral structural components.

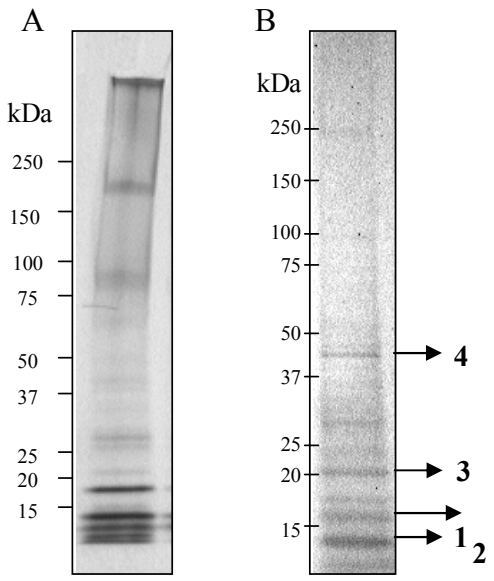

Fig. 12. Protein profile of exosporium extracted by sonication. A. *B. cereus* ATCC 4342 exosporium proteins were separated on a 4-20% SDS-PAGE and silver stained. B. Exosporium proteins were separated on a 4-15%SDS-PAGE and stained with Coomassie blue. Selected bands, indicated by arrows, were analyzed by LC-MS/MS. The molecular weight of each protein standard is indicated on the left.

Table 3: Proteins identified by LC-MS/MS from selected bands of 1D SDS-PAGE of *B. cereus* ATCC 4342 exosporium extracted by sonication.

band[a]	protein name	MW[b] (kDa)	pI	*B. cereus* ATCC 4342[c]	*B. cereus* ATCC 14579[c]	*B. anthracis* Ames[c]	*B. anthracis* Sterne[c]	description
4	Alr	43.6	5.84	bcere0010_02170	Bc_0264	Ba_0252	BAS0238	alanine racemase[d]
4	hyp protein[e]	35.5	8.99	bcere0010_45630	Bc_3712	Ba_3841	BAS3557	collagen-like protein
1, 2, 4	CotY	19.7	4.65	bcere0010_10880	Bc_1222	Ba_1238	BAS1145	exosporium protein[d]
3	CotE	20.4	4.39	bcere0010_35320	Bc_3770	Ba_3906	BAS3619	exosporium protein[d]
2, 3	ExsY	16.1	4.95	bcere0010_10840	Bc_1218	Ba_1234	BAS1141	exosporium protein[d]
2	ExsFA	17.3	4.29	bcere0010_10870	Bc_1221	Ba_1237	BAS1144	exosporium protein[d]
2	GerQ	16.1	5.27	bcere0010_51240	Bc_5391	Ba_5641	BAS5242	
2	hyp proteins[e]	17.6	4.99	bcere0010_01680	Bc_0212	Ba_0190	BAS0191	putative lipoprotein
1	thioredoxin	11.5	4.51	bcere0010_43060	Bc_4521	Ba_4758	BAS4417	
1	hyp protein (ExsM)	15.2	9.64	bcere0010_49400	Bc_5206	Ba_5438	BAS5053	Chordin (CHRD) domain

[a] Band apparent molecular weight: 4=43 kDa; 3=20 kDa; 2=17 kDa; 1=13 kDa. [b] MW, molecular weight; [c]NCBI locus tag

[d] exosporium characterized protein (references herein the text); [e] hypothetical protein

Exosporium protein extraction under reducing conditions

Analysis of a *B. cereus* ATCC 4342 exosporium preparation by SDS-PAGE in non-reducing conditions showed a remarkable change in the protein profile (Fig. 13), suggesting the presence of protein multimers stabilized by disulfide bonds.

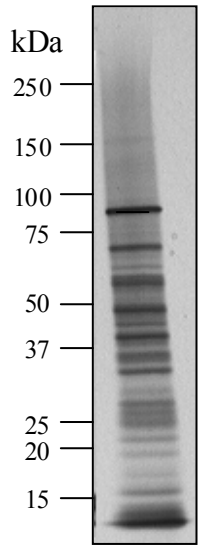

Fig. 13: Protein profile of exosporium in non-reducing conditions. Proteins were separated on a 4-15% SDS-PAGE in non-reducing conditions and silver stained. The molecular weight of each protein standard is indicated on the left.

Therefore, proteins were released from the spore surface by treatment with 2% β-mercaptoethanol under alkaline conditions. Before the extraction, purified spores were washed consecutively with high salt and an anionic detergent (SDS) to eliminate possible adsorbed proteins, including remnants of the mother cell. After β-mercaptoethanol treatment, the extracted proteins were separated from the spores by centrifugation and filtration. The treated spores were later examined by SEM, to confirm that this gentle extraction method did not alter the exosporium integrity and allowed the extraction of

mainly spore surface proteins, minimizing coat protein contamination (Fig. 14A). Analysis of the supernatant under negative staining TEM, showed the presence of spore appendages and soluble proteins, but not exosporium fragment as in the case of extraction by sonication (Fig. 14B).

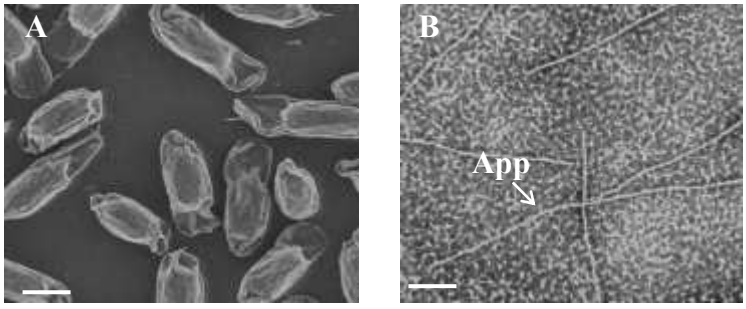

Fig. 14: Exosporium protein extraction with 2% β-mercaptoethanol. In A, scanning electron micrograph of *B. cereus* ATCC 4342 after β-mercaptoethanol treatment. Bar represents 1μm. In B, negative stained electron micrographs showing appendages and soluble exosporium protein. App, spore appendage. Bar represents 200 nm..

The extracted exosporium proteins were separated on a 1-D SDS-PAGE gel (Fig. 15). Comparison of the protein profiles from the sonication and β-mercaptoethanol extractions showed the presence of shared bands while others were unique to each treatment (Fig. 15A and B). Also, the intensity of the band corresponding to CotE is reduced in the β-mercaptoethanol profile, which coincides with a previous report that CotE may be localized on the interspace side of the exosporium instead the surface (Giorno *et al.*, 2007).

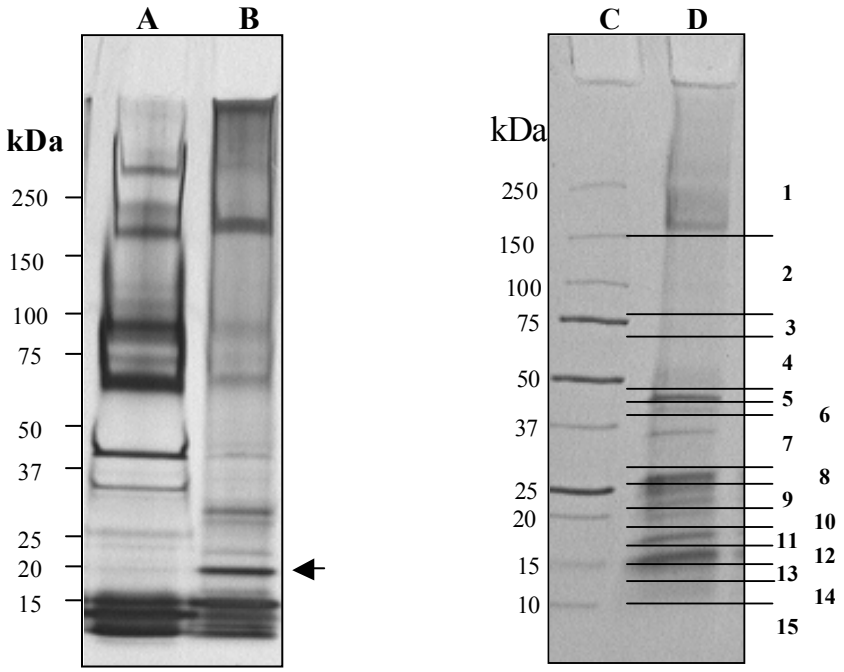

Fig. 15: Protein profile of exosporium protein extracted with β-mercaptoethanol. Lanes A and B. Exosporium proteins extracted with β-mercaptoethanol (A) or sonication (B) were run on a 4-20% SDS-PAGE and silver stained. The arrow marks the position of CotE. Lanes C and D. Protein weight standards (C), and exosporium proteins extracted with β-mercaptoethanol (D) were run on a 4-20% SDS-PAGE and stained with Coomassie blue. The numbers on the right indicate the gel slice that was analyzed by LC-MS/MS. The molecular weight of each protein standard is indicated on the left.

Mass spectrometry analysis

Identification of the proteins extracted by β-mercaptoethanol under reducing conditions was performed by LC-MS/MS, after trypsin in-gel digestion. In this case, the whole gel was divided in 15 slices and analyzed (Fig. 15D). The resulting peptide sequences were matched against a database containing *B. anthracis* and *B. cereus* genomes (Table 4).

Table 4: Proteins identified by LC-MS/MS from *B. cereus* ATCC 4342 exosporium extracted with 2% β-mercaptoethanol.

[a] MW, molecular weight; [b] NCBI locus tag

[c] exosporium characterized protein (references herein the text); [d] hypothetical protein

gel slice	protein name	MW [a] (kDa)	pI	*B. cereus* ATCC 4342 [b]	*B. cereus* ATCC 14579 [b]	*B. anthracis* Ames [b]	*B. anthracis* Sterne [b]	description
1	Rbp	221.1	4.23	bcere0010_34240	Bc_3546	Ba_3601	BAS3340	
2	BclC	52.1	3.86	bcere0010_20940	Bc_3345	Ba3841	BAS3557	Collagen-like protein
2	EA1	90.5	5.83	bcere0010_07850	---	Ba_0887	BAS0842	S-layer protein
3	ExsJ/BclB	32.8	4.3	bcere0010_22120	Bc_2382	Ba_2450	BAS2281	Exosporium protein [c]
4, 5, 6, 7	Alr	43.6	5.84	bcere0010_02170	Bc_0264	Ba_0252	BAS0238	Alanine racemase
4, 5, 6, 7, 8, 9, 10, 11, 12, 13	Cot B	16.7	6.59	bcere_0010_3100	Bc_0390	----	BAS0341	
4, 5, 6, 7, 8, 9, 10, 11, 12, 13	ExsK	32.8	4.3	bcere0010_22120	Bc_2493	Ba_2459	BAS2281	Exosporium protein [c]
4, 8, 9	ExsB	23.7	9.7	bcere0010_18510	Bc_3030	Ba_2045	BAS1898	
4, 5	PG-lytic enzyme	48.1	9.27	bcere0010_33640	Bc_607	Ba_3668	BAS3402	cortex-lytic
5, 6, 7, 9, 10, 13	cotE	20.4	4.39	bcere0010_35320	Bc_3770	Ba_3906	BAS3619	Exosporium protein [c]
6, 7	IunH	35.6	5.6	bcere0010_48710	Bc_2331	Ba_5338	BAS4961	Inosine-uridine hydrolase
8,12	hyp protein [d]	14.6	8.25	bcere0010_29950	Bc_3195	----	----	

Gel slice	protein name	MW [a] (kDa)	pI	*B. cereus* ATCC 4342 [b]	*B. cereus* ATCC 14579 [b]	*B. anthracis* Ames [b]	*B. anthracis* Sterne [b]	description
9	SODA1	22.6	5.31	bcere0010_40690	Bc_4272	Ba_4499	BAS4177	Superoxide dismutase
7, 10, 11, 12	hyp protein [d]	13.7	6.58	bcere0010_38120	Bc_4047	Ba_4266	BAS3957	
11	GerQ	16.1	5.27	bcere0010_51240	Bc_5391	Ba_5641	BAS5242	
11	ExsY	16.1	4.95	bcere0010_10840	Bc_1218	Ba_1234	BAS1141	Exosporium protein [c]
12	hyp protein [d]	24.5	9.7	bcere0010_42210	Bc_4419	Ba_4658	BAS4323	Cortex lipoprotein
12	thioredoxin	4.51	11.5	bcere0010_43060	Bc_4521	Ba_4758	BAS4417	
12	hyp protein (ExsM)	15.2	9.64	bcere0010_49400	Bc_5206	Ba_5438	BAS5053	CHRD domain
13	Csp	7.3	4.84	bcere0010_53280	Bc_3539	Ba_3594	BAS3333	Cold shock protein
13	hyp protein [d]	11.2	9.97	bcere0010_23240	Bc_2481	Ba_2545	BAS2367	*B. cereus* group protein
13	hyp protein [d]	9.7	4.23	bcere0010_22100	Bc_2375	Ba_2431	BAS2264	*B. cereus* group protein
14, 15	SASP	6.8	6.13	bcere0010_44320	Bc_4646	Ba_4898	BAS4544	Small acid soluble protein
14	SASP	7.2	8.21	bcere0010_17940	Bc_1984	Ba_1987	BAS1844	Small acid soluble protein
14	hyp protein [d]	9.3	4.74	bcere0010_35460	Bc_3784	Ba_3920	BAS3634	similar IG 16623
14	SASP	6.5	9.4	bcere0010_11710	Bc_1311	Ba_1324	BAS1225	Small acid soluble protein

Two collagen-like proteins, BclC and ExsJ/BclB and a novel cell surface protein, reticulocyte binding protein (Rbp), were identified on *B. cereus* ATCC 4342 exosporium. BclA was not found in this exosporium preparation, as it extensive glycosylation makes mass spectrometry analysis difficult (Sylvestre *et al.*, 2002). Other proteins such as ExsK, CotB, CotE, SODA1, Alr, IunH have been already reported as components of *B. anthracis* and *B. cereus* ATCC 10789 exosporium preparations (Lai *et al.*, 2003; Redmond *et al.*, 2004; Steichen *et al.*, 2003; Todd *et al.*, 2003). ExsK, CotB and CotE were found across several gel slices, suggesting that they formed protein complexes with other exosporium proteins (Steichen *et al.*, 2005). While ExsF and CotY were present in the exosporium sample extracted by sonication, they were not identified in exosporium extracted by β-mercaptoethanol treatment, indicating that 2% β-mercaptoethanol treatment is not solubilizing all of the basal layer proteins. This result agrees with the integrity of the exosporium of β-mercaptoethanol treated spores as seen under SEM (Fig. 14A). Thioredoxin, an enzyme that allows disulfide bond formation (Kadokura *et al.*, 2003), was also found for the first time in the exosporium suggesting that some of the disulfide bonds between exosporium proteins may be enzymatically catalyzed (Fig. 13). In addition, several hypothetical proteins with no orthologs in *B. subtilis* were identified. Only one of these proteins, encode in locus bcere0010_49400, was also found in the sonication sample. This protein was named ExsM and its characterization is described later in this work. Hypothetical protein encoded in the bcere0010_ 29950 locus is only present in *B. cereus* strains but not in *B. anthracis*. Also, CotB is not encoded in *B. anthracis* Ames and *B. cereus* ATCC 10789. Interestingly, several SASP proteins that are

usually synthetized and located in the core were found in the exosporium fraction, as well as cortex proteins.

Comparison of exoporium profiles between *B. cereus* and *B. anthracis*

Equal number of *B. cereus* ATCC 14579, ATCC 10789, ATCC 4342 and *B. anthracis* ΔSterne spores were sonicated or treated with 2% β-mercaptoethanol to isolate exosporium proteins. The protein profiles obtained showed little co-migration of proteins between *B. cereus* strains and *B. anthracis* in both sonication and β-mercaptoethanol samples (Fig. 16A and B). The differences observed between the profiles originated from: 1- the presence of strain specific proteins on the spore surface, 2- variability in the processing of common proteins and 3- protein polymorphisms between strains and species. In particular, the differences were bigger in the case of comparison with the *B. anthracis* profile. *B. cereus* strains also showed a prominent band after glycoprotein staining, which was absent in *B. anthracis* (Fig. 16C). Although this protein, ExsJ/BclB, has been previously characterized as a component of *B. anthracis* exosporium (Thompson *et al.*, 2007), its expression or extractability may be lower than in the *B. cereus* exosporium. In all, these results showed that the surface of spores is highly heterogenous, especially when comparing *B. anthracis* to *B. cereus* strains, probably reflecting adaptations to different environments and lifestyles.

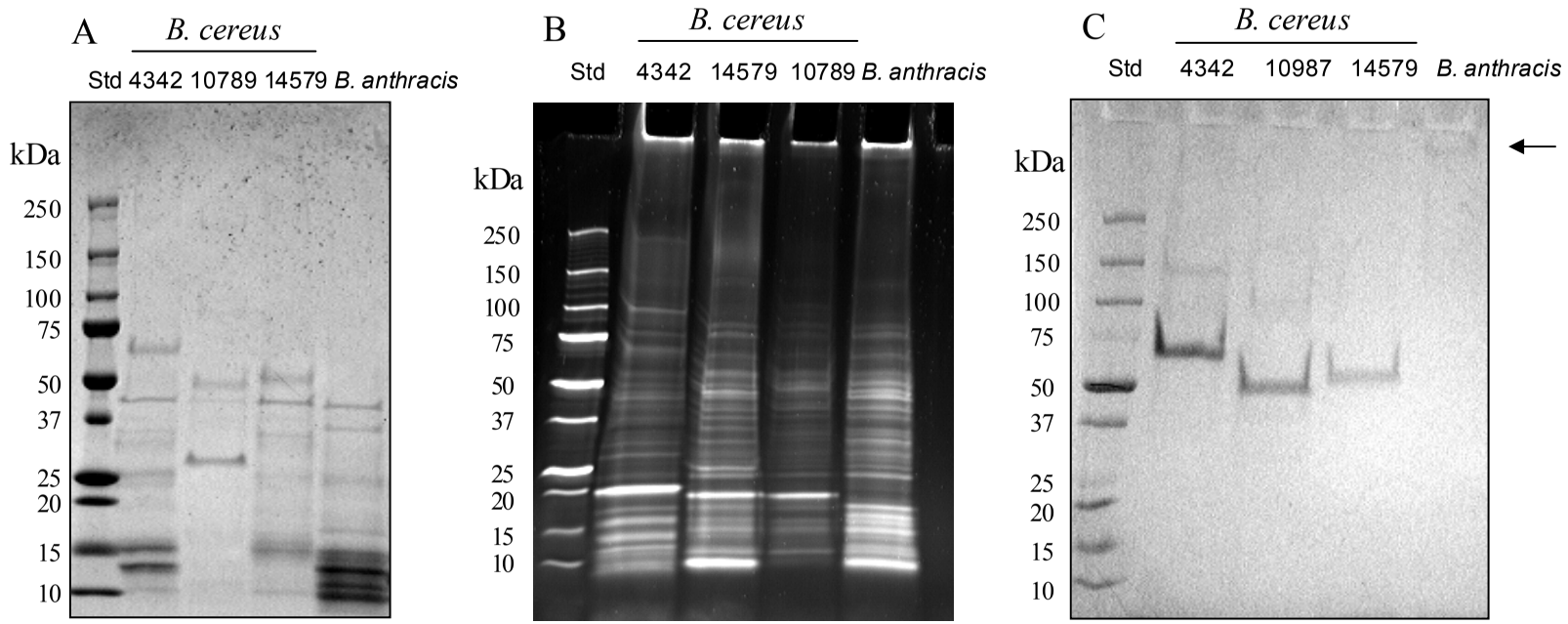

Fig. 16: Comparison of exosporium protein profiles between *B. cereus* strains and *B. anthracis*. In A, exosporium proteins were extracted with β-mercaptoethanol, run on a 4-20% SDS-PAGE and stained with Coomassie blue. In B, exosporium proteins were extracted by sonication, run on a 4-20% SDS-PAGE and stained with Sypro Ruby. In C, exosporium proteins were extracted with β-mercaptoethanol, run on a 4-20% SDS-PAGE. Glycoproteins were detected with a glycoprotein detection kit. The arrow indicates a faint glycoprotein band in the *B.anthracis* lane. Std, protein weight standards. The molecular weight of each protein standard is indicated on the left.

Proteins from the exosporium of *B. cereus* ATCC 14579 were extracted with 2% β-mercaptoethanol and separated by SDS-PAGE. The gel was then divided into slices and after in-gel trypsin digestion (Fig. 17), the proteins were identified by LC-MS/MS (Table 5). A core of proteins were conserved between *B.cereus* ATCC 4342 and *B. cereus* ATCC 15479 such as Rbp, Alr, CotB, CotG/ExsB, CotE and Iunh. In addition, several hypothetical proteins encode in loci Bc_0996, Bc_2267, Bc_0843 and Bc_5456 were only identified in *B. cereus* ATCC 14579. A novel collagen-like protein, Bc_3526 was also found in this exosporium preparation. The variability in the composition of *B. cereus* ATCC 14579 and *B. cereus* ATCC 4342 agreed with the variability observed when the exosporium protein profiles of these *B. cereus* strains were compared.

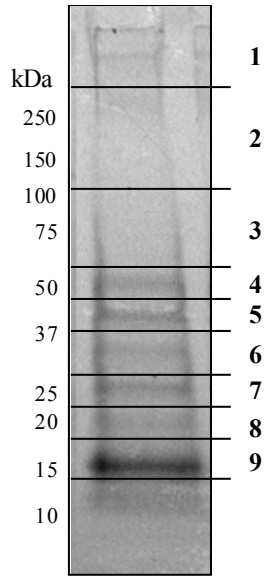

Fig. 17: Protein profile of *B. cereus* ATCC 14579 exosporium. Proteins were extracted with 2% β-mercaptoethanol, run on a 4-20% SDS-PAGE and stained with Coomassie blue. The numbers on the right indicate the gel slice that was analyzed by LC-MS/MS. The molecular weight of each protein standard is indicated on the left.

Table 5: Proteins identified by LC-MS/MS from *B. cereus* ATCC 14579 exosporium.

Gel slice	Protein name	MW [a] kDa	pI	*B. cereus* ATCC 14579 [b]	*B. cereus* ATCC 4342 [b]	*B. anthracis* Ames [b]	*B. anthracis* Sterne [b]	description
1, 2	Rbp [c]	163.2	3.95	BC_3546	bcere0010_34240	Ba_3601	BAS3340	Reticulocyte binding protein
1	Adhesion protein	120	6.48	BC_3526	bcere0010_48390	Ba_5258	BAS4884	Collagen-like protein
1	hyp protein [e]	17.9	8.98	BC_5456	bcere0010_51900	Ba_5708	BAS5312	
3	hyp protein [e]	32.7	6.91	BC_1280	bcere0010_11390	Ba_1289	BAS1193	
4, 5, 9	CotB1	19.2	5.32	BC_0389	bcere0010_3090	-----	BAS0340	
4, 5, 6, 7, 9, 10	CotB2 [c]	16.8	6.52	BC_0390	bcere0010_3100	-----	BAS0341	
4, 5	Alr [c]	43.7	5.35	BC_0264	bcere0010_2170	Ba_0252	BAS0238	Alanine racemase
4, 10	hyp protein [e]	40.5	5.94	BC_0843	bcere0010_7300	Ba_0824	BAS0785	Outer surface protein
6	IunH [c]	36.2	5.42	BC_2889	bcere0010_48710	Ba_5338	BAS4961	Inosine-uridine hydrolase

Gel slice	Protein name	MW [a] kDa	pI	*B. cereus* ATCC 14579 [b]	*B. cereus* ATCC 4342 [b]	*B. anthracis* Ames [b]	*B. anthracis* Sterne [b]	description
7, 10	ExsB	22.9	9.64	BC_2030	bcere0010_18510	Ba_2045	BAS1898	
8, 9	hyp protein [e]	21.5	21.5	BC_2267	bcere0010_22940	Ba_2334	BAS2176	
8	CotE [c]	20.3	4.42	BC_3770	bcere0010_35320	Ba_3906	BAS3619	Exosporium protein [d]
9, 10	hyp protein [c e]	14.7	8.33	BC_3195	bcere0010_29950	----	----	
9	hyp protein [e]	15.4	6.5	BC_0996	bcere0010_51810	Ba_5699	BAS5303	

[a] MW, molecular weight; [b]NCBI locus tag

[c] protein identified in *B. cereus* 4342 exosporium; [d] exosporium characterized protein (references herein the text);

[e] hypothetical protein

Characterization of *B. cereus* mutant spores

From the list of proteins identified in *B. cereus* ATCC 4342 exosporium, a few were selected to inactivate their respective encoding genes. The hypothetical proteins encoded in locus*:* bcere0010_22100, bcere0010_38120, bcere0010_29950, bcere0010_42210 have no homologs outside the *B. cereus* group and thus, they are good candidates for exosporium proteins. Additionally, ExsK and GerQ have been identified in other proteomics studies but have not been characterized. It has been previously reported that exosporium proteins may have more than one localization in the spore (Moody *et al.*, ; Severson *et al.*, 2009). Therefore, two SASP and the putative cortex protein encoded in locus bcere0010_42210 were also chosen to study their role in the exosporium. All knockouts were generated by insertional mutagenesis directed to the first 200 bp of their respective coding sequences. The resulting mutant strains were named as indicated in table 4. This strains were sporulated, and the mutant spores were visualized under TEM and SEM to study their morphology.

Table 6: *B. cereus* mutant strains.

Strain	*B. cereus* ATCC 4342 locus inactivated	protein name
MF20	becer0100_44320	SASP
MF22	becer0100_22100	hypothetical protein
MF24	becer0100_42210	hypothetical protein
MF26	becer0100_22120	ExsK
MF28	becer0100_38120	hypothetical protein
MF30	becer0100_51240	GerQ
MF33	becer0100_29950	hypothetical protein

Ultrastructural analysis

Under SEM, none of the mutant spores had major defects in their exosporium (Fig. 18). The morphology of the mutant spores were similar to wild-type spores in all the cases, and they all possessed appendages on their surface. In addition, there were no visible changes in the outer surface of the spores. With the exception of MF20 and MF31, the structure (including the exosporium) of the mutant spores was normal when studied by thin-section TEM (Fig. 19). The cortex of MF20 spores stained lighter than the cortex of wild-type spores, and the spores spontaneously turned phase gray, as seen under phase-contrast microscopy, due to loss of DPA (dipicolinic acid, data not shown), indicating that MF20 spores had a defective cortex. These observations were in agreement with the prediction that the hypothetical protein encoded in locus bcere0010_42210 is a cortex lipoprotein that could be participating in the attachment of the cortex to either the inner or outer membrane of the spore. In addition, spore preparations of MF23 (GerQ deficient strain) showed a more fragile exosporium than wild-type. In *B. subtilis*, GerQ is a coat protein that is crosslinked by transglutaminase (Tgl) (Ragkousi and Setlow, 2004), suggesting that *B. cereus* GerQ is also crosslinked in the exosporium. Thus, the lack of crosslinking may affect the structural stability of the exosporium in the GerQ deficient spores.

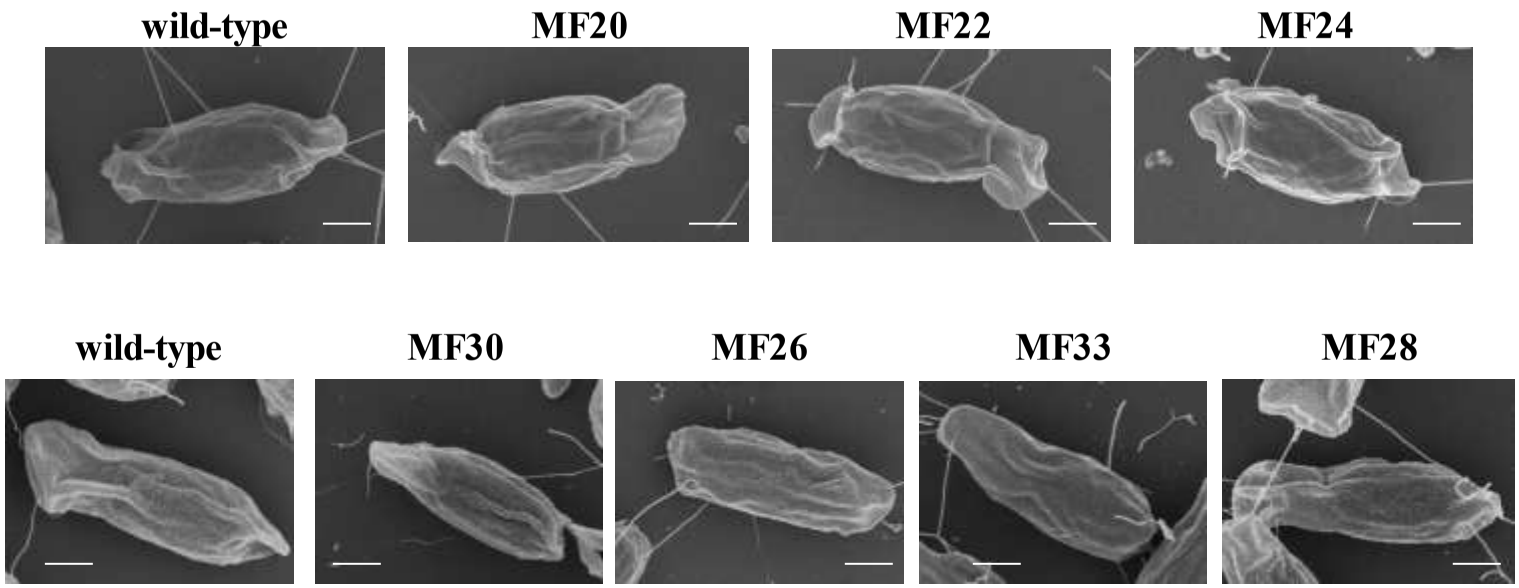

Fig. 18: Scanning electron micrographs of *B. cereus* mutant spores. *B. cereus* ATCC 4342 (wild-type) spores and mutant spores were analyzed under SEM.

Scale bar, 1μm.

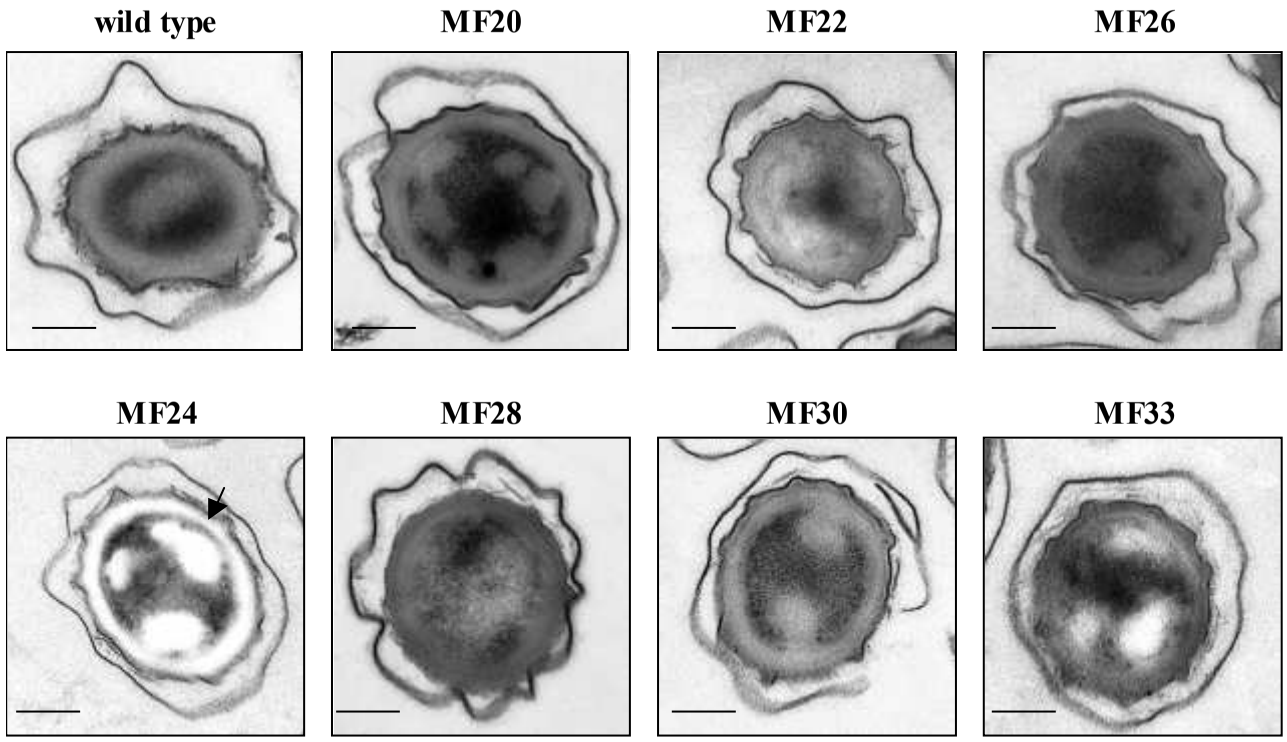

Fig. 19: Transmission electron micrographs of *B. cereus* mutant spores. *B. cereus* ATCC 4342 (wild-type) and mutant spores were analyzed under TEM. The arrow points to the cortex of MF24 spore. Scale bar, 500 nm.

Exosporium protein profiles

Proteins from mutant exosporiums were extracted with 2% β-mercaptoethanol under alkaline conditions, and were run on a 1-D SDS-PAGE. The resulting protein profiles of the mutant exosporiums did not show any major reproducible differences when compared to wild-type (Fig. 20). This result was expected as the mutant spores had a complete exosporium in all cases. Interestingly, there were also no protein bands missing in any of the profiles, probably because there were other exosporium proteins migrating in the same position.

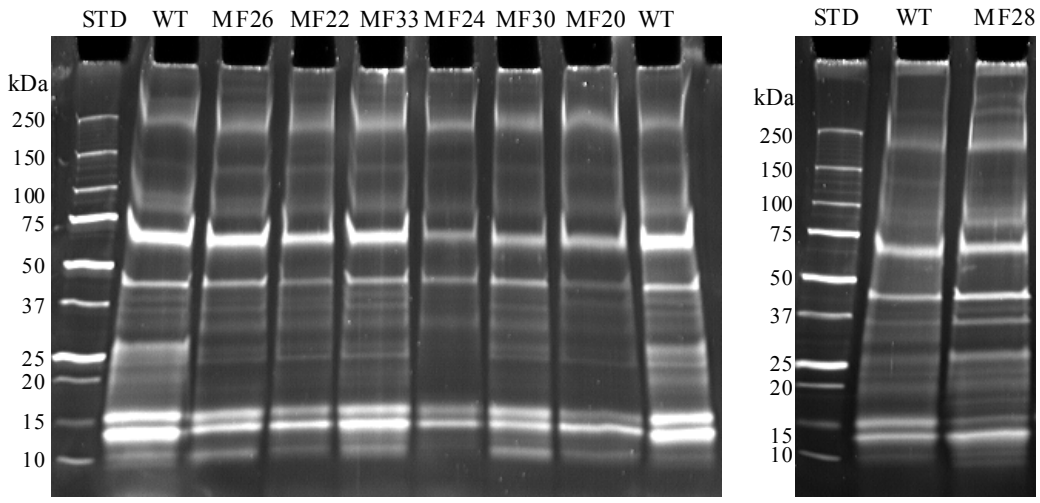

Fig. 20: Exosporium protein profiles of spore mutants. *B. cereus* ATCC 4342 (wt) and mutant exosporiums were extracted with 2% β-mercaptoethanol and run on a 4-20% SDS-PAGE. Proteins were stained with Sypro Ruby. Std, protein weight standards. The molecular weight of each protein standard is indicated on the left.

Sporulation rate

The sporulation rates of wild-type and mutant strains were assessed by plating serial dilutions of bacteria culture onto sporulation media, and then exposing the bacteria to chloroform vapors at differents time points. The chloroform only kills vegetative bacteria but not spores, so the number of colonies after treatment represents the amount of spores present in the culture at each time point. Most of the mutants showed sporulation rates similar to wild-type, with a small delay at 18 h (Fig. 21). MF22 had a slower sporulation rate than wild-type, with a spore yield that was two and three orders of magnitude lower than wild-type at 18 h and 24 h time points, respectively. However, sporulation was not blocked, as MF22 sporulation reached wild-type levels after 48 hs.

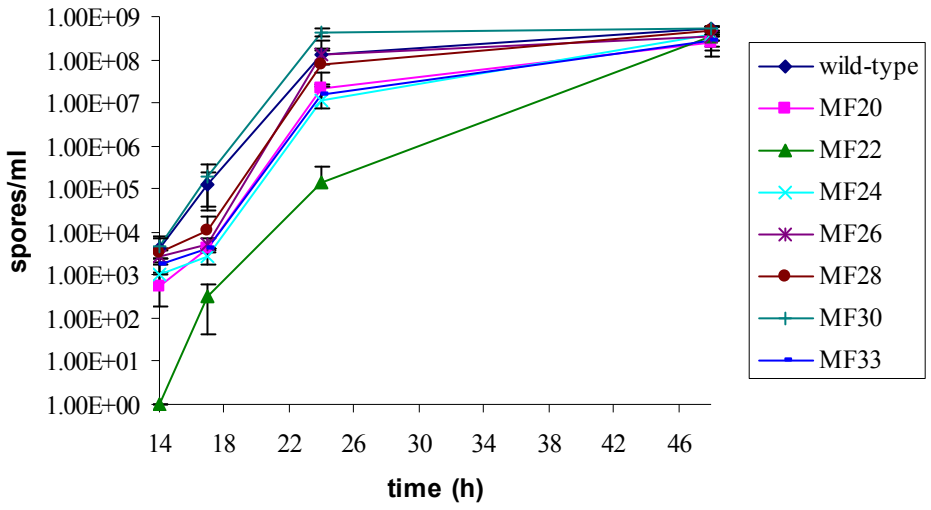

Fig. 21: Sporulation rate. *B. cereus* ATCC 4342 (wild-type) and mutant strain sporulation rate was studied by exposure to chloroform vapors at 14 h, 17 h, 24 h and 48 h after plating onto sporulation media.

B. anthracis spore mutants

To study if the roles of GerQ (BAS5242) and the cortex lipoprotein (BAS4323) were conserved in *B. anthracis*, the respective genes were inactivated by insertional mutagenesis in the non-pathogenic strain, *B. anthracis* ΔSterne. The resulting mutant strain for *gerQ* was called MF61, and the null mutant for BAS4323, MF46. *B. anthracis* GerQ has an 88% similarity with *B. cereus* GerQ and the chromosomal region surrounding *gerQ* locus are also very similar in both organisms. Thin-section TEM revealed that MF61 spores had a collapsed and brittle exosporium (Fig. 22B). In addition, several exosporium fragments that had detached from the spores were observed (Fig 22C). Therefore, like in *B. cereus*, *B. anthracis* GerQ was important for exosporium integrity.

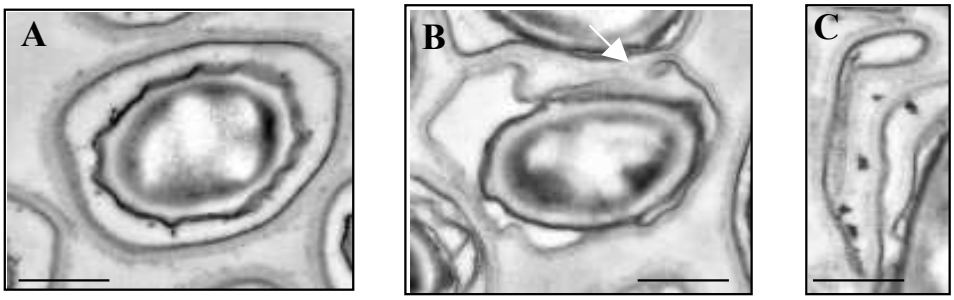

Fig. 22: Transmission electron micrograph of MF61. *B. anthracis* ΔSterne (A) and MF61 (B) were contrasted with Alcian blue to visualized the 'hair-like' nap on the surface of the exosporium. The arrow points to a broken exosporium. In C, fragment of exosporium lost from MF61 spores. Scale bar, 250 nm.

The cortex lipoprotein BAS4323 is 98% similari to bcere0010_42210, and their chromosome regions are also highly syntenic. The MF46 spores, deficient in BAS4323, presented a thinner cortex when studied under TEM; thus, repeating the *B. cereus* mutant phenotype (Fig. 23B).

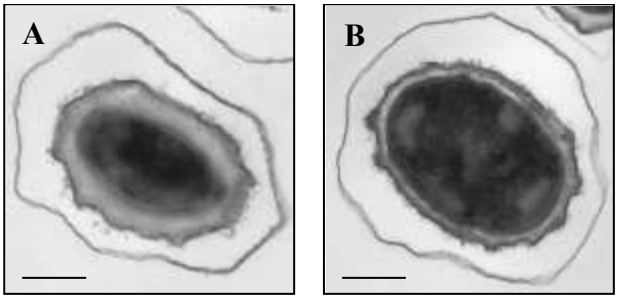

Fig. 23: Transmission electron micrograph of MF46. A. *B. anthracis* ΔSterne wild-type. B. MF46 spores. Scale bar, 250 nm.

Also, we tested whether inactivation of the gene BAS2264 (*B. anthracis* homolog for bcere0010_22100) affected the rate of sporulation when measured by chloroform vapors exposure. In this case, the slow sporulation phenotype observed in *B. cereus* was also seen in the *B. anthracis* background (Fig. 24), although the differences were seen at 14 and 18 h after plating in sporulation media.

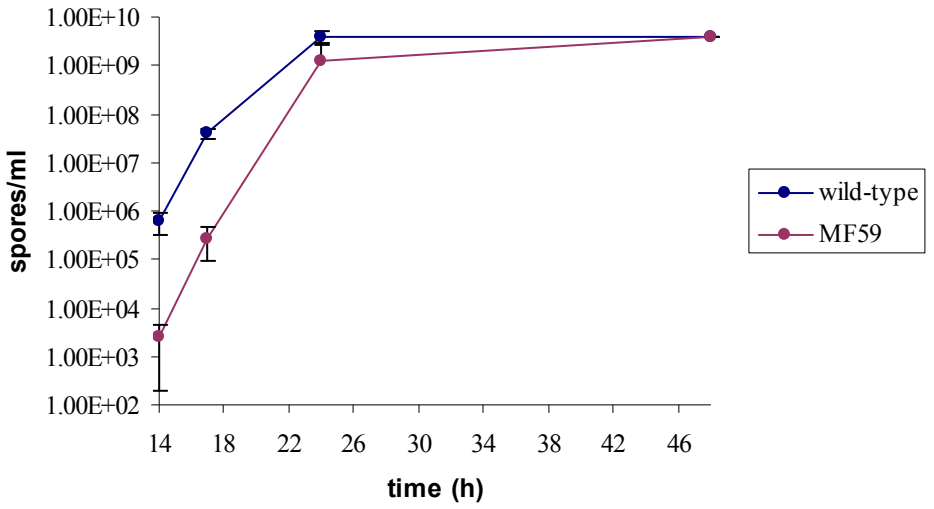

Fig. 24: Sporulation rate of MF59. Sporulation rate of *B. anthracis* ΔSterne (wild-type) and MF59 was measured at 14 h, 17 h, 24 h, 48 h time points.

Role of transglutaminase in exosporium maturation

Absence of GerQ during sporulation resulted in a fragile exosporium, suggesting that crosslinking of exosporium proteins provide mechanical resistance. As aforementioned, *B. subtilis* GerQ is crosslinked by Tgl in the spore coat (Ragkousi and Setlow, 2004). Tgl activity provides rigidity and resistance to degradation to the spore coat, and probably to the exosporium. To assess the role of Tgl in exosporium crosslinking, the enzyme was inhibited during sporulation, and the resulting exosporium protein profile was analyzed.

Tgl catalyzes the formation of an isopeptide bond between a lysine donor residue in one protein and the acceptor glutamine residue from the same or another protein (Lorand and Graham, 2003). To inhibit Tgl activity, sporulation plates were supplemented with monodansylcadaverine (MDC), a competitor inhibitor that mimics the lysine donor. Spores formed in the presence of MDC were harvested and washed and their exosporiums were extracted with 2% β-mercaptoethanol and separated by 1-D SDS-PAGE. MDC had a dose-dependent effect on solubilization of exosporium proteins (Fig. 25). A series of low molecular weight bands appeared with higher concentrations of MDC and overall, the efficiency of protein extraction increased with MDC treatment. However, high molecular weights bands were not affected by Tgl inactivation. Several types of crosslinking, such us O-O' dityrosine crosslinking, may stabilize high molecular weight complexes; hence, the lack Tgl activity may not be sufficient to break them apart. In all, Tgl may participate in exosporium assembly and maturation by crosslinking small proteins and processed peptides, which may provide structural stability and resistance to degradation to the spore surface.

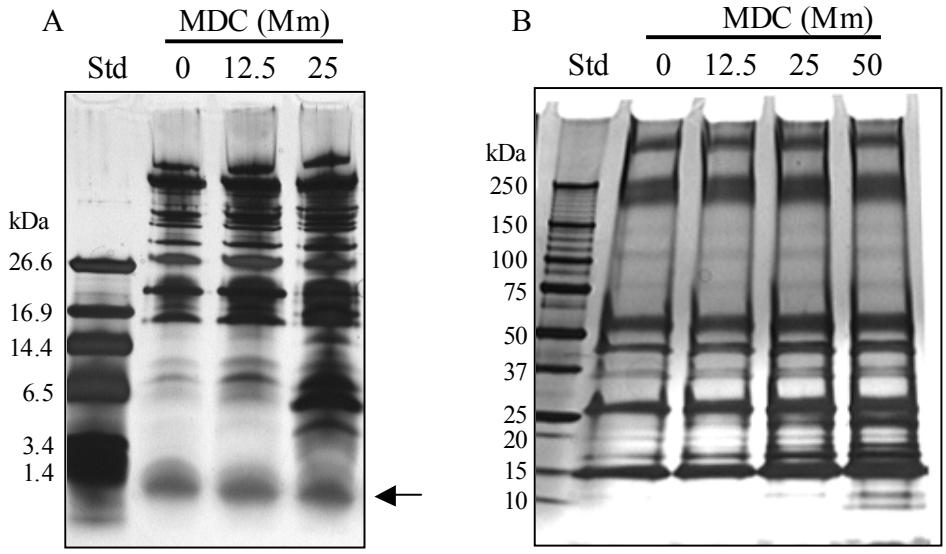

Fig. 25: Inhibition of Tgl. Exosporium proteins were extracted with 2% β-mercaptoethanol from *B. cereus* ATCC 4342 sporulated in media containing the indicated concentration of MDC. A. 16.5% Tricine SDS-PAGE, silver stained. The arrow indicates the gel front. B. 4-20% SDS-PAGE, silver stained. Std, protein weight standards. The molecular weight of each protein standard is indicated on the left.

Characterization of reticulocyte binding protein

BclA, a collagen-like protein, has been described as the main component of the hair-like nap (Sylvestre *et al.*, 2002). Other collagen-like proteins, BclB/ExsJ, BclC, BclD and BclE, have also been identified in the genome of *B. anthracis* and *B. cereus* (Leski *et al.*, 2009). BclB/ExsJ plays a role in exosporium integrity; the role in exosporium function and structure of BclC and BclD has not been studied yet. Rbp (reticulocyte binding protein) is an uncharacterized cell surface protein present in the exosporium of *B. cereus* ATCC 4342, *B. cereus* ATCC 14579 and also *B. cereus* 10789

(data not shown). To study the role of Rbp on the exosporium, *B. cereus* ATCC 4342 *rb*p null mutants were constructed by insertional mutagenesis, and the resulting *rbp* spores were visualized under TEM and SEM. The *rbp* mutant strain was named MF38.

TEM revealed that *rbp* mutant spores were devoid of the hair-like nap typical of the exosporium (Fig. 26B). In addition, the MF38 spores associated more tightly with the SEM grid than wild-type spores, which agreed with changes on the surface of these spores (Fig 26D). Thus, Rbp could be a new component of the exosporium nap or could have a role in the assembly of BclA. Futher experiments, such us immunoelectromicroscopy with antibody against Rbp and BclA, are necessary to clarify the role of Rbp in nap formation.

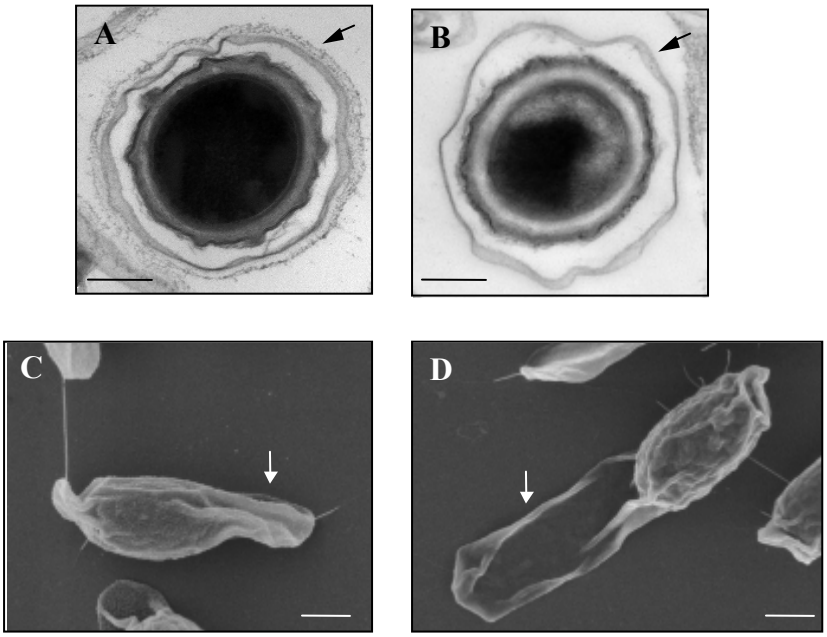

Fig. 26: Electron micrographs of MF38 spores. A and B. Transmission electron micrographs of *B. cereus* ATCC 4342 (A) and MF38 (B) spores, contrasted with Alcian Blue. The arrows mark the presence (A) or absence (B) of the hair-like nap. Scale bar, 250 nm. C and D. Scanning electron micrographs of *B. cereus* ATCC 4342 (C) and MF38 (D) spores. The arrows indicates the difference in interaction with the SEM grid between wild-type and mutant spores. Scale bar, 500 nm.

Besides a missing band that likely corresponded to Rbp, the rest of the protein profile of the Rbp mutant exosporium did not have any other differences when compared to the wild-type exosporium. Then, lack of Rbp only affected assembly of the nap but not the rest of the exosporium (Fig. 27).

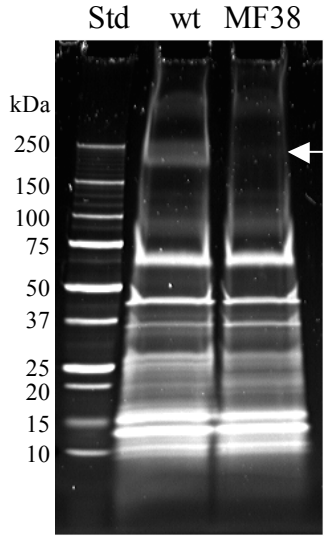

Fig. 27: Exosporium protein profile of MF38 spores. *B. cereus* ATCC 4342 (wt) and MF38 exosporiums were extracted with 2% β-mercaptoethanol, run on a 4-20% SDS-PAGE and stained with Sypro Ruby. The arrow marks Rbp putative position. Std, protein weight standards. The molecular weight of each protein standard is indicated on the left.

To study the adhesion properties of Rbp, we compared pellicle formation between *B. cereus* ATCC 4342 and MF38 strains. A pellicle is a biofilm produce on the liquid/air interface of an standing culture and consists on vegetative bacteria and spores embedded in an extracellular matrix composed of protein, DNA and extracellular polysaccharide (EPS) (Wijman et al., 2007). Thus, interaction of the spore surface with EPS is important for establishment and maintenance of the biofilm. After 3 days of culture in LD standing media, *B. cereus* ATCC 4342 pellicle was visible, but MF38 bacteria did not form a pellicle (Fig. 28A). After 10 days of culture, a dense pellicle had grown on the liquid/air

interface of both strains cultures (Fig. 28B). While wild-type strain pellicle contained mainly spores, MF38 pellicle was composed mainly of vegetative cells and sporangias (Fig. 28C). In conclusion, *rbp* null mutant strains had a delay in the formation of pellicle, which could be related to an altered interaction between mutant spores and EPS.

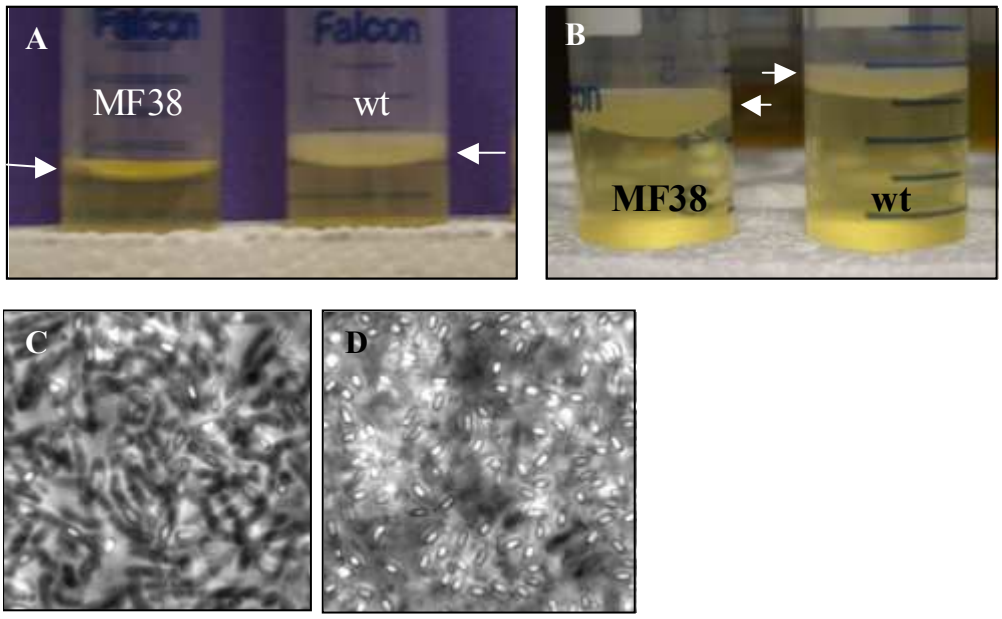

Fig. 28: Pellicle formation. Formation of pellicle in standing culture in LD media. In A, 3 days old MF38 or *B. cereus* ATCC 4342 (wt) pellicle. In B, 10 days old MF38 or *B. cereus* ATCC 4342 (wt) pellicle. Arrows point to pellicles. In C, phase contrast micrographs of 10 day old MF38 (C) and wild-type (D) pellicle (1000X).

Results: Characterization of ExsM, a novel exosporium protein

Identification of ExsM

ExsM was identified from a proteomic analysis of *B. cereus* ATCC 4342 exosporium extracted with 2% β-mercaptoethanol treatment under alkaline conditions (Table 4). From the list of putative proteins obtained, an uncharacterized protein (becer0010_49400) was identified within a prominent band running at 12 kDa, which also contained ExsK, CotB and other hypothetical proteins. Interestingly, this protein was also identified by LC-MS/MS in a *B. cereus* ATCC 4342 exosporium sample extracted by sonication (Table 3). This protein was a good candidate to be part of the exosporium as it has no homolog in *B. subtilis*, whose spores do not have a conspicuous exosporium separated by an interspace. We decided to call it ExsM, following the nomenclature established by Todd *et al*. (Todd *et al.*, 2003), and pursue its study.

ExsM is a small basic protein with a theoretical molecular weight of 15.4 kDa, which differs from its apparent molecular weight of 12 kDa, possibly due to processing or partial degradation. It is encoded by a monocistronic operon and contains a CHRD domain. CHRD is a recently defined protein motif identified in Chordin, a key developmental protein in vertebrates that, in simple terms, dorsalizes early embryonic tissues (Hyvonen, 2003). Actually, the entire ExsM sequence constitutes the CHRD domain, with a positively charged, conserved C-terminal. As yet, there is no functional prediction for CHRD domain (Fig. 29).

```
  1 ttcgtaatta acacttgaaa aagtcataaa tgattatgta taaaccataa agtagtagaa
 61 gtagtgctgg gaaatttata taaggagaat gcccgtatga caacacattt ctttgcgagg
121 ttaacaggta agagggaaat acccccctgta aatacagaag cttatggcgt agcagagttt
181 atatttagtg aggatttaaa gaagttgcaa tatcgggtca tattgaaaaa catcgaaaaa
241 gttacatcat gccaaattca tttagggaaa gcagatcaaa ttggtccaat tgttttaagt
301 ttatttggtc cattaaagca aggtattagt gtaaatgaag gggtcgtcac tggtgtagtt
361 aatgtggggg attttgaagg acctttacag gggcgagcgt ttgatagctt acttcaagaa
421 atcattcagg cgaatgtata tgtaaatgtt tatacgaagt cccataagaa gggcgaaata
481 agggggagaa ttaggaaagt aaagaagtag aaaaaaggct gtccatattt tggaacagcc
```

Fig. 29A: *B. cereus* ATCC 4342 *exsM* sequence. Consensus sequence for σ^E (Eichenberger *et al.*, 2004) is highlighted in blue and *exsM* sequence is highlighted in yellow.

```
  1  MTTHFFARLT GKREIPPVNT EAYGVAEFIF SEDLKKLQYR VILKNIEKVT SCQIHLGKAD
 61  QIGPIVLSLF GPLKQGISVN EGVVTGVVNV GDFEGPLQGR AFDSLLQEII QANVYVNVYT
121  KSHKKGEIRG RIRKVKK
```

Fig. 29B: *B. cereus* ATCC 4342 ExsM sequence. Red colored amino acids correspond to highly conserved residues in the CHRD domain (Hyvonen, 2003).

Localization of ExsM-GFP during sporulation

To study the subcellular localization of ExsM, we constructed a C-terminal in-frame fusion with a GFP coding sequence (Webb *et al.*, 1995), which was incorporated into the *B. cereus* ATCC 4342 genome by allelic replacement. Expression of the ExsM-GFP fusion was then followed at different time-points, before and during sporulation. To localize the forespore and estimate the stage of sporulation by phase-contrast microscopy, cell membranes were stained with the membrane stain FM4-64.

ExsM-GFP fluorescence was detected only during sporulation, shortly after the beginning of forespore engulfment. Furthermore, fluorescence was restricted to the mother cell, with no visible fluorescence in the forespore. Three hours after the start of sporulation, the ExsM fusion was localized at the forespore pole facing the middle of the mother cell (Fig. 30A). At 5 h, the ExsM fusion was then found at both poles of the forespore. At 6 h, as the nascent spore became visible by phase-contrast microscopy, the fluorescence intensified at the poles. At 8 h, ExsM-GFP unevenly surrounded the whole circumference phase-bright spore still inside the mother cell. It was not possible to localize ExsM-GFP on the mature spore once released from the mother cell, which showed no fluorescence. Western blots probed with anti-GFP IgG showed that at 10 h after sporulation, there was a sharp decrease in the signal for ExsM-GFP. This coincided with the sharply increased in intensity of a 27 kDa band, which matched the molecular weight of GFP. This suggests that ExsM was either processed or degraded during lysis of the mother cell or the GFP was cleaved from ExsM-GFP complex at this stage (data not

shown). The cleavage of GFP from a GFP-protein complex during sporulation is not uncommon and has been reported with other spore protein-GFP fusion proteins (Kim *et al.*, 2006). To diminish the action of sporulation specific proteases, sporulation was carried at 25°C; in this case, we were able to detect fluorescence from ExsM-GFP on the exosporium of mature spores (Fig. 30B).

The dynamic pattern of ExsM-GFP localization, starting at the forespore pole closer to the middle of the mother cell and moving towards the opposite pole, is shared with other outer-spore proteins (Kim *et al.*, 2006; Thompson and Stewart, 2008). This agrees with the presence of a putative σ^E promoter sequence upstream of *exsM* (Eichenberger *et al.*, 2004). CotE and ExsA, two proteins that participate during the formation of the exosporium, are also under the control of σ^E (Bailey-Smith *et al.*, 2005; Giorno *et al.*, 2007).

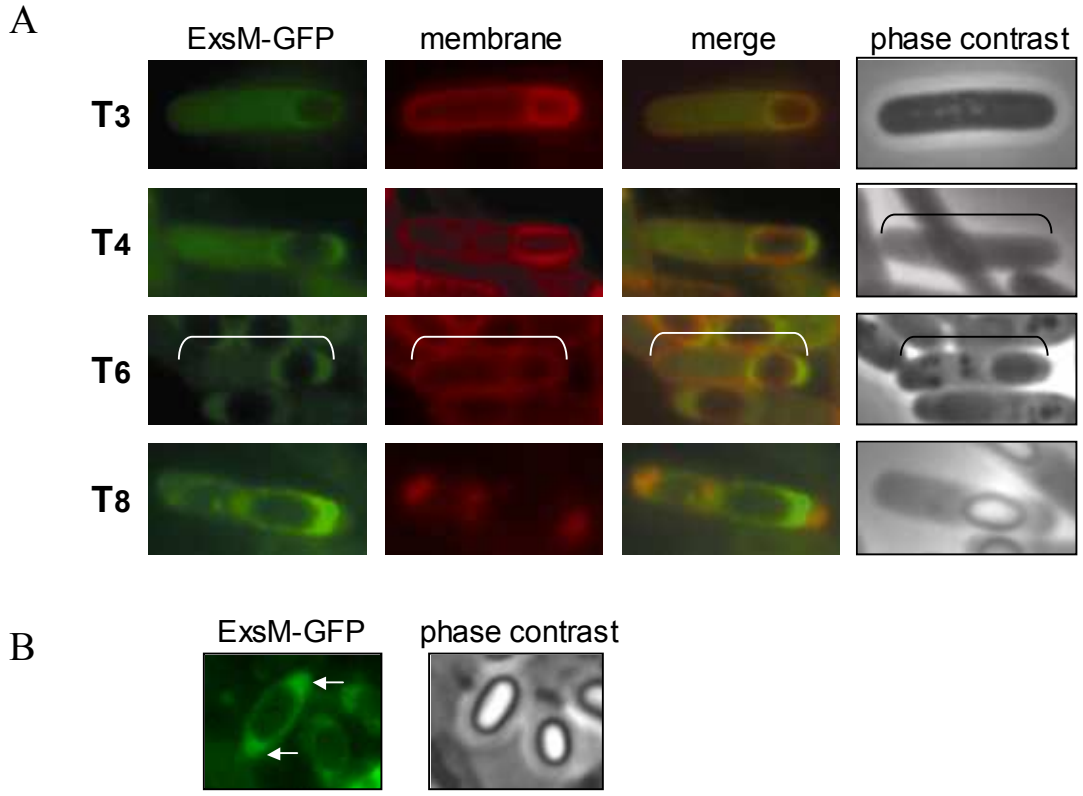

Fig. 30: Fluorescence microscopic localization of ExsM-GFP during sporulation. A. Fluorescence micrographs (1000X) of representative cells producing ExsM-GFP that were collected at 3 h (T3), 4 h (T4), 6 h (T6) and 8 h (T8) after sporulation. The cell membranes were stained with FM4-64 (red fluorescence). The figure also shows the merged images of GFP fusion protein and FM4-64, and same field view under phase-contrast. The brackets indicate individual sporangia. B. Fluorescence and phase-contrast micrographs (2000X) of ExsM-GFP carrying mature spores. The white arrows point to the spore exosporium.

Ultrastructural analysis of *exsM* spores

To gain further insight into the role of ExsM in spore formation, we inactivated the *exsM* gene in *B. cereus* strain ATCC 4342 by insertional mutagenesis targeted to its first 200 bp. The resulting mutant was named: *exsM*. Spores were prepared from the *exsM* mutant strain and visualized by SEM. The mutant *exsM* spores were morphologically different from wild-type spores, mainly due to changes in the mutant exosporium (Fig. 31). While wild-type spores presented an extended exosporium, which gave the appearance of a 'tail' (Fig. 31A), the mutant spores had a tightly wrapped exosporium, which lacked this characteristic (Fig. 31B). As a result, *exsM* spores were significantly shorter than wild-type when the whole spore including the exosporium was measured. There was no difference when the spore width was measured. In addition, the wild-type spore population had a greater variability in size than the *exsM* spore population, in which the length distribution was more constricted (Table 7, Fig. 32).

Fig. 31: SEM analysis of *exsM* spores. Scanning electron micrographs of *B. cereus* ATCC 4342 wild-type spores showing the typical morphology with a 'tail-like' side (A) and of e*xsM* spores (B). Scale bar, 1 μm.

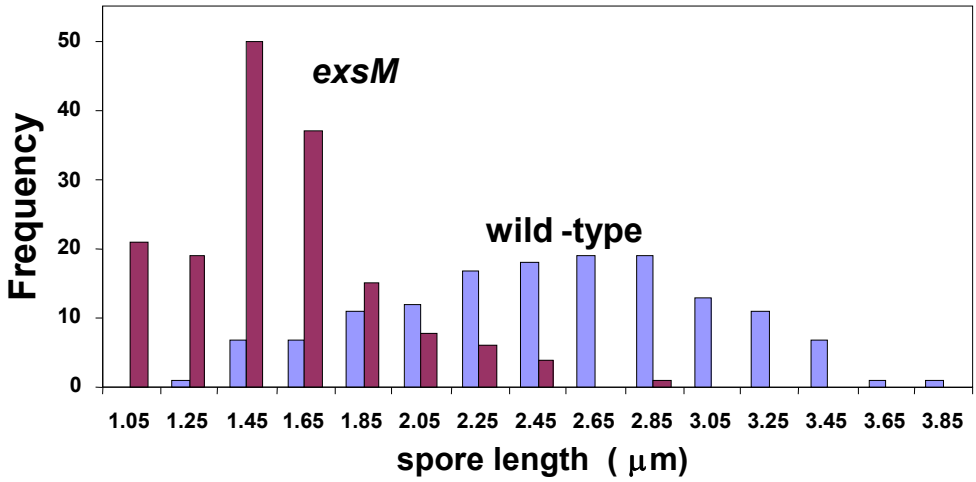

Fig. 32: *B. cereus* ATCC 4342 wild-type and *exsM* spore length distribution. Spore length distribution, including the exosporium, of more than 150 individual wild-type (in blue) and e*xsM* spores (in red).

Table 7: *B. cereus* ATCC 4342 wild-type and *exsM* spore size.

	wild-type	*exsM*
Length	2.40 ± 0.56 μm	1.66 ± 0.38 μm*
Width	0.90 ± 0.05 μm	0.87 ± 0.1 μm

*wt vs *exsM* spores $p<0.001$ (Mann-Whitney *U* test)

Thin-section TEM was performed to further visualize the differences between the wild-type and mutant exosporium. While the *exsM* spores showed no major disruption in any of the spore concentric layers, the majority (77%) were actually encased in two distinct exosporium layers (Fig. 33). To test if each layer constituted a complete exosporium and not simply an invagination of a single exosporium, the contrast agent Alcian blue was used to distinguish the exosporium hair-like nap from the basal layer on the mutant spores. The hair-like nap was present on each of the exosporium layers and facing the same direction, towards the exterior of the spore (Fig. 33C), which argues against invagination.

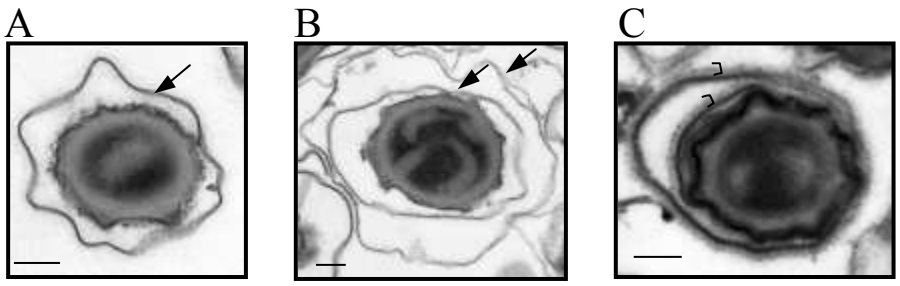

Fig. 33: TEM analysis of exsM spores. Transmission electron micrographs of *B. cereus* ATCC 4342 wild-type (A) and *exsM* spores (B). The black arrows points to a single layer exosporium in panel A and a double layer exosporium in panel B. Panel C shows a representative spore from ExsM-deficient strain stained with Alcian blue to increase contrast. The brackets denote the presence of a hair-like nap on the top of each exosporium layer. Scale bar, 250 nm.

An ExsM-deficient mutant was also constructed in a *B. cereus* ATCC 14579 background, which is the *B. cereus* type strain. *B. cereus* ATCC 14579 *exsM* spores showed the same morphological changes seen with the *B. cereus* ATCC 4342 e*xsM* spores under SEM and TEM. SEM revealed that *exsM* spores were shorter than wild-type and lacked the typical exosporium 'tail' seen in wild-type spores (Fig. 34 and 35, Table 8). *B. cereus* ATCC 14579 spores were also composed of a double layer exosporium, with each layer having a hair-like nap with an outward orientation (Fig. 34 D, E).

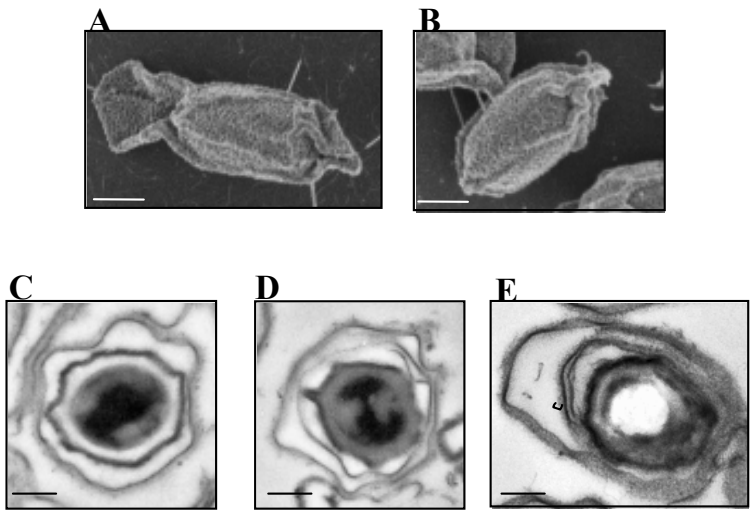

Fig. 34: Ultrastructural analysis of *B. cereus* ATCC 14579 *exsM* spores. Scanning electron micrographs of wild-type spores showing the typical morphology with a 'tail-like' side (A) and e*xsM* spores (B). Scale bar, 1 μm. Transmission electron micrographs of wild-type (C) and *exsM* spores (D). Panel E shows a representative spore from ExsM-deficient strain stained with Alcian blue to increase contrast. The bracket denote the presence of a hair-like nap. Scale bar 250 nm.

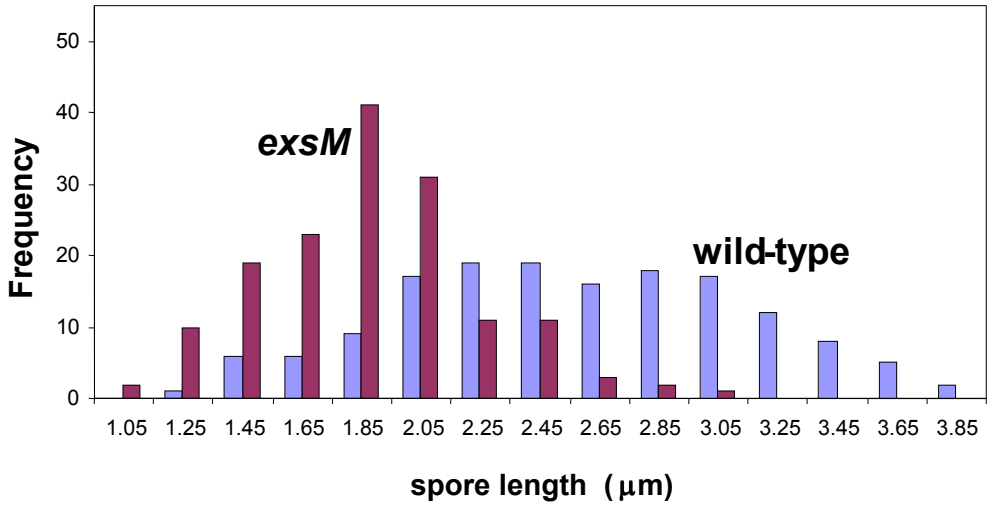

Fig. 35. *B. cereus* ATCC 14579 wild-type and *exsM* spore length distribution. Spore length distribution of more than 150 individual *B. cereus* ATCC 14579 wild-type (in blue) and e*xsM* spores (in red).

Table 8: *B. cereus* ATCC 14579 wild-type and *exsM* spore size.

	B. cereus ATCC 14579	*exsM*
length	2.49 ± 0.59 μm	1.76 ± 0.37 μm*
width	0.88 ± 0.05 μm	0.86 ± 0.06 μm

*wt vs *exsM* spores $p<0.001$ (Mann-Whitney *U* test)

Spore protein profiles

Exosporium proteins from *B. cereus* ATCC 4342 wild-type and *exsM* spores were extracted with 2% β-mercaptoethanol under alkaline conditions, run on a 1-D SDS-PAGE, and stained with Coomassie blue (Fig. 36A). The resulting protein profiles showed no major differences, besides an increase of the intensity of the band running at 26 kDa in the *exsM* profile. A similar result was obtained when wild-type and mutant exosporiums were extracted by sonication (Fig. 36B). In this case, the *exsM* protein profile presented a low-intensity band at 19 kDa and a more intense band at 45 kDa. It was not possible to precisely know which proteins were affected as these bands represented more than one protein as determined by LC-MS/MS. The similarity between the protein composition of wild-type and *exsM* exosporiums discounts a grossly defective exosporium as the reason for duplicating this layer. However, a few proteins appeared up- and down- regulated in the mutant, suggesting that ExsM may have a small effect on the overall exosporium protein content.

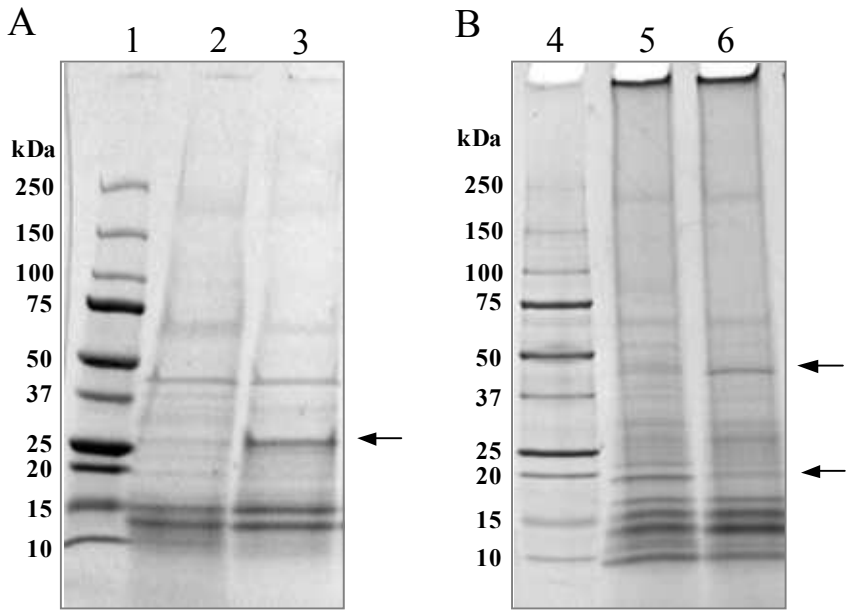

Fig. 36: SDS-PAGE analysis of exosporium proteins in wild-type and *exsM* spores. Proteins were separated in a 4-20% polyacrylamide gel and stained with colloidal Coomassie blue. Panel A shows the exosporium protein profile from *B. cereus* ATCC 4342 wild-type (lane 2) and *exsM* spores (lane 3) obtained after treatment with 2% β-mercaptoethanol for 2 h at 37°C. In panel B, exosporium proteins from wild-type (lane 5) and *exsM* spores (lane 6) were extracted by sonication and stained with colloidal Coomassie blue. The protein standards (lane 1 and 4) molecular weight is indicated on the left. The black arrows indicate the positions of bands whose intensities changed in the *exsM* mutant.

To study if inactivation of *exsM* had any effect on the spore coat composition, the coat and exosporium proteins were extracted concurrently, as extraction of only coat proteins without exosporium contamination was not feasible. The exosporium and coat protein were then extracted by incubation with 8M urea and 1% SDS under reducing conditions (Aronson and Fitz-James, 1971; Cheng and Aronson, 1977), or 4% SDS and

10% β-mercaptoehtanol (Henriques *et al.*, 1995). In both cases, the protein profiles were nearly identical (Fig. 37). Therefore, inactivation of ExsM showed no visible effect on the coat plus exosporium protein composition.

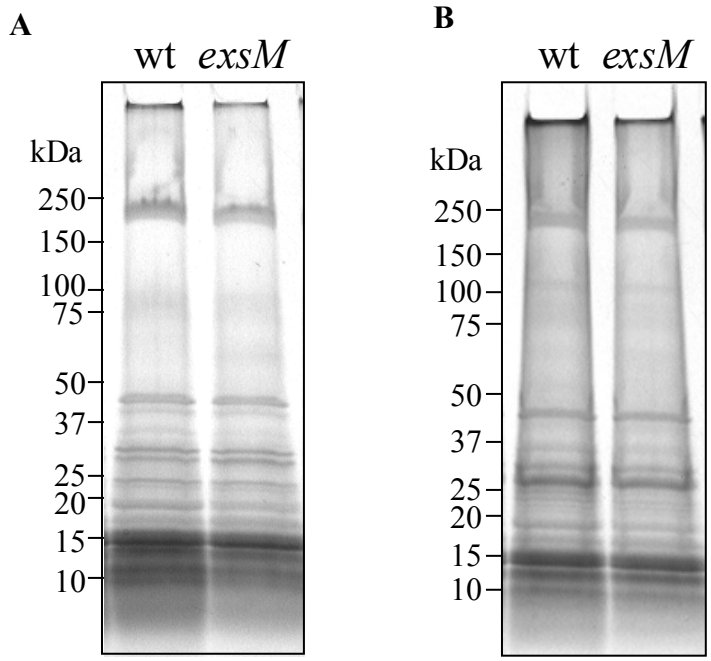

Fig. 37: SDS-PAGE analysis of exosporium plus coat proteins in wild-type and *exsM* spores. In A, the coat and exosporium proteins were extracted with 8M urea and 4%SDS from *B. cereus* ATCC 4342 (wt) and *exsM* spores. In B, the coat and exosporium proteins were extracted with 4% SDS and 10% β-mercaptoethanol. In both cases, proteins were stained with colloidal Coomassie blue. The molecular weight of each protein standard is indicated on the left.

Spore properties

Wild-type and ExsM-deficient strains had very similar growth (Fig. 38) and sporulation rates (Fig. 39). In addition, when the spore resistance to heat (80°C, 10 min) and organic solvents (chloroform, methanol and phenol) were compared following standard protocols (Cutting *et al.*, 1990b), no differences between wild-type and mutant spores were found, indicating that *exsM* spore coat, at least for these resistance properties, was not compromised (Table 9).

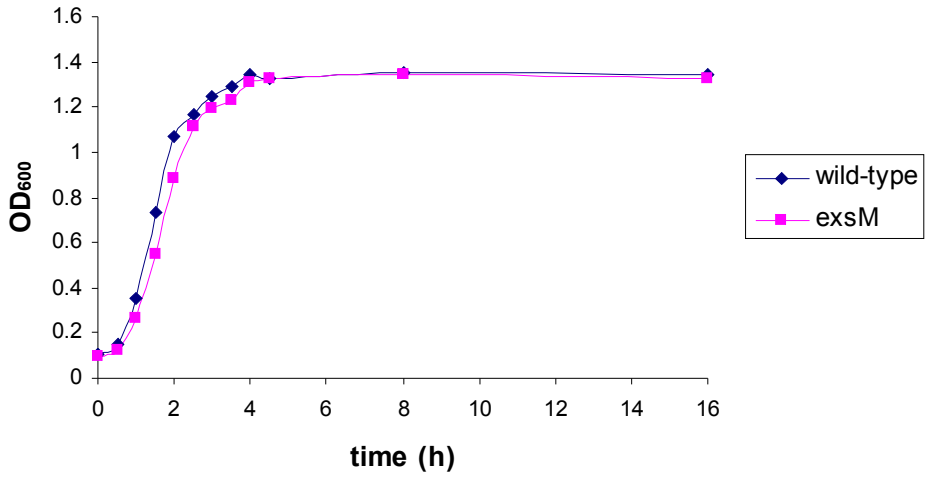

Fig. 38: Growth curve of *B. cereus* ATCC 4342 wild-type and *exsM*. Growth was measured in BHI media at 37°C.

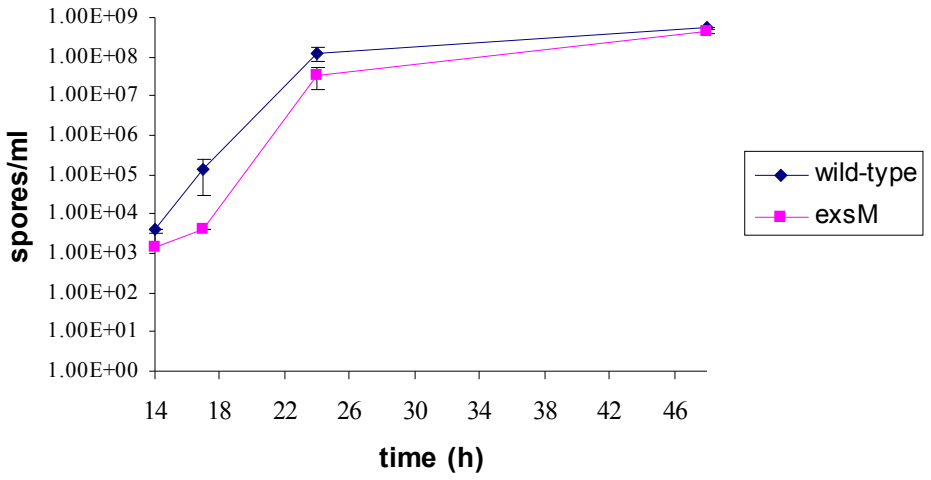

Fig. 39: Sporulation rate of *B. cereus* ATCC 4342 wild-type and *exsM*. Sporulation rate was studied by exposure to chloroform vapors at 14 h, 18 h, 24 h and 48 h after plating on sporulation agar.

Table 9: *B. cereus* ATCC 4342 wild type and *exsM* spore resistance properties.

Resistance to	Wild-type	*exsM*
Heat (80°C, 10 min)	83 ± 8%	91 ± 8%
Chloroform	16 ± 1%	18 ± 4%
Methanol	91 ± 12%	92 ± 6%
Phenol	9 ± 1%	10 ± 1%

It has been reported that in the absence of the exosporial nap, sensitivity to lysozyme moderately increases (Steichen *et al.*, 2003); hence, spore resistance to 250 mg/ml egg lysozyme treatment was tested at several time points. Double exosporium spores were more resistant to treatment with lysozyme after 5, 10 and 20 min (Fig. 40), which is consistent with the exosporium being a semipermeable barrier to harmful macromolecules (Ball *et al.*, 2008; Gerhardt and Black, 1961; Gerhardt, 1967).

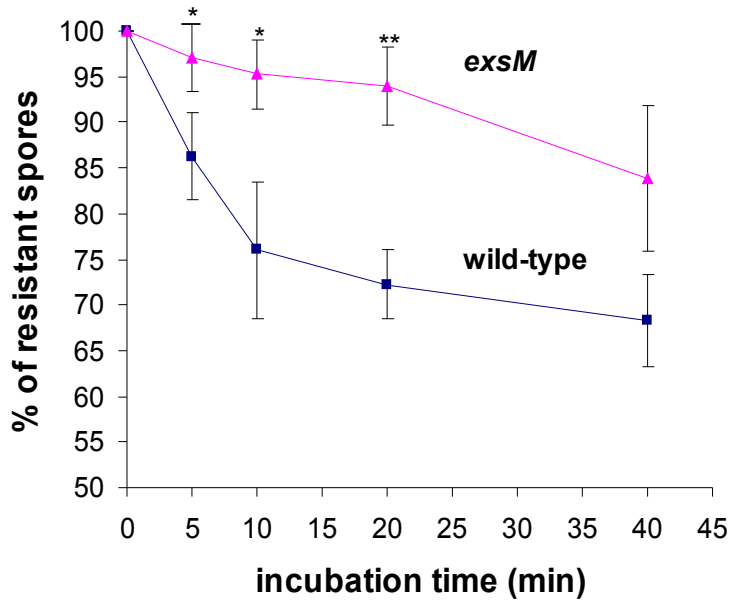

Fig. 40: Lysozyme resistance assay. *B. cereus* ATCC 4342 wild-type (blue) and *exs*M spores (red) were incubated with 250 μg/ml of lysozyme and aliquots were taken at 0, 5, 10, 20 and 40 min. Serial dilutions of each aliquot was plated on BHI agar. After overnight incubation, the survivors were enumerated. The graphic shows the mean and SD of three independent experiments done with different preparations of wild-type and mutant spores.* $p<0.05$ and **$p<0.005$ wild-type versus *exsM*, Student's *t* test.

Germination

The characteristic architecture of the spore not only contributes to its resistance properties, but also to the resumption of vegetative growth under proper conditions. In particular, the exosporium may regulate the timing of germination, as this structure includes enzymes that modify or hydrolyze germinants. Alr converts L-alanine to its competitive inhibitor D-alanine, and IunH degrades inosine and related nucleosides (Boydston *et al.*, 2006; Steichen *et al.*, 2007; Todd *et al.*, 2003).

To investigate the response of *exsM* spores to L-alanine (50mM), both loss of the spore heat resistance and fall in optical density at 580nm (OD_{580}) was assessed after the addition of the germinant. Loss of heat resistance reflects the loss of the spore core content (mainly DPA) and rehydration, and measures early and intermediate germination events (Paidhungat, 2002). Loss of OD_{580} represents depletion of the content of the core and also cortex hydrolysis, which are intermediate events during germination. When compared to wild-type spores, ExsM-deficient spores showed a lower rate of germination but the efficiency of germination after 15 min was ultimately equal (Fig. 41 and Fig. 42A).

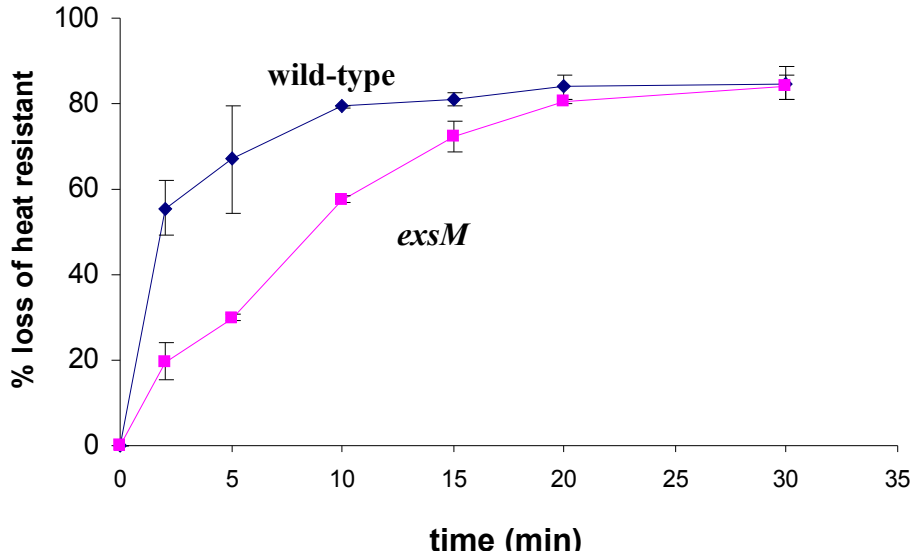

Fig. 41: Spore germination in the presence of L-alanine. Heat activated *B.cereus* ATCC 4342 wild-type (blue) and *exsM* spores (red) were incubated in the presence of 50 mM L-alanine, and germination was monitored by loss of heat resistance at selected time points. Mean and SD of one representative experiment done in duplicate is shown.

To investigate if the slower rate in germination was due to the action of Alr, wild-type and *exsM* spores were preincubated with D-cycloserine (DCS, 1mM) to inhibit Alr before addition of L-alanine (50mM). Germination was monitored by following the change in OD_{580}. The pretreatment with the Alr inhibitor increased the germination rate of *exsM* spores to wild-type levels, and also the germination efficiency to levels higher than wild type (Fig. 42). DCS treatment did also increase the germination efficiency of wild-type spores, as expected (Gould, 1966).

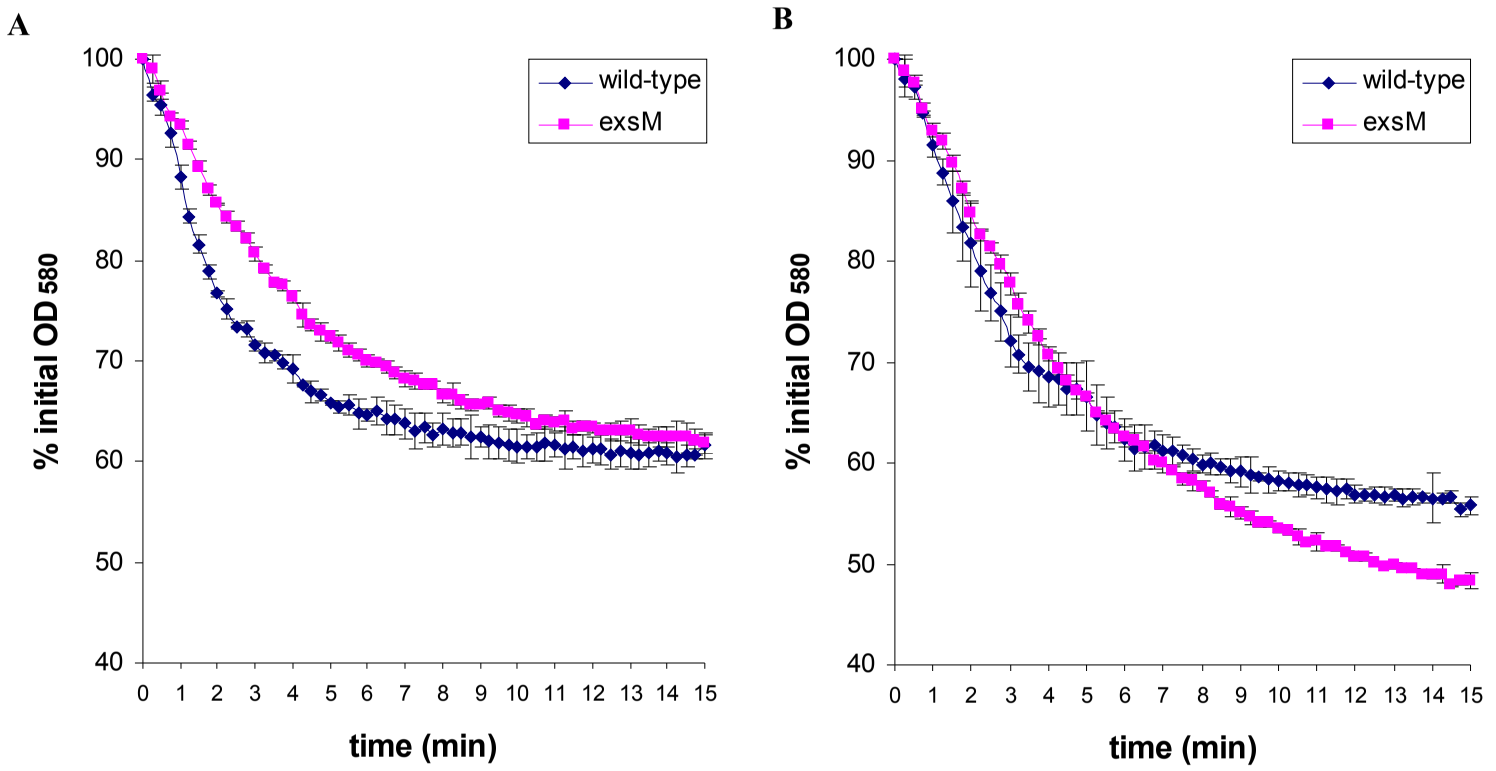

Fig. 42: Effect of DCS on spore germination with L-alanine. Loss of OD_{580} was measured as an indicator of spore germination. *B. cereus* ATCC 4342 wild-type (blue) and *exsM* spores (red) were germinated in the presence of 50 mM L-alanine (panel A). Also, spores were pretreated for 15 min with 1mM D-cycloserine (DCS) and then germinated with 50 mM L-alanine (panel B). Mean and SD of triplicate measurements of representative experiments are shown.

When germination was induced with L-alanine (1mM) and inosine (1mM), the germination response from wild-type and mutant spores was overall enhanced (Clements and Moir, 1998; Foerster and Foster, 1966; Ireland and Hanna, 2002; Warren and Gould, 1968). In this case, *exsM* spores exhibited a faster and more complete germination than wild-type spores (Fig. 43A). There was no effect on the germination rate when either spore populations were pretreated with DCS (Fig. 43B), which agrees with a previous report that Alr has no effect when germination is activated by both L-alanine and inosine (Chesnokova *et al.*, 2009).

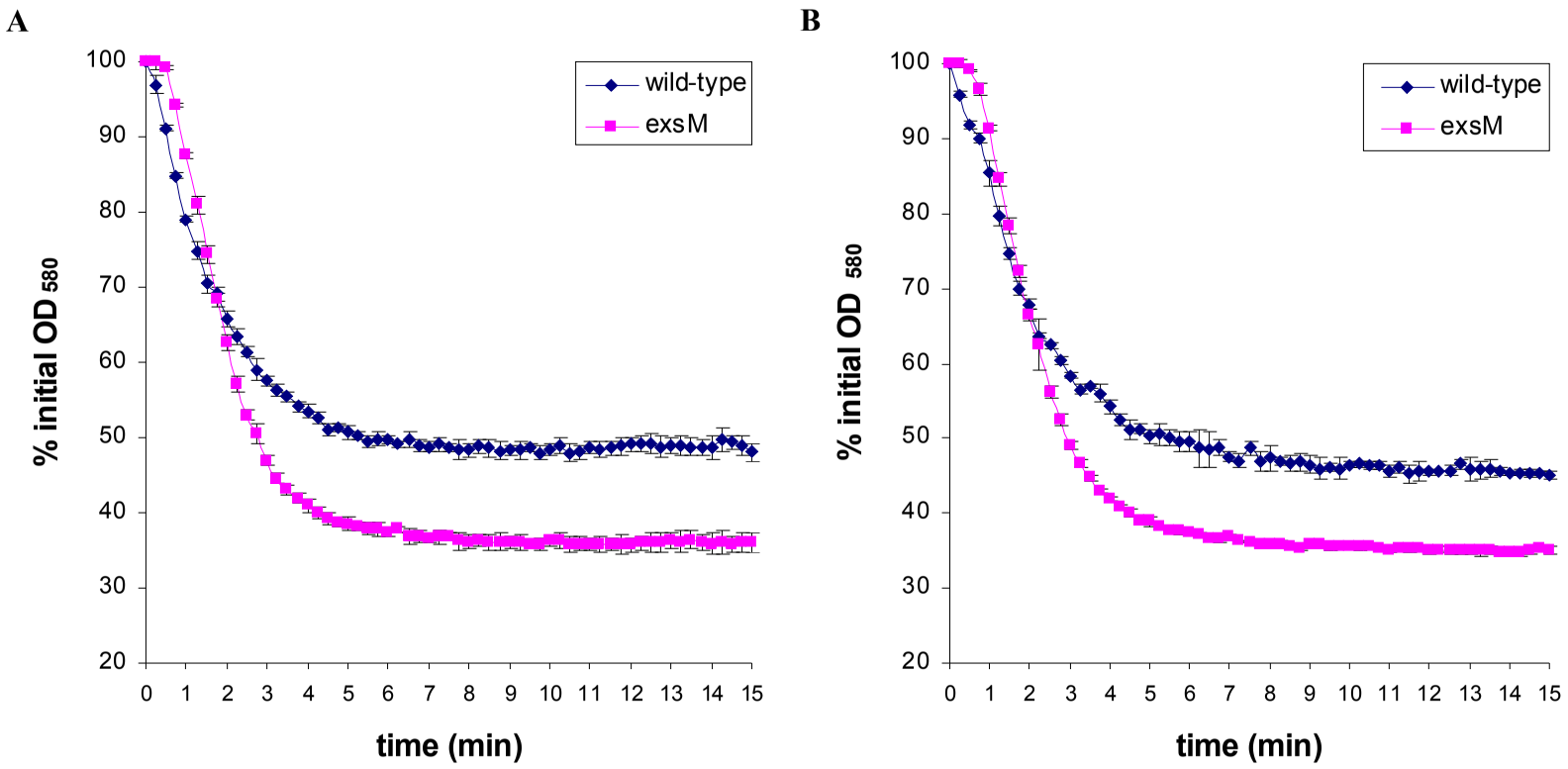

Fig. 43: Spore germination with L-alanine and inosine. *B. cereus* ATCC 4342 wild-type (blue) and *exsM* spores (red) were germinated in the presence of 1mM L-alanine and 1 mM of inosine (panel A). Also, spores were pretreated for 15 min with 1mM D-cycloserine (DCS) and then germinated with 1mM L-alanine and 1 mM inosine (panel B). Mean and SD of triplicate measurements of representative experiments are shown.

ExsM-deficient spores also showed a higher germination efficiency than wild-type when germinated with: inosine (1M), inosine (1M) plus L-serine (1M) or complete medium (50% BHI). While germination of wild-type spores with inosine resulted in a biphasic curve, this was not the case for *exsM* (Fig. 44). The change in the kinetics of germination was probably due to the activity of Iunh. In addition, *exsM* spores showed a slight delay in germination with inosine plus L-serine (Fig. 45) and when germinated in complete medium (Fig. 46).

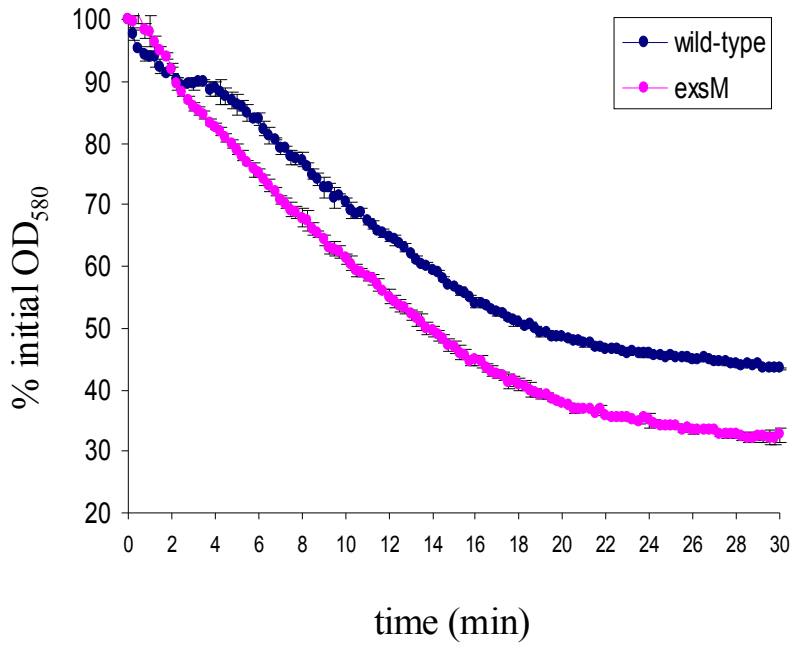

Fig. 44: Spore germination with inosine. *B. cereus* ATCC 4342 wild-type (blue) and *exsM* spores (red) were germinated in the presence of 1mM inosine. Mean and SD are shown for triplicate measurements of a representative experiment.

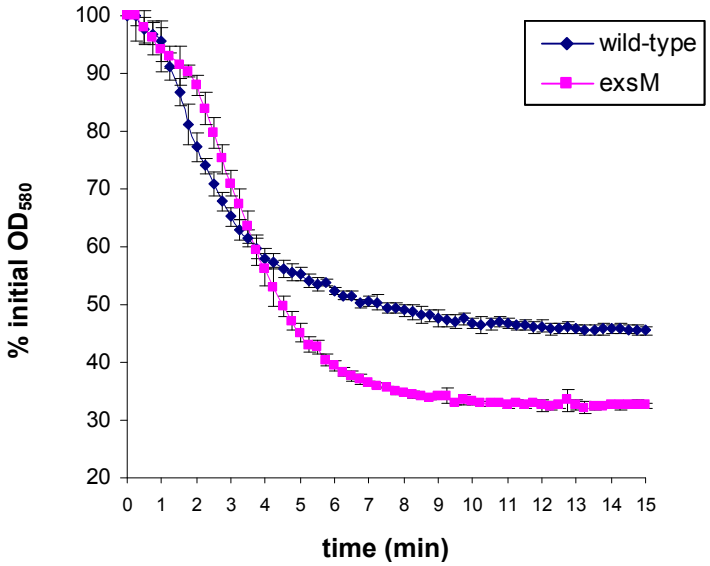

Fig. 45: Spore germination with L-serine and inosine. *B. cereus* ATCC 4342 wild-type (blue) and *exsM* spores (red) were germinated with 1mM L-serine and 1 mM inosine. Mean and SD are shown for triplicate measurements of one representative experiments.

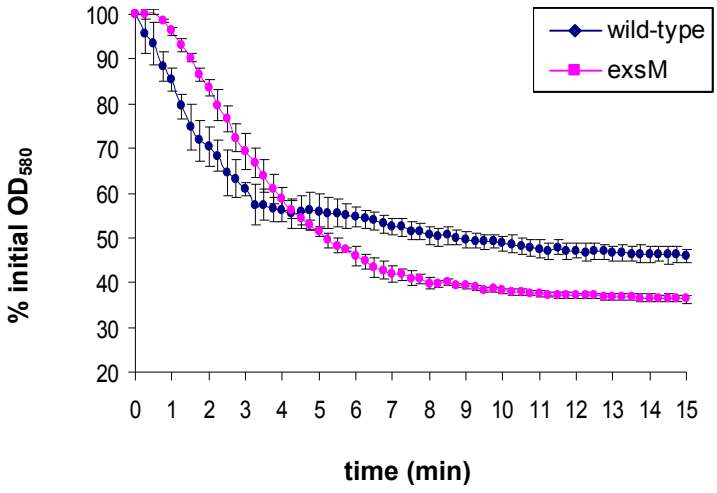

Fig. 46: Spore germination in complete media. Wild-type (blue) and *exsM* spores (red) were germinated in 50% BHI. Mean and SD are shown for triplicate measurements of a representative experiment .

Outgrowth

The resumption of metabolism after germination of wild-type and *exsM* spores was tested using a variant of the semiquantitative tetrazolium (TTZ) overlay assay (Cutting *et al.*, 1990b; Giorno *et al.*, 2007). TTZ turns red when it is reduced by active dehydrogenases present in the germinated spore. Thus, TTZ is an indicator of outgrowth. After two hours of incubation at 37°C*, exsM* mutants were less red than wild-type (Fig. 47A), though when the incubation was held for longer times (16 h), the color intensity was the same as wild-type (fig 47B), which suggested that spore outgrowth might be delay but not blocked in the mutants. Outgrowth of spores in BHI was compared by monitoring changes in OD_{580}. In this case, spores were resuspended at a lower initial OD_{580} to allow for bacteria growth, which explains why the drop in OD_{580} observed was not as high as in the germination assays, when a higher initial OD_{580} was used (Fig. 46). It has been demonstrated that the extent of germination is positively correlated with spore density (Caipo *et al.*, 2002); (Dodatko *et al.*, 2009). ExsM-deficient spores showed a more efficient germination on BHI but lower rate of vegetative growth (Fig. 47C), confirming the results obtained with the semiquantitative assay. Also, outgrowth can be visualized as a change from spherical (spore) to cylindrical shape (outgrowing cell) (Morris and Hansen, 1981), so phase-contrast microscopy was used to assess the percentage of outgrowing cells. After 60 min of incubation in BHI, the wild-type sample contained 76 ±1.7 % outgrowing cells versus 44.5 ± 2.5% in the ExsM deficient sample. Thus, the escape mechanism of the nascent cell may not be forceful enough to rapidly burst from the mutant double layer exosporium, which may be reflected as a diminishing outgrowth rate.

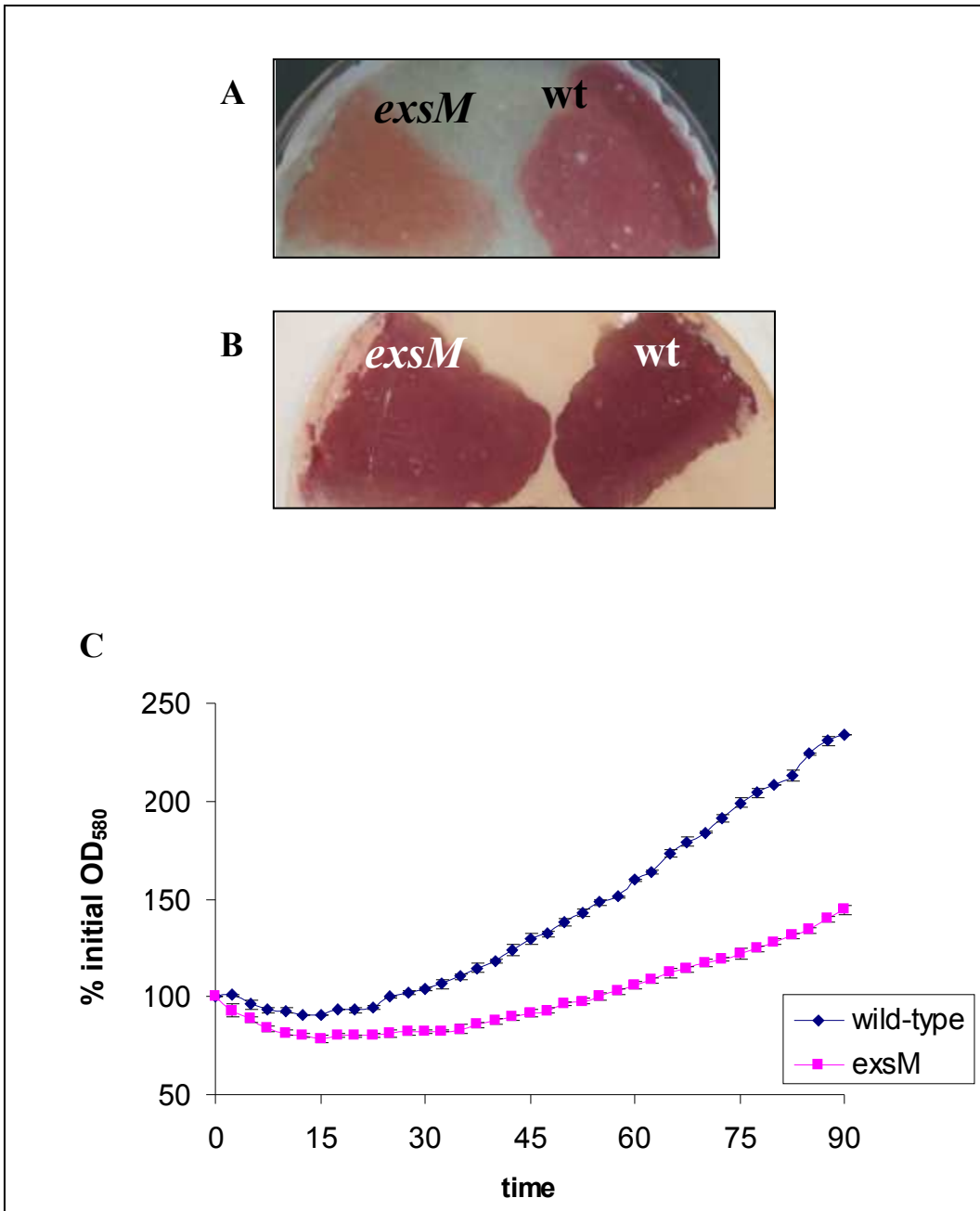

Fig. 47. Spore outgrowth in complete media. A photograph of a representative tetrazolium overlay assay of *B. cereus* ATCC 4342 wild-type and *exsM* strains after 2 h incubation (A) or 16 h (B) is shown. In B, changes in OD_{580} were used to assess wild-type (blue) and *exsM* spores (red) germination and outgrowth in BHI media. Mean and SD are shown for one representative experiment done in triplicate.

B. anthracis ExsM-deficient mutants

Inactivation of *exsM* in *B. anthracis* ΔSterne was achieved by insertional mutagenesis, and the resulting mutant spores were studied under SEM and TEM. The morphological differences seen between the *B. anthracis* wild-type and *exsM* spores were not as large as the ones between *B. cereus* wild-type and *exsM* spores, because *B. anthracis* spores do not have a tail-like extended exosporium (Fig. 48A and B). Still, as with *B. cereus*, *B. anthracis exsM* spores were shorter and rounder than wild-type (Fig 49, table 10). Additionally, we observed that several mutant exosporiums were partially or fully detached from the spores (Fig. 48C). Thin section TEM revealed that 30% of the *exsM* spores had a partial double exosporium versus only 4% for the wild type spores with both layers of exosporium presenting a basal layer and a hair-like nap in the correct orientation (Fig. 48E and F).

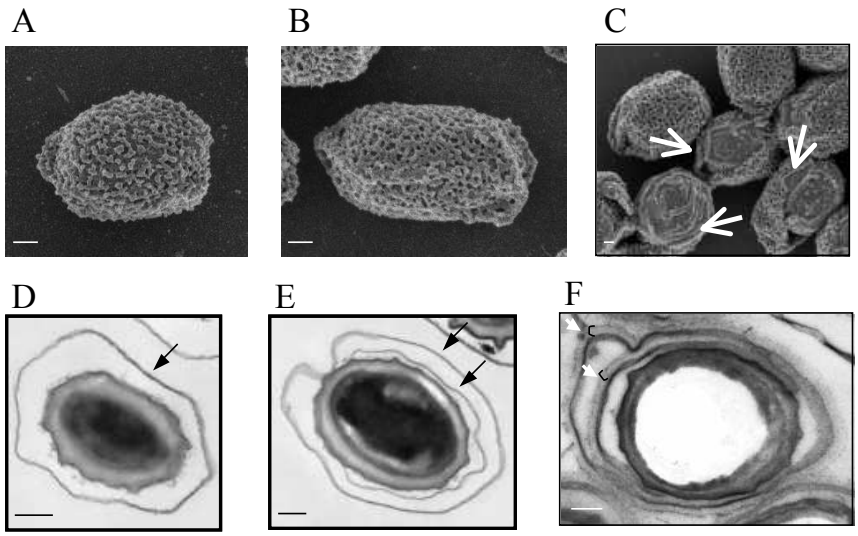

Fig. 48: Ultrastructural analysis of *B. anthracis exsM* spores. Scanning electron micrographs of *B. anthracis* ΔSterne (A) and e*xsM* spores (B and C). In C, the white arrows indicate spores that have partially lost their exosporium. Scale bar, 500 nm. Transmission electron micrographs of *B. anthracis* ΔSterne (D) and *exsM* spores (E). The black arrows point to a single layer exosporium in panel D and a double layer exosporium in panel E. Panel F shows a representative *exsM* spore stained with Alcian blue to increase contrast. The brackets denote the presence of the hair-like nap on top of the exosporium in both layers. Scale bar, 250 nm.

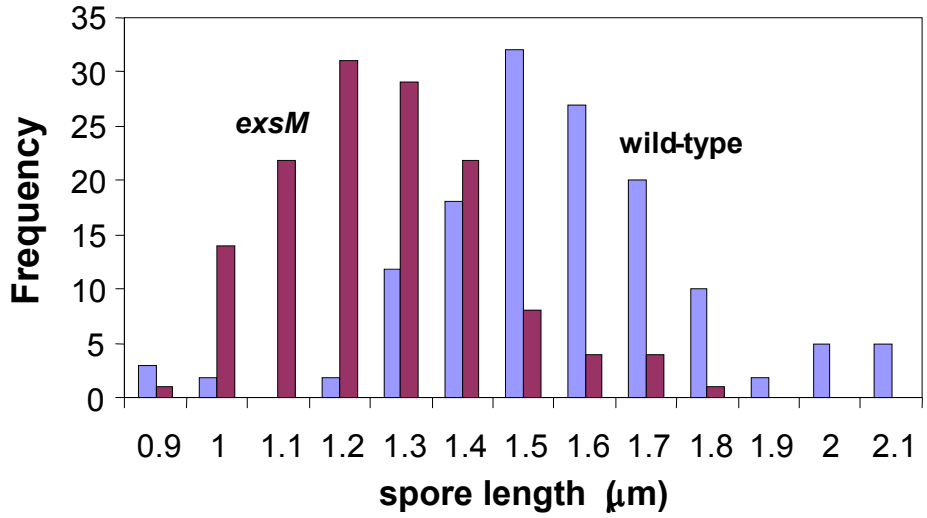

Fig. 49: *B. anthracis* ΔSterne wild-type and *exsM* spore length distribution. Spore length distribution of more than 100 individual *B. anthracis* ΔSterne wild-type (in blue) and e*xsM* spores (in red).

Table 10: *B. anthracis* ΔSterne wild-type and *exsM* spore size.

	B. anthracis ΔSterne	*exsM*
length	1.63 ± 0.21 μm	1.30 ± 0.21 μm*
width	0.97 ± 0.08 μm	1.04 ± 0.11 μm

*wt vs *exsM* spores $p<0.001$ (Student's *t* test)

A paralogue with 40% identity to ExsM has been identified in the exosporium of *B. anthracis* and named BxpC (Steichen *et al.*, 2003). Inactivation of this gene alone did not affect the structure of the exosporium (Fig. 50), or the size of the spore (Fig. 51, table 11). However, it could be compensating for the function of ExsM during exosporium formation in the *B. anthracis* mutants.

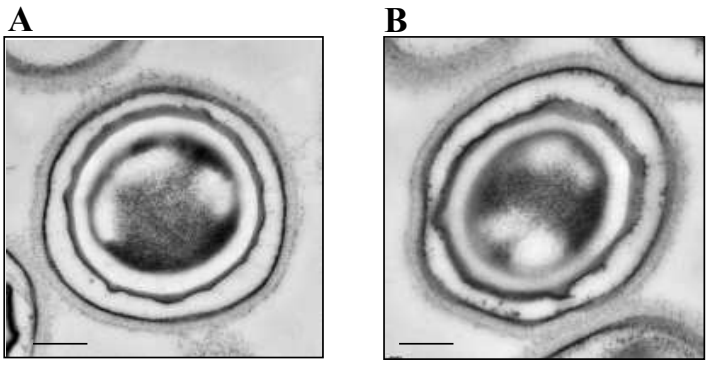

Fig. 50: Ultrastructural analysis of *B. anthracis bxpC* spores. Transmission electron micrographs of *B. anthracis* ΔSterne (A) and *bxpC* spores (B). The spores were stained with Alcian blue to increase contrast. Scale bar, 250 nm.

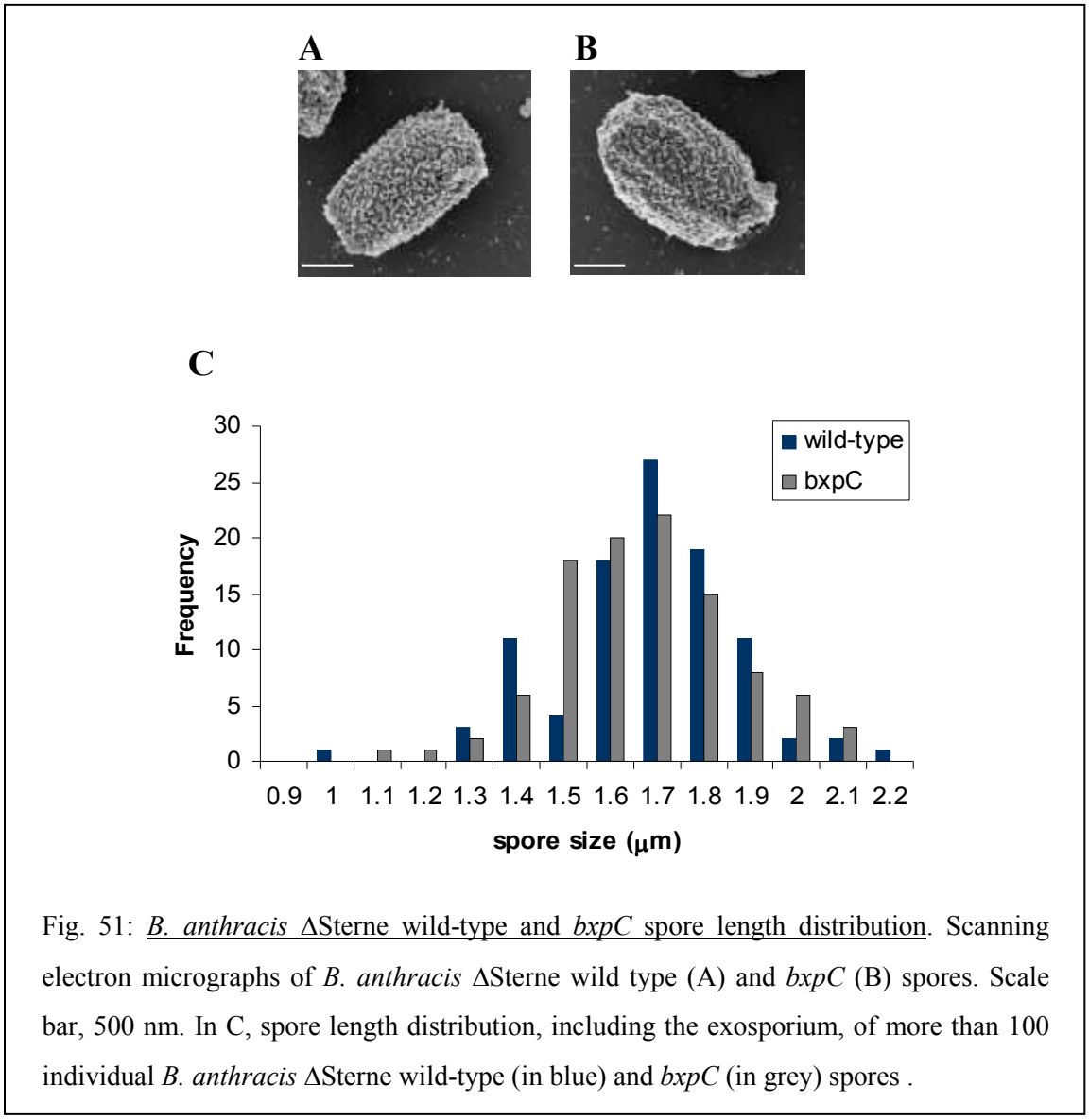

Fig. 51: *B. anthracis* ΔSterne wild-type and *bxpC* spore length distribution. Scanning electron micrographs of *B. anthracis* ΔSterne wild type (A) and *bxpC* (B) spores. Scale bar, 500 nm. In C, spore length distribution, including the exosporium, of more than 100 individual *B. anthracis* ΔSterne wild-type (in blue) and *bxpC* (in grey) spores .

Table 11: *B. anthracis* ΔSterne wild-type and *bxpC* spore size.

	B. anthracis ΔSterne	*bxpC*
length	1.65 ± 0.19 μm	1.66 ± 0.19 μm
width	0.97 ± 0.07 μm	1.01 ± 0.08 μm

Results: Spore appendages characterization

Appendages isolation

Under SEM, two morphological distinct appendages could be seen emanating from the surface of *B. cereus* ATCC 4342 and *B. cereus* 14579 spores (Fig. 52). These appendages were separated from *B. cereus* ATCC 14579 spores by extraction with 2% β-mercaptoethanol under alkaline conditions. The extraction resulted in a mixture of spore appendages with soluble exosporium proteins, as before noted (Fig. 53A). To further isolate the appendages, the sample was then subjected to a CsCl discontinous gradient ultracentrifugation (DesRosier and Lara, 1981), which resulted in 2 bands floating at different density points (Fig. 53B). Both bands were composed of purified appendages mostly stripped of exosporium soluble proteins, based on negative staining TEM (Fig. 53A and B). While the less dense band contained thin appendages, the denser band showed thicker appendages. This result indicates that CsCl gradient ultracentrifugation allowed the separation of the two types of appendages observed on *B. cereus* spores.

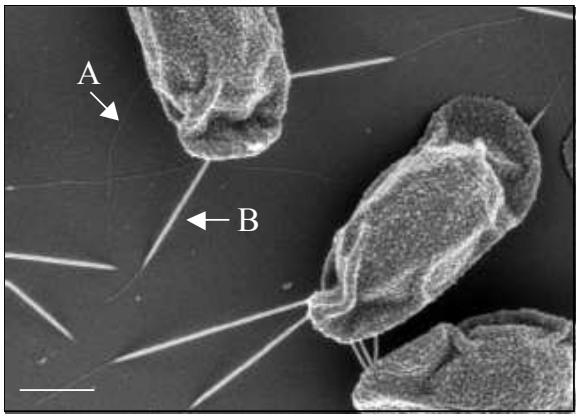

Fig. 52: Types of spore appendages. Transmission electron micrograph of *B. cereus* ATCC 14579 spores. A, thin appendage, B, thick appendage. Scale bar, 500 nm.

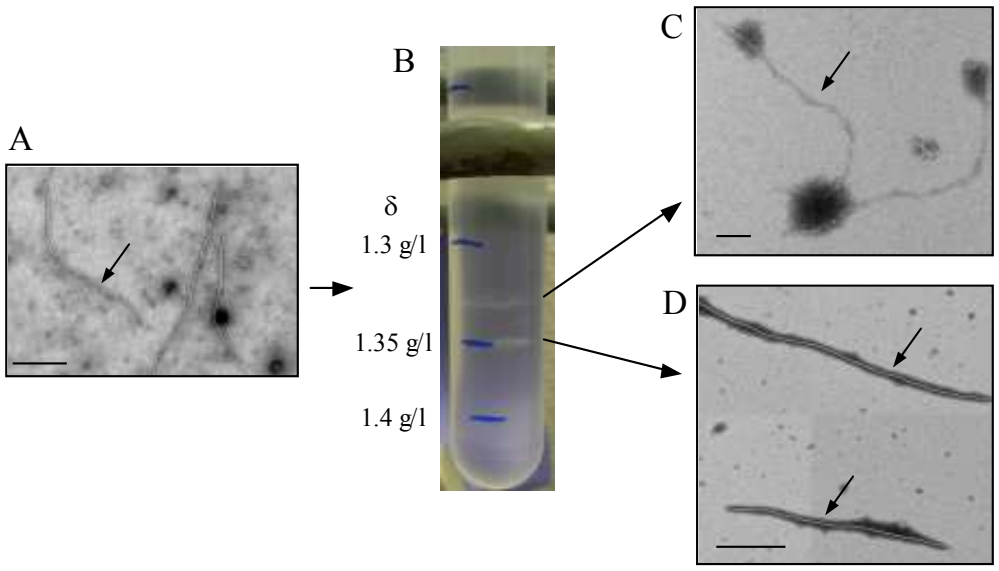

Fig. 53: Purification of spore appendages. Negative staining transmission electron micrograph of β-mercaptoethanol spore extract (A), appendages upper (C) and lower band (D). Scale bar, 100 nm. Representative result of CsCl gradient ultracentrifugation (B). The density of each CsCl solution step is indicated on the left.

Appendages were reported to be composed of protein (DesRosier and Lara, 1981; Kozuka and Tochikubo, 1985). However, SDS-PAGE analysis of appendages boiled in Laemmli buffer for 10 min resulted in no visible protein band after staining with Coomassie Blue, Sypro Ruby or silver nitrate. Addition of 8 M urea did not solubilize the spore appendages. Several treatments tried to extract proteins from the spore appendages were also unsuccessful. Appendages were not solubilized after treatment with 2 N NaOH for 2 hs at 50°C, 70% formic for 30 min at 37°C, or 5%TCA for 25 min at 90°C. Appendages were also resistant to treatment with pronase and trypsin. These results agree with previous reports that have indicated that *B. cereus* appendages can withstand several

denaturalization treatments such as extreme pH, organic solvents, detergents, high salt solution, reducing agents and protease digestion (DesRosier and Lara, 1981; Kozuka and Tochikubo, 1985).

The highly insoluble nature showed by *B. cereus* spore appendages is in part expected as they are part of spores, and therefore, they need to maintain their structure and their function in harsh conditions. The spore coat is also known to withstand protein denaturants and proteolysis, and approximately 30% of the coat proteins are highly crosslinkend and refractory to extraction (Zilhao *et al.*, 2004). Then, appendage insolubility may be due to irreversible crosslinking between the protein monomers composing these structures. Another possibility is that appendages contain non-ribosomally encoded products. Non-ribosomal peptides are often cyclic or branched structures that can contain modified or D-amino acids and are highly stable and resistant to proteolysis (Moffitt and Neilan, 2000). These peptides are produced by large enzymatic complexes, known as non-ribosomal peptide synthetases (NRPS), without a RNA template (Stachelhaus and Marahiel, 1995). For example, *B. cereus* emetic toxin, cereulide is a nonribosomal peptide as well as gramicidin S produced by *B. subtilis*. *B. cereus* ATCC 14579 has several putative non-ribosomal synthetase operons that contain consensus sequence for the sporulation factors σ^E and σ^K, suggesting that production of non-ribosomal product takes place during sporulation (Fig. 54).

.

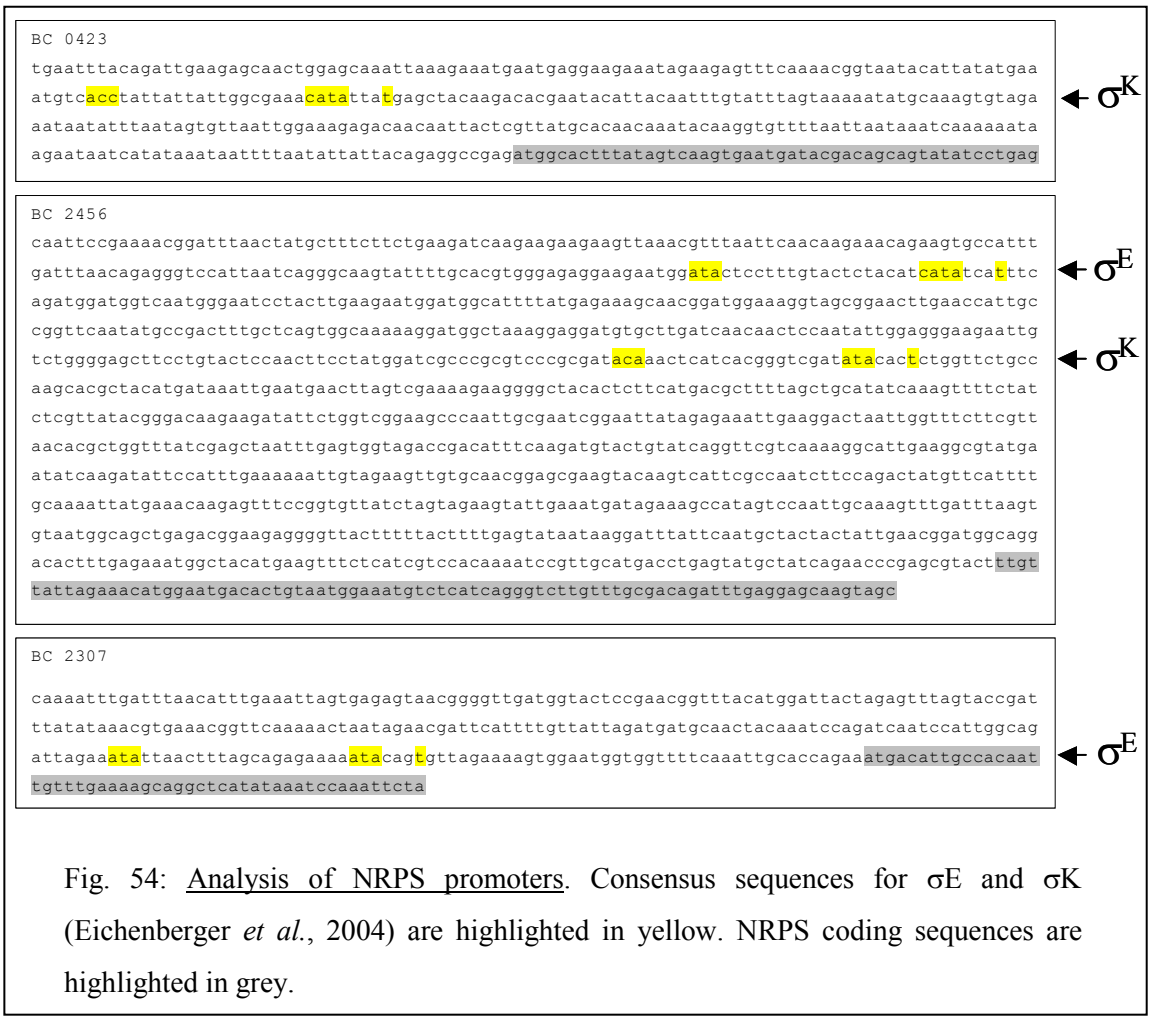

Fig. 54: Analysis of NRPS promoters. Consensus sequences for σE and σK (Eichenberger *et al.*, 2004) are highlighted in yellow. NRPS coding sequences are highlighted in grey.

Proteins associated with the appendages

Analysis of a highly concentrated appendage sample obtained after CsCl gradient ultracentrifugation revealed the presence of two bands after SDS-PAGE (Fig. 55). LC-MS/MS analysis identified spore coat-associated protein N (CotN) and Camelysin (CalY) as the main components of the two protein bands with traces of CotE and InhA (table 12).

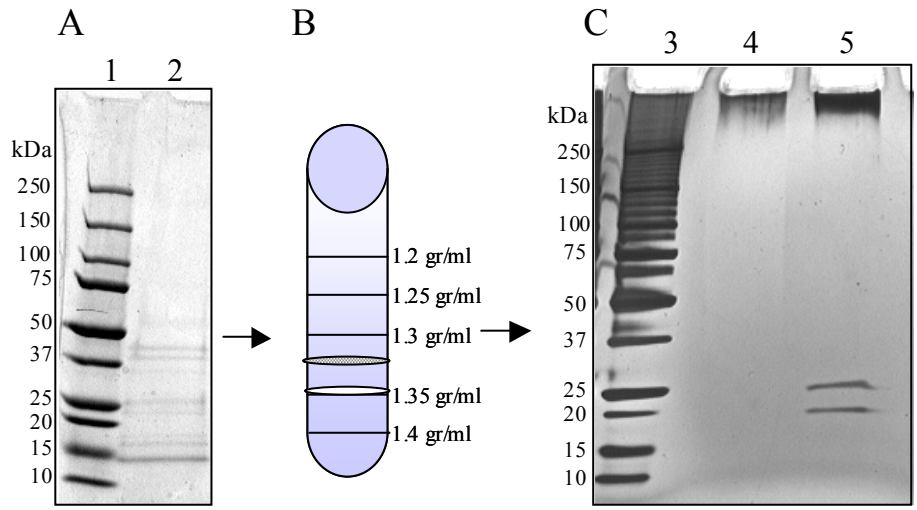

Fig. 55: SDS-PAGE analysis of isolated appendages. In A, SDS-PAGE of a 2% β-mercaptoethanol extraction of *B. cereus* 14579 spores (2). Proteins were stained with Coomassie blue. In B, CsCl gradient centrifugation scheme showing appendages bands. In C, SDS-PAGE of higher (4) and lower (5) bands. Proteins were silver stained. Lane 1, 3: Protein weight standards. The molecular weight of each protein standard is indicated on the left.

Table 12: Proteins identify by LC-MS/MS from isolated appendages.

Apparent MW[a] (kDa)	protein name	MW[a] (kDa)	pI	NCBI locus tag *B. cereus* ATCC 14579
25, 18.5	CalY	20.7	4.2	Bc_1281
18.5	CotN	21.6	5.8	Bc_1279
25	CotE	20.3	4.1	Bc_3770
18.5	InhA	86.5	4.9	Bc_1284

[a] MW, molecular weight.

Insertional mutagenesis of *cotN* had no effect on either the morphology or number of appendages present on the surface of *B. cereus* 14579 spores, but *calY* null (MF84) spores presented fewer appendages per spore than wild type (wild-type= 2.22 appendages/spore vs MF84= 1.31 appendages/spore*, * wild-type vs MF84 $p< 0.001$, Student's *t* test) (Fig. 56). CalY and CotN have 73% identity to each other, suggesting that both proteins have a rebundant and combinatorial role in the formation of appendages. Then, double inactivation of both *cotN* and *calY* loci and immuno-electron microscopy with antibodies against CalY and CotN are necessary to identity the actual role of these proteins in the formation of spore appendages.

Both CotN and CalY have 51% similarity with TasA, the main component of *B. subtilis* biofim extracellular matrix (Branda *et al.*, 2006). Interestingly, TasA forms amyloids fibrils that hold the cells together and provide structure to the extracellular matrix (Romero *et al.*). Then, like TasA, CalY and CotN may form appendages with amyloid characteristics. This could explain the resistance to solubilization shown by *B. cereus* spore appendages, as amyloids are extremely stable structures and difficult to disrupt (Romero *et al.*). Additionally, *calY* transcription is upregulated during biofilm formation in *B. thuringiensis* (Fagerlund *et al.*, 2009). Therefore, spore appendages may play a role in biofilm formation, acting like a scaffold for the biofilm matrix and holding the spores together.

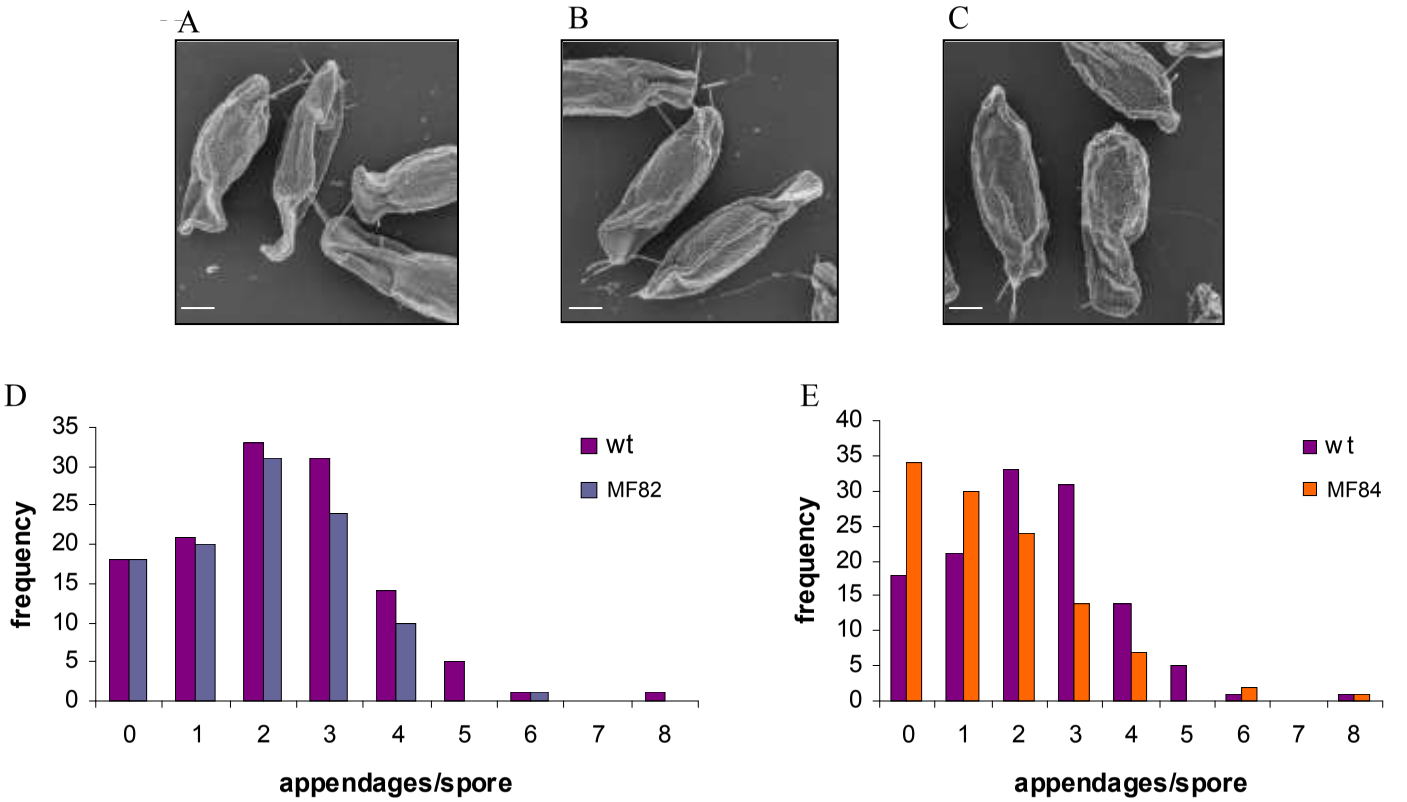

Fig. 56: Analysis of MF82 and MF84 spore appendages. Transmission electron micrograph of *B. cereus* ATCC 14579 wild-type (A), MF82 (*cotN* null mutant, B) and MF84 (*calY* null mutant, C) spores. Scale bar, 500 nm. Distribution of number of appendages per spores in wild-type (wt) and MF82 spores (D), or wild-type (wt) and MF84 spores (E).

Inactivation of CotE, resulted in spores with severely damaged exosporiums that possessed less appendages per spore (Fig. 57). Therefore, CotE not only affected the attachment of the exosporium to the spore (Giorno *et al.*, 2007) but also the presence of spore appendages. More studies are necessary to distinguished whether the effect on the number of appendages per spore is secondary to the defect in the attachment of the exosporium or CotE participates directly in the formation of spore appendages.

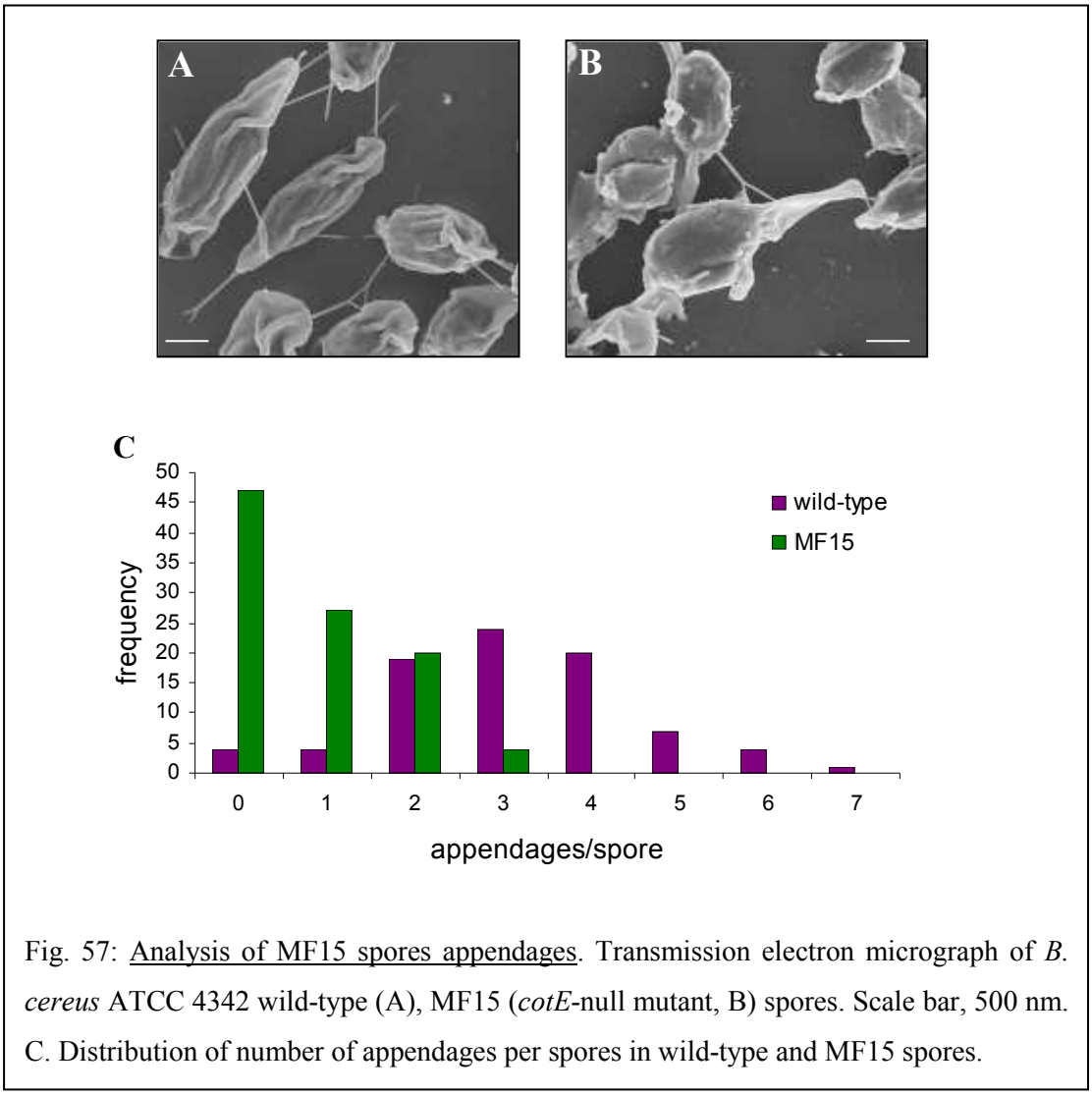

Fig. 57: Analysis of MF15 spores appendages. Transmission electron micrograph of *B. cereus* ATCC 4342 wild-type (A), MF15 (*cotE*-null mutant, B) spores. Scale bar, 500 nm. C. Distribution of number of appendages per spores in wild-type and MF15 spores.

Discussion

Exosporium Protein Composition

In 1970, Matz *et al.* described the exosporium as biochemical complex, with protein as it main component (Matz *et al.*, 1970). In 1971 (Beaman *et al.*, 1971), and later in 1984 (DesRosier and Lara, 1984), the exosporium was reported to be composed of several polypeptides; however, no attempt was made to identify or characterize any of these proteins. It was not until 2001, after the anthrax terrorist mail attacks, that the study of exosporium composition regained interest and by 2002, the first exosporium protein, BclA, was characterized as the main component of the hair-like exosporium nap (Sylvestre *et al.*, 2002). To date, more than 20 proteins have been identified in the exosporium fraction (Lai *et al.*, 2003; Redmond *et al.*, 2004; Steichen *et al.*, 2003; Todd *et al.*, 2003), and at least 10 proteins, ExsFA/BxpB, ExsA, CotY, ExsY, ExsFB, CotE, Alr, ExsJ/BclB, ExsK, BxpA have been described as actual components (Bailey-Smith *et al.*, 2005; Boydston *et al.*, 2006; Giorno *et al.*, 2007; Johnson *et al.*, 2006; Moody *et al.*, ; Severson *et al.*, 2009; Steichen *et al.*, 2005, 2007; Sylvestre *et al.*, 2005; Thompson *et al.*, 2007). In this work, the composition of the exosporium of *B. cereus* ATCC 4342 is described. *B. cereus* ATCC 4342 is a gamma phage-susceptible strain, which also displays other features typical of *B. anthracis* such as colony morphology, filamentous growth and characteristic sequences in the hypervariable *vrra* locus (Schuch *et al.*, 2002). Therefore, the results obtained with *B. cereus* ATCC 4342 may also be applicable for *B.*

anthracis. In this respect, all of the exosporium proteins identified are encoded in the chromosome, and there are no differences in exosporium composition between fully virulent *B. anthracis* and strains lacking pXO1 or pX01 and pX02 (Redmond *et al.*, 2004).

This is the first analysis of exosporium proteins extracted with 2% β–mercaptoethanol under alkaline conditions. In previous studies, exosporium proteins were extracted either with a combination of urea and β–mercaptoethanol from *B. anthracis* spores (Redmond *et al.*, 2004; Sylvestre *et al.*, 2003), or SDS and β–mercaptoethanol from *B. cereus* and *B. anthracis* isolated exosporiums (Steichen *et al.*, 2003; Todd *et al.*, 2003). The study of proteins extracted under different conditions is important because, as with the case of coat protein extraction, each treatment solubilizes a different set of proteins (Henriques and Moran, 2000). For example, in this study, two characterized components of the basal layer exosporium, ExsFA/BxpB and CotY, were not found in the β–mercaptoethanol extract, but were identified when the exosporium was extracted by sonication. As seen under SEM, β–mercaptoethanol treatment did not alter the overall integrity of the exosporium, thus, it may have not solubilized all the proteins present on the basal layer. In addition, approximately 40% of the proteins extracted with β–mercaptoethanol had not been previously reported. While a few of these proteins are probably strain-specific and therefore only present in *B. cereus* ATCC 4342 exosporium, others may only be extracted under these conditions. A few hypothetical proteins (bcere0010_29950, bcere0010_42210, bcere001023240, Bc_5206,) have no

homologs in *Bacillus subtilis* whose spores do not have a conspicuous exosporium. Consequently, these proteins are probably *bona fide* components of the exosporium.

Analysis of the protein composition of the exosporium revealed proteins that are not usually present in the outer layers of the spores. Small acid soluble proteins (SASP) are synthesized in the forespore and localized in the core of the mature spore (Setlow and Waites, 1976). The large amount of SASP (20% of the total spore protein content) suggests that these proteins are present as a contaminant in other spore layers. For example, in *B. subtilis*, two SASP proteins, SspA and SspE, also have been found in the coat (Lai *et al.*, 2003). Therefore, traces of SASP present in the exosporium were probably detected by highly sensitive techniques such as LC-LC/MS. However, the passage of proteins from the core to the outer layers is highly restricted due to the presence of the cortex and the coat. In this respect, SASP proteins may then be actual components of the exosporium. Inactivation of locus bcere0010_44320, which encodes a SASP identified in *B. cereus* ATCC 4342 exosporium, had no effect on the exosporium structure. While no additional exosporium functions were assessed in this mutant, it is most probable that SASP bcere0010_44320 is not a structural component of the exosporium.

Exosporium proteins SoaA, BxpA, ExsK have an alternative localization in the spore, and when studied by immuno-electron microscopy, they are found predominantly in the cortex (Cote *et al.*, 2008; Moody *et al.*, ; Severson *et al.*, 2009). In this study, a putative cortex protein, bcere0010_42210, belonging to the *B. subtilis* YhcN/YlaJ

superfamily, was identified in *B. cereus* ATCC 4342 exosporium. While absence of SoaA, BxpA and ExsK during sporulation has no effect on the spore structure (Cote *et al.*, 2008; Moody *et al.*, ; Severson *et al.*, 2009), inactivation of bcere0010_42210 resulted in spores with an abnormal cortex that turned phase gray spontaneously due to loss of dipicolinic acid (DPA) from the spore core. The abnormal cortex phenotype was also conserved in *B. anthracis* ΔSterne BAS4323 null mutant spores. Interestingly, *B. subtilis yhcN* null mutant spores show no structural defects on the cortex (Bagyan *et al.*, 1998). Absence of bcere0010_42210 had no effects on the structure of the exosporium. Consequently, further functional and localization studies are necessary to corroborate that bcere0010_42210 is an actual exosporium component. In *B. subtilis*, YhcN/YlaJ expression is under the regulation of σ^G (Bagyan *et al.*, 1998), but the bcere0010_42210 promoter region did not contain a clear consensus sequence for any of the sporulation sigma factors. In the chromosome, the bcere0010_42210 locus is next to *exsA*, a protein that participates in the assembly of both the coat and exosporium (Bailey-Smith *et al.*, 2005), although it does not appear that they form part of a single operon, due to the size of the intergenic region between these two genes. In all, protein bcere0010_42210 may be participating in the assembly of the spore cortex in *B. cereus* and *B. anthracis*.

Crosslinking of proteins is an important mechanism for spore maturation. It has been mainly studied in *B. subtilis* coat, where protein crosslinking contributes to its chemical and mechanical resistance properties (Henriques and Moran, 2000). The extent of protein crosslinking in the exosporium has not yet been studied, and only one exosporium protein, BxpA, has been found to be processed and crosslinked in *B.*

anthracis (Moody *et al.*). Comparison of reducing and non-reducing SDS-PAGE of exosporium proteins extracted by sonication showed the prevalence of disulfide bonds in this layer. In addition, the identification of thioredoxin in *B. cereus* ATCC 4342 exosporium suggests that di-cysteine bonds are enzymatically facilitated (Kadokura *et al.*, 2003). Tgl, an enzyme that catalyzes ε–(γ glutamyl)-lysine bonds, is also present in the exosporium, and participates in BxpA crosslinking. In this regard, inactivation of *gerQ* resulted in a brittle exosporium that appeared fragmented under TEM in both *B. cereus* ATCC 4342 and *B. anthracis* ΔSterne. GerQ is crosslinked by Tgl in the spore coat of *B. subtilis* (Ragkousi and Setlow, 2004); therefore absence of GerQ may alter the level of crosslinking in the exosporium, affecting its rigidity and mechanical resistance. When Tgl was inhibited with the competitor inhibitor monodansylcadaverine (MDC) during *B. cereus* ATCC 4342 sporulation, solubilization of exosporium small peptides was increased after treatment with β–mercaptoethanol. These results suggest that, like in the coat, exosporium maturation involves formation of insoluble protein complexes by YabG proteolysis and Tgl crosslinking, as well as disulfide bonds catalyzed by thioredoxin. Other types of protein crosslinking, such as O-O' di-tyrosine bonds may also be present in the exosporium.

Only one of the *B. cereus* ATCC 4342 spore mutants, bcere0100_22100 null strain, had a delay in sporulation. Resistance to chloroform vapors reached wild-type levels at 48 hs, indicating that sporulation was not blocked. Mutant spores have no visible structural defects under TEM and SEM. Then, absence of this protein (bcere0100_22100) during sporulation may affect deposition of the coat, which is the

spore layer that confers resistance to organic solvent, retarding the appearance of chloroform resistant spores. A *B. anthracis* BAS2264 null strain also showed a similar delay when tested, which was expected as BAS2264 has 100% similarity to bcere0100_22100. There are no homologs for bcere0010_22100 outside the *B. cereus* group and it does not contain any known protein domains. The chromosomal region where bcer0010_22100 is located contains three other genes that encode for *B. cereus* group specific proteins. All these genes are expressed during sporulation in *B. anthracis* (Bergman *et al.*, 2006), suggesting that they constitute a gene cluster that is involved in assembly of *B. cereus*/*B. anthracis* spore outer layer. Deletion of the whole gene cluster and study of its effects on the mutant spores would provide insights in exosporium formation in *B. cereus* and *B. anthracis* spores.

Rbp is a novel exosporium protein that may participate in the formation of the hair-like nap of *B. cereus* ATCC 4342 spores. Rbp has neither homology to BclA, the main component of *B. anthracis* nap, nor it is a collagen-like protein. Rather, it contains 23 N-glycosylation sites and 9 DUF11 domains, which are usually present in cell surface proteins (Finn *et al.*, 2006). To distinguish whether Rbp is an actual component of the hair-like projections or participates in their assembly, immuno-electron microscopy studies are necessary. Still, Rbp appeared to have no visible effect on the assembly of most of the exosporium proteins, as a comparison of wild-type and *rbp* exosporium protein profiles only differed in one band that corresponded to Rbp based on LC-MS/MS data. Interestingly, *Clostridium taeniosporum*, whose spores also have a hair-like nap on their surface, contains two homologs of Rbp, p29a and p29b, and a BclA homolog, GP85

(Walker *et al.*, 2007). In the chromosome, *GP85, p29a, p29,* loci are contiguous suggesting that these proteins act together. In the mass spectrometry of *B. cereus* ATCC 4342, Rbp as well as BclA were identified, arguing that both proteins are present in the exosporium and are not mutually exclusive components of the hair-like nap. Participation of Rbp in *B. anthracis* hair-like nap formation has not yet been studied. However, previous proteomic studies of the *B. anthracis* exosporium have not identified Rbp in their samples (Lai *et al.*, 2003; Redmond *et al.*, 2004; Steichen *et al.*, 2003). Whether Rbp forms part of the *B. anthracis* nap is important, as it can be used for the development of assays to distinguish between these two organisms. Also, differences in protein composition of the nap, which is the first point of contact with the host, may reflect adaptation to the different pathogenicity displayed by *B. anthracis* and *B. cereus*. For example, since BclA inhibits adhesion to epithelial cells of *B. anthracis* spores (Bozue *et al.*, 2007b), the presence of Rbp on the surface of *B. cereus* spores may promote interaction with epithelial cells and increase the persistence of *B. cereus* in the intestinal milleu.

Several putative exosporium proteins had no effect on the structure of the exosporium when their encoding genes were inactivated by insertional mutagenesis. These proteins, becer0100_38120 and bcer0010_22100, have no homologs in *B. subtilis* and hence are good candidates to compose the exosporium. Additional studies based on immuno-techniques are necessary to determine the actual localization of these proteins on the spore. In addition, the absence of any of these proteins (ExsK, bcer0100_38120 and bcer0010_22100) did not alter the rate of sporulation or the overall exosporium protein

composition. However, we cannot discard the idea that these proteins may play a role in germination or other functional parameters of the exosporium that were not assessed in this work. In *B. subtilis*, deletion of several coat genes has no obvious effect on the coat, indicating that many of these proteins are redundant (Driks, 2002). The same phenomenon may be happening in the exosporium as its properties may emerge from the interaction of many proteins that can compensate for the absence of just one.

The exosporium is the first point of contact with the environment, so variability in its composition is expected between organisms that differ in ecology and pathogenecity. Comparison of the composition of the exosporium extracted by sonication or β–mercaptoethanol treatment between *B. cereus* strains and *B. anthracis* revealed little co-migration of proteins in SDS-PAGE. Some of the differences seen on the *B. cereus*/*B. anthracis* protein profiles correspond to protein polymorphism, such as the case of BclA and ExsJ/Bclb, while others differences are the result of the presence of strain specific proteins. In this regard, *B. cereus* ATCC 14579 and *B. cereus* ATCC 4342 shared certain core exosporium proteins, but differed with others based on proteomic analysis. Post-translational modifications (proteolysis, crosslinking and glycosilation) that occur during maturation of the exosporium also contribute to the differences observed in the protein profiles. For example, CotE had an apparent molecular weight of 20 kDa in *B. cereus* ATCC 4342 but in *B. cereus* ATCC 10579, its apparent molecular weight was 12 kDa (Todd *et al.*, 2003). The glycosylation pattern of the exosporium also differs between *B. cereus* strains and *B. anthracis*. In *B. cereus* exosporium, Bclb/ExsJ was the main glycosylated protein, while BclA is the major glycosylated protein in *B. anthracis*

exosporium (Steichen *et al.*, 2003; Thompson *et al.*, 2007). It is important to note that *B. anthracis* exosporium also contains BclB/ExsJ (Thompson *et al.*, 2007). Therefore, the differences observed between *B. anthracis* and *B. cereus* glycoprotein profiles could respond to different levels of ExsF/BclB glycosylation in these organisms, or differences in the extractability of this protein from each exosporium. This is the first time that the main glycosilated protein of the *B. cereus* exosporium was identified. However, differences in the sugar residues present in the exosporium of these two organisms have previously been described (Dong *et al.*, 2008). The exosporium of *B. anthracis* (and other highly virulent strains: *B. cereus* E33L and *B. thuringiensis* Al Hakam) contains high amount of anthrose, an unusual terminal sugar, which is only present in very low quantities or not at all in *B. cereus*. Protein glycosylation is linked to pathogenesis (Schmidt *et al.*, 2003), therefore it would be interesting to study how different patterns of glycosilation of ExsJ/BclB and BclA affect the infectivity properties of *B. cereus* and *B. anthracis*. While *B. cereus* spores have to persist on the intestinal epithelial long enough to germinate and produce enterotoxins, *B. anthracis* phagocytosis by macrophages is an essential step for initiation of infection (Guidi-Rontani, 2002).

Assembly of the Exosporium

Absence of either BclA, ExsY, ExsFA/BxpB, ExsA, CotE or BclB during sporulation results in an exosporium that is incomplete, damaged or unattached, depending on the specific protein that is missing (Bailey-Smith *et al.*, 2005; Boydston *et al.*, 2006; Giorno *et al.*, 2007; Johnson *et al.*, 2006; Steichen *et al.*, 2005; Sylvestre *et al.*, 2005; Thompson *et al.*, 2007). In this study, a new exosporium protein is described, ExsM, and a new phenotype, the double layer exosporium that resulted from its absence. These two separate layers that surrounded the spore possessed a hair-like nap facing the exterior of the spore, implying that the double layer exosporium is not the product of a simple invagination; yet, we cannot discard that the double layer configuration could have been the result of one convoluted layer, which may appear like two layers under the electron microscope.

While exosporium formation occurs without a visible connection to the rest of the spore, some communication through the interspace between these two structures is necessary to obtain a closed layer (Giorno *et al.*, 2007). It is possible that ExsM forms part of this communication system and its absence promotes disorder in the interspace that leads to the construction of a second exosporium. Also, it could be also possible that ExsM inhibits the formation an extra exosporium layer. Since the exosporium is a self-assembled structure, its synthesis needs to be tightly regulated to avoid spontaneous aggregation of exosporium protein at the wrong location or time. In this regard, a low percentage of wild-type *B. anthracis* spores presented lamellas in their interspace (Data

not shown), indicating the importance of this kind of regulation. Another possibility is that ExsM may participate in formation of the cap. In this case, absence of a defined cap during sporulation of *exsM* spores can lead to lack of polarity of the exosporium and result in duplication of this structure. Although additional experiments are needed to distinguish between these different options, studies with the ExsM-GFP showed that ExsM is present at the correct time and initial site of exosporium formation and suggested that this protein acts as a regulator of this process.

ExsM conforms a single CHRD domain, a novel protein motif identified in chordin, a secreted animal protein that participates in embryonic development (Hyvonen, 2003). In vertebrates, chordin dorsalizes early embryonic tissue by binding and sequestering bone morphogenetic proteins or BMP (De Robertis and Kuroda, 2004). BMP interaction is mediated through the cysteine rich domains of chordin (also known as vWC domains), while there is no functional prediction for CHRD (Yu *et al.*, 2004). Other microbial proteins containing a CHRD domain have been identified in *Brucella melitensis, Streptomyces avermitilis, Burkholderia fungorum, Bradyrhizobium japonicum* between others; however, none of these proteins have been characterized (Hyvonen, 2003). These bacterial proteins differentiate from ExsM in that they are larger, and thus, the CHRD domain does not constitute the whole protein. In addition, no protein with a CHRD motif has been identified in archae, yeast or plants. The C-terminus of ExsM is positively charged, while a very negatively charge C-terminal domain is present in ExsA and CotE, two proteins that participate in the attachment of the exosporium to the rest of the spore (Bailey-Smith *et al.*, 2005; Giorno *et al.*, 2007). While the actual role of ExsM

during exosporium assembly is unknown, its C-terminal domain may play a role in the localization of ExsM at the site of exosporium formation or in assembly of the exosporium itself by electrostatic interactions with CotE and ExsA. This interaction between ExsM and other negatively charged proteins might even form part of the proposed communication system between the spore and the nascent exosporium through the interspace (Giorno *et al.*, 2007).

In *B. anthracis*, the effect of *exsM* inactivation resulted in a partial phenotype in which the internal layer did not surround the whole spore. This partial double layer exosporium could be due to the presence of a paralogue of *exsM* in the *B. anthracis* genome. A paralogue with 40% identity and 62% similarity to ExsM has been identified in the exosporium of *B. anthracis* and named BxpC (Steichen *et al.*, 2003). While inactivation of this gene alone did not affect neither the spore size nor the structure of the exosporium, it could be compensating for the function of ExsM during exosporium formation in the mutants, even though BxpC does not have a positively charged C-terminal domain like ExsM (Fig. 58). Alternatively, the *B. anthracis exsM* partial phenotype may be due to insufficient production of enough exosporium protein to construct two complete layers. Exosporium protein expression was not upregulated in the *B. cereus* ATCC 4342 *exsM* mutant. But, *B. cereus* spores have a larger exosporium; thus, there is more protein available for a double layer exosporium. Additional studies with double mutants for ExsM and BxpC are necessary to distinguish between these two options.

ExsM

MTTHFFARLTGKREIPPVNTEAYGVAEFIFSEDLKKLQYRVILKNIEKVTSCQIHLGKSDQIGPIVLSL
LGPLKQGISVNEGVVTGVVNVEEFEGPLQGRAFDSLLQEIIQANVYVNVYTKSNKKGEIRGRIRKVKK

BxpC

MFFAKLRGRNEVPPVETDARGEAFFKLSRDELSLKFKLDLFDIEDVVAAHLHIGAKGTNGPVVAFLFGP
ITNPVSIECATLTGMITQEDLVGPLAGQTLGTLINEIISGNIYINVHTVQHPNGEIRGQLNYC

Fig. 58: ExsM and BxpC sequence. *B. anthracis* Sterne ExsM and BxpC amino acid sequence. Positively charged residues are colored in red.

Roles of the Exosporium

Exosporium and coat protein profiles showed that ExsM-deficient spores did not have a defect in the composition of the exosporium or the coat. In addition, spore resistance to organic solvents, usually associated with coat functionality, was not affected either. However, the presence of a double layer exosporium increased spore resistance to lysozyme, which agrees with one of the proposed functions of the exosporium as a barrier for harmful macromolecules (Ball *et al.*, 2008; Gerhardt and Black, 1961; Gerhardt, 1967). Electron crystallography analysis revealed that the exosporium is indeed a semi-permeable layer that would prevent the passage of degradative enzymes (Ball *et al.*, 2008). In the past, there have been conflicting results about the contribution of this outer spore layer to lysozyme resistance when the exosporium is missing or has been mechanically removed (Johnson *et al.*, 2006). Here, we found some variability in the susceptibility to lysozyme between different preparations of wild-type spores, which can explain how a small effect of the exosporium could have been missed.

The exosporium contains proteins that inhibit germination: Alr, Iunh (Chesnokova *et al.*, 2009; Liang *et al.*, 2008; Yan *et al.*, 2007). While spores with a double exosporium germinated more slowly in response to L-alanine, it is not clear if the Alr inhibitory effect seen with *exsM* spores was due to an increased amount of this enzyme or its particular localization in two consecutive layers. Extraction of the mutant exosporium with 2% β-mercaptoethanol showed an increased amount of protein running at 45 kDa, which could reflect an increase in Alr whose theoretical molecular weight is 43.7 kDa. However, this increment was very subtle and it was not observed in the protein profiles from exosporium extracted by sonication. No suppressing effect on germination was noticed by Alr and Iunh when spores were germinated with both L-alanine and inosine mixture, aside from a very small lag (1½ min) in the germination of mutant *exsM* spores. L-alanine and inosine act synergically to induce germination (Clements and Moir, 1998), and therefore the inhibitory effects may not be measurable in this case. When wild-type spores were germinated only with inosine, they showed a biphasic response curve, which is unique to *B. cereus* ATTC 4342. This was not the case for *exsM* spores, which did not present the fast response phase, probably due to effect of Iunh. The kinetics of germination in the presence of inosine and L-serine also differed between wild-type and *exsM* spores. In all, a negative role for the exosporium on the initiation of germination was slightly enhanced in the double layer exosporium spores.

At the same time, double exosporium spores also presented a more efficient germination induced by inosine, L-alanine and inosine, L-serine and inosine, and when germination was tested in complete medium (50% BHI). Also, after pretreatment with an

inhibitor of Alr, the mutant spores had a more complete germination in the presence of L-alanine. The positive effect of the exosporium in germination efficiency may be related to its role in protecting the spore from the action of hydrolytic enzymes (Ball *et al.*, 2008; Gerhardt and Black, 1961; Gerhardt, 1967). Germination depends on the integrity of all layers of the spore, and if the cortex, coat or another layer has been compromised, germination will typically be blocked (Paidhungat, 2002). It has been previously described that presence of Alr on the exosporium spores suppresses premature germination of nascent *B. anthracis* spores during late stages of sporulation, when mother lysis occurs and there is an abundance of germinants (Chesnokova *et al.*, 2009). Likewise, the exosporium could also be protecting the spore from hydrolytic enzyme damage during cell mother lysis. Presence of a double exosporium may then increase the amount of spores with less damage that could respond more readily to the presence of germinants. In addition, efficiency of germination increases with the concentration of germinant or the number of receptors per the spores (Ghosh and Setlow, 2009); and so, an alternative but not mutually exclusive possibility is that the exosporium promotes interaction between germinants and germinant receptors by an unknown mechanism that may involve the interspace environment. When *B. cereus* 569 spore germination is induced with inosine, the bacteria release L-alanine that then acts as a co-germinant, like an autocrine signal (Dodatko *et al.*, 2009). The exosporium and/or interspace may play a role in this positive feedback loop, for example, by limiting the diffusion of L-alanine into the environment and thus, increasing the interaction of L-alanine with the spore own germinant receptors.

In conclusion, the role of the exosporium in germination is more complex than ever thought before. The results in this study suggest that the exosporium not only affects the timing of germination by degrading small amounts of germinants, but also promotes germination in the presence of the right amount of nutrients, which agrees with previous observations that the absence of a functional exosporium affects negatively germination (Giorno *et al.*, 2007; Giorno *et al.*, 2009).

Steichen *et al*. showed that outgrowing cells always escape from the spore shell through the exosporium cap, which may be a weakened spot to facilitate such escape (Steichen *et al.*, 2007). Using this escape mechanism, the new vegetative cell is able to suddenly burst and separate from its exosporium in less than 1 s. We have shown that the presence of the double layer exosporium slowed down outgrowth, probably because it presented a greater physical barrier to the escape process. It would be interesting to see how our result fits the "bottle cap model" by investigating if the mutant double exosporium possesses one cap on each layer or if any of the layers are homogeneous.

Although the presence of a double exosporium seems to benefit the spore in terms of lysozyme resistance and germination, it also altered the outgrowth process and the overall morphology of the spore. Being in direct contact with the environment, the exosporium is believed to participate in adhesion to abiotic surfaces and live tissues. In *B. cereus*, interaction with epithelial tissues has been shown to start by attachment of the exosporium 'tail' (Panessa-Warren *et al.*, 2007). Therefore, a change in the shape of the exosporium could be detrimental to the spore, especially for food-poisoning strains that

need to persist in the intestinal tract to germinate and produce enterotoxins (Granum, 1997). In addition, *exsM* spores presented less size variability across its population. This constriction in the spore size can be a direct by-product of the presence of a double layer exosporium or it could be related to a compromised interspace, which is believed to have a spring-like nature (Giorno *et al.*, 2007). It is not clear how this may affect the survival of the mutant spores in the environment, but it is possible that a reduction in heterogeneity of the spore population can diminish adaptation to an environment that may have changed since the moment of sporulation.

Summary

The surface of *B. cereus* and *B. anthracis* spores is highly adapted to the different pathogenicity and ecological properties of each organism. While sharing a set of common proteins, variability in the exosporium composition between *B.cereus* strains and *B. anthracis* resulted not only from the presence of strain–specific proteins, but also from differences in glycosilation, processing and crosslinking that occurs during exosporium maturation. The study of the *B. cereus* ATCC 4342 exosporium also helped to understand the *B. anthracis* exosporium, as the phenotypes of the mutant spores were conserved across both organisms. A new protein, Rbp, involved in nap formation was also described, indicating that the spore surface is defined by more than one protein. Construction of the exosporium is a non-continuous process that needs to be strictly controlled to ensure the correct self-assembly of at least 20 proteins. In this study, a novel spore protein ExsM, which participates in the regulation of exosporium assembly, has

been identified and characterized. Absence of this protein during sporulation affected spore morphology and resulted in spores that were shorter than wild-type. Additionally, *exsM* spores, encased by a double layer exosporium, allowed us to investigate the role of the exosporium in a new way. It was demonstrated that the exosporium provides protection against lysozyme, enhances germination efficiency and participates in the outgrowth of the nascent cell. In all, the exosporium seems to play an important role in timing both germination and outgrowth, two processes that need to occur under the right conditions to maximize the survival of the nascent vegetative cell and are central to the pathogenesis of *B. cereus* and *B. anthracis* (Mock and Fouet, 2001; Stenfors Arnesen *et al.*, 2008).

References

Abanes-De Mello, A., Sun, Y.L., Aung, S., and Pogliano, K. (2002) A cytoskeleton-like role for the bacterial cell wall during engulfment of the Bacillus subtilis forespore. *Genes Dev* **16**: 3253-3264.

Abrami, L., Reig, N., and van der Goot, F.G. (2005) Anthrax toxin: the long and winding road that leads to the kill. *Trends Microbiol* **13**: 72-78.

Agaisse, H., Gominet, M., Okstad, O.A., Kolsto, A.B., and Lereclus, D. (1999) PlcR is a pleiotropic regulator of extracellular virulence factor gene expression in Bacillus thuringiensis. *Mol Microbiol* **32**: 1043-1053.

Agata, N., Mori, M., Ohta, M., Suwan, S., Ohtani, I., and Isobe, M. (1994) A novel dodecadepsipeptide, cereulide, isolated from Bacillus cereus causes vacuole formation in HEp-2 cells. *FEMS Microbiol Lett* **121**: 31-34.

Agata, N., Ohta, M., Mori, M., and Isobe, M. (1995) A novel dodecadepsipeptide, cereulide, is an emetic toxin of Bacillus cereus. *FEMS Microbiol Lett* **129**: 17-20.

Agrawal, A., Lingappa, J., Leppla, S.H., Agrawal, S., Jabbar, A., Quinn, C., and Pulendran, B. (2003) Impairment of dendritic cells and adaptive immunity by anthrax lethal toxin. *Nature* **424**: 329-334.

Alam, S., Gupta, M., and Bhatnagar, R. (2006) Inhibition of platelet aggregation by anthrax edema toxin. *Biochem Biophys Res Commun* **339**: 107-114.

Alper, S., Duncan, L., and Losick, R. (1994) An adenosine nucleotide switch controlling the activity of a cell type-specific transcription factor in B. subtilis. *Cell* **77**: 195-205.

Anderson, I., Sorokin, A., Kapatral, V., Reznik, G., Bhattacharya, A., Mikhailova, N., Burd, H., Joukov, V., Kaznadzey, D., Walunas, T., Markd'Souza, Larsen, N., Pusch, G., Liolios, K., Grechkin, Y., Lapidus, A., Goltsman, E., Chu, L., Fonstein, M., Ehrlich, S.D., Overbeek, R., Kyrpides, N., and Ivanova, N. (2005) Comparative genome analysis of Bacillus cereus group genomes with Bacillus subtilis. *FEMS Microbiol Lett* **250**: 175-184.

Andersson, A., Ronner, U., and Granum, P.E. (1995) What problems does the food industry have with the spore-forming pathogens Bacillus cereus and Clostridium perfringens? *Int J Food Microbiol* **28**: 145-155.

Andersson, A., Granum, P.E., and Ronner, U. (1998) The adhesion of Bacillus cereus spores to epithelial cells might be an additional virulence mechanism. *Int J Food Microbiol* **39**: 93-99.

Ankolekar, C., and Labbe, R.G. Physical characteristics of spores of food-associated isolates of the Bacillus cereus group. *Appl Environ Microbiol* **76**: 982-984.

Arigoni, F., Duncan, L., Alper, S., Losick, R., and Stragier, P. (1996) SpoIIE governs the phosphorylation state of a protein regulating transcription factor sigma F during sporulation in Bacillus subtilis. *Proc Natl Acad Sci U S A* **93**: 3238-3242.

Aronson, A.I., and Fitz-James, P.C. (1971) Reconstitution of bacterial spore coat layers in vitro. *J Bacteriol* **108**: 571-578.

Aronson, A.I., and Fitz-James, P. (1976) Structure and morphogenesis of the bacterial spore coat. *Bacteriol Rev* **40**: 360-402.

Ash, C., Farrow, J.A., Dorsch, M., Stackebrandt, E., and Collins, M.D. (1991) Comparative analysis of Bacillus anthracis, Bacillus cereus, and related species on

the basis of reverse transcriptase sequencing of 16S rRNA. *Int J Syst Bacteriol* **41**: 343-346.

Atrih, A., Zollner, P., Allmaier, G., Williamson, M.P., and Foster, S.J. (1998) Peptidoglycan structural dynamics during germination of Bacillus subtilis 168 endospores. *J Bacteriol* **180**: 4603-4612.

Atrih, A., and Foster, S.J. (2001) In vivo roles of the germination-specific lytic enzymes of Bacillus subtilis 168. *Microbiology* **147**: 2925-2932.

Bagyan, I., Hobot, J., and Cutting, S. (1996) A compartmentalized regulator of developmental gene expression in Bacillus subtilis. *J Bacteriol* **178**: 4500-4507.

Bagyan, I., Noback, M., Bron, S., Paidhungat, M., and Setlow, P. (1998) Characterization of yhcN, a new forespore-specific gene of Bacillus subtilis. *Gene* **212**: 179-188.

Bai, U., Mandic-Mulec, I., and Smith, I. (1993) SinI modulates the activity of SinR, a developmental switch protein of Bacillus subtilis, by protein-protein interaction. *Genes Dev* **7**: 139-148.

Bailey-Smith, K., Todd, S.J., Southworth, T.W., Proctor, J., and Moir, A. (2005) The ExsA protein of Bacillus cereus is required for assembly of coat and exosporium onto the spore surface. *J Bacteriol* **187**: 3800-3806.

Baldus, J.M., Green, B.D., Youngman, P., and Moran, C.P., Jr. (1994) Phosphorylation of Bacillus subtilis transcription factor Spo0A stimulates transcription from the spoIIG promoter by enhancing binding to weak 0A boxes. *J Bacteriol* **176**: 296-306.

Ball, D.A., Taylor, R., Todd, S.J., Redmond, C., Couture-Tosi, E., Sylvestre, P., Moir, A., and Bullough, P.A. (2008) Structure of the exosporium and sublayers of spores of

the Bacillus cereus family revealed by electron crystallography. *Mol Microbiol* **68**: 947-958.

Banks, D.J., Barnajian, M., Maldonado-Arocho, F.J., Sanchez, A.M., and Bradley, K.A. (2005) Anthrax toxin receptor 2 mediates Bacillus anthracis killing of macrophages following spore challenge. *Cell Microbiol* **7**: 1173-1185.

Barbosa, T.M., Serra, C.R., La Ragione, R.M., Woodward, M.J., and Henriques, A.O. (2005) Screening for bacillus isolates in the broiler gastrointestinal tract. *Appl Environ Microbiol* **71**: 968-978.

Barlass, P.J., Houston, C.W., Clements, M.O., and Moir, A. (2002) Germination of Bacillus cereus spores in response to L-alanine and to inosine: the roles of gerL and gerQ operons. *Microbiology* **148**: 2089-2095.

Bartkus, J.M., and Leppla, S.H. (1989) Transcriptional regulation of the protective antigen gene of Bacillus anthracis. *Infect Immun* **57**: 2295-2300.

Basu, S., Kang, T.J., Chen, W.H., Fenton, M.J., Baillie, L., Hibbs, S., and Cross, A.S. (2007) Role of Bacillus anthracis spore structures in macrophage cytokine responses. *Infect Immun* **75**: 2351-2358.

Beaman, T.C., Pankratz, H.S., and Gerhardt, P. (1971) Paracrystalline sheets reaggregated from solubilized exosporium of Bacillus cereus. *J Bacteriol* **107**: 320-324.

Beaman, T.C., Pankratz, H.S., and Gerhardt, P. (1972) Ultrastructure of the exosporium and underlying inclusions in spores of Bacillus megaterium strains. *J Bacteriol* **109**: 1198-1209.

Beecher, D.J., and Macmillan, J.D. (1991) Characterization of the components of hemolysin BL from Bacillus cereus. *Infect Immun* **59**: 1778-1784.

Beecher, D.J., Schoeni, J.L., and Wong, A.C. (1995) Enterotoxic activity of hemolysin BL from Bacillus cereus. *Infect Immun* **63**: 4423-4428.

Beecher, D.J., and Wong, A.C. (1997) Tripartite hemolysin BL from Bacillus cereus. Hemolytic analysis of component interactions and a model for its characteristic paradoxical zone phenomenon. *J Biol Chem* **272**: 233-239.

Ben-Yehuda, S., and Losick, R. (2002) Asymmetric cell division in B. subtilis involves a spiral-like intermediate of the cytokinetic protein FtsZ. *Cell* **109**: 257-266.

Ben-Yehuda, S., Rudner, D.Z., and Losick, R. (2003) RacA, a bacterial protein that anchors chromosomes to the cell poles. *Science* **299**: 532-536.

Bergman, N.H., Anderson, E.C., Swenson, E.E., Niemeyer, M.M., Miyoshi, A.D., and Hanna, P.C. (2006) Transcriptional profiling of the Bacillus anthracis life cycle in vitro and an implied model for regulation of spore formation. *J Bacteriol* **188**: 6092-6100.

Beyer, W., and Turnbull, P.C. (2009) Anthrax in animals. *Mol Aspects Med* **30**: 481-489.

Bongiorni, C., Stoessel, R., Shoemaker, D., and Perego, M. (2006) Rap phosphatase of virulence plasmid pXO1 inhibits Bacillus anthracis sporulation. *J Bacteriol* **188**: 487-498.

Bowen, W.R., Fenton, A.S., Lovitt, R.W., and Wright, C.J. (2002) The measurement of Bacillus mycoides spore adhesion using atomic force microscopy, simple counting methods, and a spinning disk technique. *Biotechnol Bioeng* **79**: 170-179.

Boydston, J.A., Chen, P., Steichen, C.T., and Turnbough, C.L., Jr. (2005) Orientation within the exosporium and structural stability of the collagen-like glycoprotein BclA of Bacillus anthracis. *J Bacteriol* **187**: 5310-5317.

Boydston, J.A., Yue, L., Kearney, J.F., and Turnbough, C.L., Jr. (2006) The ExsY protein is required for complete formation of the exosporium of Bacillus anthracis. *J Bacteriol* **188**: 7440-7448.

Bozue, J., Cote, C.K., Moody, K.L., and Welkos, S.L. (2007a) Fully virulent Bacillus anthracis does not require the immunodominant protein BclA for pathogenesis. *Infect Immun* **75**: 508-511.

Bozue, J., Moody, K.L., Cote, C.K., Stiles, B.G., Friedlander, A.M., Welkos, S.L., and Hale, M.L. (2007b) Bacillus anthracis spores of the bclA mutant exhibit increased adherence to epithelial cells, fibroblasts, and endothelial cells but not to macrophages. *Infect Immun* **75**: 4498-4505.

Branda, S.S., Chu, F., Kearns, D.B., Losick, R., and Kolter, R. (2006) A major protein component of the Bacillus subtilis biofilm matrix. *Mol Microbiol* **59**: 1229-1238.

Brunsing, R.L., La Clair, C., Tang, S., Chiang, C., Hancock, L.E., Perego, M., and Hoch, J.A. (2005) Characterization of sporulation histidine kinases of Bacillus anthracis. *J Bacteriol* **187**: 6972-6981.

Burbulys, D., Trach, K.A., and Hoch, J.A. (1991) Initiation of sporulation in B. subtilis is controlled by a multicomponent phosphorelay. *Cell* **64**: 545-552.

Caipo, M.L., Duffy, S., Zhao, L., and Schaffner, D.W. (2002) Bacillus megaterium spore germination is influenced by inoculum size. *J Appl Microbiol* **92**: 879-884.

Callegan, M.C., Kane, S.T., Cochran, D.C., Gilmore, M.S., Gominet, M., and Lereclus, D. (2003) Relationship of plcR-regulated factors to Bacillus endophthalmitis virulence. *Infect Immun* **71**: 3116-3124.

Callegan, M.C., Cochran, D.C., Kane, S.T., Ramadan, R.T., Chodosh, J., McLean, C., and Stroman, D.W. (2006) Virulence factor profiles and antimicrobial susceptibilities of ocular bacillus isolates. *Curr Eye Res* **31**: 693-702.

Camp, A.H., and Losick, R. (2008) A novel pathway of intercellular signalling in Bacillus subtilis involves a protein with similarity to a component of type III secretion channels. *Mol Microbiol* **69**: 402-417.

Camp, A.H., and Losick, R. (2009) A feeding tube model for activation of a cell-specific transcription factor during sporulation in Bacillus subtilis. *Genes Dev* **23**: 1014-1024.

Carniol, K., Eichenberger, P., and Losick, R. (2004) A threshold mechanism governing activation of the developmental regulatory protein sigma F in Bacillus subtilis. *J Biol Chem* **279**: 14860-14870.

Cataldi, A., Fouet, A., and Mock, M. (1992) Regulation of pag gene expression in Bacillus anthracis: use of a pag-lacZ transcriptional fusion. *FEMS Microbiol Lett* **77**: 89-93.

CDC (2009a) Survellaince for foodborne disease outbreak-United State 2006. *Morbid. Mortal. Weekly Rep: CDC survelliance summaries* **58**: 609-615.

CDC (2009b) Anthrax: General Information. In *http://www.cdc.gov/nczved/divisions/dfbmd/diseases/anthrax/*.

Chada, V.G., Sanstad, E.A., Wang, R., and Driks, A. (2003) Morphogenesis of bacillus spore surfaces. *J Bacteriol* **185**: 6255-6261.

Chary, V.K., Xenopoulos, P., and Piggot, P.J. (2006) Blocking chromosome translocation during sporulation of Bacillus subtilis can result in prespore-specific activation of sigmaG that is independent of sigmaE and of engulfment. *J Bacteriol* **188**: 7267-7273.

Cheng, Y.S., and Aronson, A.I. (1977) Alterations of spore coat processing and protein turnover in a Bacillus cereus mutant with a defective postexponential intracellular protease. *Proc Natl Acad Sci U S A* **74**: 1254-1258.

Chesnokova, O.N., McPherson, S.A., Steichen, C.T., and Turnbough, C.L., Jr. (2009) The spore-specific alanine racemase of Bacillus anthracis and its role in suppressing germination during spore development. *J Bacteriol* **191**: 1303-1310.

Chirakkal, H., O'Rourke, M., Atrih, A., Foster, S.J., and Moir, A. (2002) Analysis of spore cortex lytic enzymes and related proteins in Bacillus subtilis endospore germination. *Microbiology* **148**: 2383-2392.

Clements, M.O., and Moir, A. (1998) Role of the gerI operon of Bacillus cereus 569 in the response of spores to germinants. *J Bacteriol* **180**: 6729-6735.

Cleret, A., Quesnel-Hellmann, A., Mathieu, J., Vidal, D., and Tournier, J.N. (2006) Resident CD11c+ lung cells are impaired by anthrax toxins after spore infection. *J Infect Dis* **194**: 86-94.

Cleret, A., Quesnel-Hellmann, A., Vallon-Eberhard, A., Verrier, B., Jung, S., Vidal, D., Mathieu, J., and Tournier, J.N. (2007) Lung dendritic cells rapidly mediate anthrax spore entry through the pulmonary route. *J Immunol* **178**: 7994-8001.

Cohan, F.M. (2002) What are bacterial species? *Annu Rev Microbiol* **56**: 457-487.

Cortezzo, D.E., Koziol-Dube, K., Setlow, B., and Setlow, P. (2004) Treatment with oxidizing agents damages the inner membrane of spores of Bacillus subtilis and sensitizes spores to subsequent stress. *J Appl Microbiol* **97**: 838-852.

Cote, C.K., Bozue, J., Moody, K.L., DiMezzo, T.L., Chapman, C.E., and Welkos, S.L. (2008) Analysis of a novel spore antigen in Bacillus anthracis that contributes to spore opsonization. *Microbiology* **154**: 619-632.

Cowan, A.E., Olivastro, E.M., Koppel, D.E., Loshon, C.A., Setlow, B., and Setlow, P. (2004) Lipids in the inner membrane of dormant spores of Bacillus species are largely immobile. *Proc Natl Acad Sci U S A* **101**: 7733-7738.

Cutting, S., Oke, V., Driks, A., Losick, R., Lu, S., and Kroos, L. (1990a) A forespore checkpoint for mother cell gene expression during development in B. subtilis. *Cell* **62**: 239-250.

Cutting, S., Driks, A., Schmidt, R., Kunkel, B., and Losick, R. (1991) Forespore-specific transcription of a gene in the signal transduction pathway that governs Pro-sigma K processing in Bacillus subtilis. *Genes Dev* **5**: 456-466.

Cutting, S.M., , and B., V.H.P. (1990b) *Molecular Biology Methods for Bacillus.* Chichester, United Kingdom: John Wiley and Sons Ltd.

Cybulski, R.J., Jr., Sanz, P., Alem, F., Stibitz, S., Bull, R.L., and O'Brien, A.D. (2009) Four superoxide dismutases contribute to Bacillus anthracis virulence and provide spores with redundant protection from oxidative stress. *Infect Immun* **77**: 274-285.

Dai, Z., Sirard, J.C., Mock, M., and Koehler, T.M. (1995) The atxA gene product activates transcription of the anthrax toxin genes and is essential for virulence. *Mol Microbiol* **16**: 1171-1181.

Damgaard, P.H. (1995) Diarrhoeal enterotoxin production by strains of Bacillus thuringiensis isolated from commercial Bacillus thuringiensis-based insecticides. *FEMS Immunol Med Microbiol* **12**: 245-250.

Daubenspeck, J.M., Zeng, H., Chen, P., Dong, S., Steichen, C.T., Krishna, N.R., Pritchard, D.G., and Turnbough, C.L., Jr. (2004) Novel oligosaccharide side chains of the collagen-like region of BclA, the major glycoprotein of the Bacillus anthracis exosporium. *J Biol Chem* **279**: 30945-30953.

Day, W.A., Jr., Rasmussen, S.L., Carpenter, B.M., Peterson, S.N., and Friedlander, A.M. (2007) Microarray analysis of transposon insertion mutations in Bacillus anthracis: global identification of genes required for sporulation and germination. *J Bacteriol* **189**: 3296-3301.

DesRosier, J.P., and Lara, J.C. (1981) Isolation and properties of pili from spores of Bacillus cereus. *J Bacteriol* **145**: 613-619.

DesRosier, J.P., and Lara, J.C. (1984) Synthesis of the exosporium during sporulation of *Bacillus cereus*. *J Gen Microbiol* **130**: 935-940.

Didelot, X., Barker, M., Falush, D., and Priest, F.G. (2009) Evolution of pathogenicity in the Bacillus cereus group. *Syst Appl Microbiol* **32**: 81-90.

Diederich, B., Wilkinson, J.F., Magnin, T., Najafi, M., Erringston, J., and Yudkin, M.D. (1994) Role of interactions between SpoIIAA and SpoIIAB in regulating cell-specific transcription factor sigma F of Bacillus subtilis. *Genes Dev* **8**: 2653-2663.

Dierick, K., Van Coillie, E., Swiecicka, I., Meyfroidt, G., Devlieger, H., Meulemans, A., Hoedemaekers, G., Fourie, L., Heyndrickx, M., and Mahillon, J. (2005) Fatal family outbreak of Bacillus cereus-associated food poisoning. *J Clin Microbiol* **43**: 4277-4279.

Dixon, T.C., Meselson, M., Guillemin, J., and Hanna, P.C. (1999) Anthrax. *N Engl J Med* **341**: 815-826.

Doan, T., Morlot, C., Meisner, J., Serrano, M., Henriques, A.O., Moran, C.P., Jr., and Rudner, D.Z. (2009) Novel secretion apparatus maintains spore integrity and developmental gene expression in Bacillus subtilis. *PLoS Genet* **5**: e1000566.

Dodatko, T., Akoachere, M., Muehlbauer, S.M., Helfrich, F., Howerton, A., Ross, C., Wysocki, V., Brojatsch, J., and Abel-Santos, E. (2009) Bacillus cereus spores release alanine that synergizes with inosine to promote germination. *PLoS One* **4**: e6398.

Dong, S., McPherson, S.A., Tan, L., Chesnokova, O.N., Turnbough, C.L., Jr., and Pritchard, D.G. (2008) Anthrose biosynthetic operon of Bacillus anthracis. *J Bacteriol* **190**: 2350-2359.

Driks, A. (1999) Bacillus subtilis spore coat. *Microbiol Mol Biol Rev* **63**: 1-20.

Driks, A. (2002) Maximum shields: the assembly and function of the bacterial spore coat. *Trends Microbiol* **10**: 251-254.

Drobniewski, F.A. (1993) Bacillus cereus and related species. *Clin Microbiol Rev* **6**: 324-338.

Drysdale, M., Heninger, S., Hutt, J., Chen, Y., Lyons, C.R., and Koehler, T.M. (2005) Capsule synthesis by Bacillus anthracis is required for dissemination in murine inhalation anthrax. *Embo J* **24**: 221-227.

Duc le, H., Hong, H.A., Barbosa, T.M., Henriques, A.O., and Cutting, S.M. (2004) Characterization of Bacillus probiotics available for human use. *Appl Environ Microbiol* **70**: 2161-2171.

Duesbery, N.S., Webb, C.P., Leppla, S.H., Gordon, V.M., Klimpel, K.R., Copeland, T.D., Ahn, N.G., Oskarsson, M.K., Fukasawa, K., Paull, K.D., and Vande Woude, G.F. (1998) Proteolytic inactivation of MAP-kinase-kinase by anthrax lethal factor. *Science* **280**: 734-737.

Duncan, L., and Losick, R. (1993) SpoIIAB is an anti-sigma factor that binds to and inhibits transcription by regulatory protein sigma F from Bacillus subtilis. *Proc Natl Acad Sci U S A* **90**: 2325-2329.

Dutz, W., and Kohout-Dutz, E. (1981) Anthrax. *Int J Dermatol* **20**: 203-206.

Duverger, A., Jackson, R.J., van Ginkel, F.W., Fischer, R., Tafaro, A., Leppla, S.H., Fujihashi, K., Kiyono, H., McGhee, J.R., and Boyaka, P.N. (2006) Bacillus anthracis edema toxin acts as an adjuvant for mucosal immune responses to nasally administered vaccine antigens. *J Immunol* **176**: 1776-1783.

Dworkin, J., and Losick, R. (2001) Differential gene expression governed by chromosomal spatial asymmetry. *Cell* **107**: 339-346.

Ehling-Schulz, M., Fricker, M., and Scherer, S. (2004) Bacillus cereus, the causative agent of an emetic type of food-borne illness. *Mol Nutr Food Res* **48**: 479-487.

Ehling-Schulz, M., Svensson, B., Guinebretiere, M.H., Lindback, T., Andersson, M., Schulz, A., Fricker, M., Christiansson, A., Granum, P.E., Martlbauer, E., Nguyen-The, C., Salkinoja-Salonen, M., and Scherer, S. (2005a) Emetic toxin formation of Bacillus cereus is restricted to a single evolutionary lineage of closely related strains. *Microbiology* **151**: 183-197.

Ehling-Schulz, M., Vukov, N., Schulz, A., Shaheen, R., Andersson, M., Martlbauer, E., and Scherer, S. (2005b) Identification and partial characterization of the nonribosomal peptide synthetase gene responsible for cereulide production in emetic Bacillus cereus. *Appl Environ Microbiol* **71**: 105-113.

Ehling-Schulz, M., Guinebretiere, M.H., Monthan, A., Berge, O., Fricker, M., and Svensson, B. (2006) Toxin gene profiling of enterotoxic and emetic Bacillus cereus. *FEMS Microbiol Lett* **260**: 232-240.

Eichenberger, P., Fujita, M., Jensen, S.T., Conlon, E.M., Rudner, D.Z., Wang, S.T., Ferguson, C., Haga, K., Sato, T., Liu, J.S., and Losick, R. (2004) The program of gene transcription for a single differentiating cell type during sporulation in Bacillus subtilis. *PLoS Biol* **2**: e328.

Errington, J. (2003) Regulation of endospore formation in Bacillus subtilis. *Nat Rev Microbiol* **1**: 117-126.

Evans, L., Feucht, A., and Errington, J. (2004) Genetic analysis of the Bacillus subtilis sigG promoter, which controls the sporulation-specific transcription factor sigma G. *Microbiology* **150**: 2277-2287.

Fagerlund, A., Lindback, T., Storset, A.K., Granum, P.E., and Hardy, S.P. (2008) Bacillus cereus Nhe is a pore-forming toxin with structural and functional

properties similar to the ClyA (HlyE, SheA) family of haemolysins, able to induce osmotic lysis in epithelia. *Microbiology* **154**: 693-704.

Fagerlund, A., Kolsto, A.B., and Okstad, O.A. (2009) Differential gene expression and gene regulation during biofilm formation in *Bacillus thuringiensis*. In *Bacillus-ACT 2009* Santa Fe, NM, pp. 28-29.

Fawcett, P., Eichenberger, P., Losick, R., and Youngman, P. (2000) The transcriptional profile of early to middle sporulation in Bacillus subtilis. *Proc Natl Acad Sci U S A* **97**: 8063-8068.

FDA (2007) Soma beverage recalls Metromint flavor water. In *http://www.fda.gov/Safety/Recalls/ArchiveRecalls/2007/ucm112318.htm*.

FDA (2009) Unilever conducts nationwide voluntary recall of Slim Fast Ready-to-Drink products in cans due to possible health risk. In *http://www.fda.gov/Safety/Recalls/ucm192978.htm*.

Feinberg, L., Jorgensen, J., Haselton, A., Pitt, A., Rudner, R., and Margulis, L. (1999) Arthromitus (Bacillus cereus) symbionts in the cockroach Blaberus giganteus: dietary influences on bacterial development and population density. *Symbiosis* **27**: 109-123.

Fernandez J, M.S. (2009) Enzymatic Digestion of Membrane-Bound Proteins for Peptide Mapping and Internal Sequence Analysis. In *The Protein Protocols Handbook*. Walker, J.M. (ed). Totowa, NJ: Humana Press, pp. 927-940.

Finn, R.D., Mistry, J., Schuster-Bockler, B., Griffiths-Jones, S., Hollich, V., Lassmann, T., Moxon, S., Marshall, M., Khanna, A., Durbin, R., Eddy, S.R., Sonnhammer,

E.L., and Bateman, A. (2006) Pfam: clans, web tools and services. *Nucleic Acids Res* **34**: D247-251.

Fisher, N., and Hanna, P. (2005) Characterization of Bacillus anthracis germinant receptors in vitro. *J Bacteriol* **187**: 8055-8062.

Foerster, H.F., and Foster, J.W. (1966) Response of Bacillus spores to combinations of germinative compounds. *J Bacteriol* **91**: 1168-1177.

Foster, S.J.a.P.D.L. (2002) Structure and Synthesis of Cell Wall, Spore Cortex, Teichoic Acids, S-Layers, and Capsules. In *Bacillus subtilis and Its Closest Relatives: From genes to cells*. Sonenshein, A.L.H., J.A.; Losick, R. (ed). Washington D.C.: America Society of Microbiology.

Frandsen, N., and Stragier, P. (1995) Identification and characterization of the Bacillus subtilis spoIIP locus. *J Bacteriol* **177**: 716-722.

Fricker, M., Messelhausser, U., Busch, U., Scherer, S., and Ehling-Schulz, M. (2007) Diagnostic real-time PCR assays for the detection of emetic Bacillus cereus strains in foods and recent food-borne outbreaks. *Appl Environ Microbiol* **73**: 1892-1898.

Fujita, M., and Losick, R. (2002) An investigation into the compartmentalization of the sporulation transcription factor sigmaE in Bacillus subtilis. *Mol Microbiol* **43**: 27-38.

Fujita, M., and Losick, R. (2003) The master regulator for entry into sporulation in Bacillus subtilis becomes a cell-specific transcription factor after asymmetric division. *Genes Dev* **17**: 1166-1174.

Fuller, R. (1989) Probiotics in man and animals. *J Appl Bacteriol* **66**: 365-378.

Gerhardt, P., and Black, S.H. (1961) Permeability of bacterial spores. II. Molecular variables affecting solute permeation. *J Bacteriol* **82**: 750-760.

Gerhardt, P., and Ribi, E. (1964) Ultrastructure of the Exosporium Enveloping Spores of Bacillus Cereus. *J Bacteriol* **88**: 1774-1789.

Gerhardt, P. (1967) Cytology of Bacillus anthracis. *Fed Proc* **26**: 1504-1517.

Gerhardt, P.a.M., R.L. (1989) Spore thermoresistance mechanisms. In *Regulation of Prokaryotic Development*. Smith, I.S., R.A.; Setlow, P. (ed). Washington DC: America Society for Microbiology.

Ghebrehiwet, B., Tantral, L., Titmus, M.A., Panessa-Warren, B.J., Tortora, G.T., Wong, S.S., and Warren, J.B. (2007) The exosporium of B. cereus contains a binding site for gC1qR/p33: implication in spore attachment and/or entry. *Adv Exp Med Biol* **598**: 181-197.

Ghelardi, E., Celandroni, F., Salvetti, S., Fiscarelli, E., and Senesi, S. (2007) Bacillus thuringiensis pulmonary infection: critical role for bacterial membrane-damaging toxins and host neutrophils. *Microbes Infect* **9**: 591-598.

Ghosh, S., and Setlow, P. (2009) Isolation and characterization of superdormant spores of Bacillus species. *J Bacteriol* **191**: 1787-1797.

Giebel, J.D., Carr, K.A., Anderson, E.C., and Hanna, P.C. (2009) The germination-specific lytic enzymes SleB, CwlJ1, and CwlJ2 each contribute to Bacillus anthracis spore germination and virulence. *J Bacteriol* **191**: 5569-5576.

Giorno, R., Bozue, J., Cote, C., Wenzel, T., Moody, K.S., Mallozzi, M., Ryan, M., Wang, R., Zielke, R., Maddock, J.R., Friedlander, A., Welkos, S., and Driks, A. (2007) Morphogenesis of the Bacillus anthracis spore. *J Bacteriol* **189**: 691-705.

Giorno, R., Mallozzi, M., Bozue, J., Moody, K.S., Slack, A., Qiu, D., Wang, R., Friedlander, A., Welkos, S., and Driks, A. (2009) Localization and assembly of proteins comprising the outer structures of the Bacillus anthracis spore. *Microbiology* **155**: 1133-1145.

Gohar, M., Faegri, K., Perchat, S., Ravnum, S., Okstad, O.A., Gominet, M., Kolsto, A.B., and Lereclus, D. (2008) The PlcR virulence regulon of Bacillus cereus. *PLoS One* **3**: e2793.

Gomez, M., Cutting, S., and Stragier, P. (1995) Transcription of spoIVB is the only role of sigma G that is essential for pro-sigma K processing during spore formation in Bacillus subtilis. *J Bacteriol* **177**: 4825-4827.

Gould, G.W. (1966) Stimulation of L-alanine-induced germination of Bacillus cereus spores by D-cycloserine and O-carbamyl-D-serine. *J Bacteriol* **92**: 1261-1262.

Granum, P.E. (1997) *Bacillus cereus*. In *Food Microbiology: Fundamentals and Frontiers*. Doyle, P.M., Beuchat, L.R., Montville, T.J. (ed). Washington, DC: ASM Press, pp. 327-336.

Granum, P.E., O'Sullivan, K., and Lund, T. (1999) The sequence of the non-haemolytic enterotoxin operon from Bacillus cereus. *FEMS Microbiol Lett* **177**: 225-229.

Griffith, J., Makhov, A., Santiago-Lara, L., and Setlow, P. (1994) Electron microscopic studies of the interaction between a Bacillus subtilis alpha/beta-type small, acid-soluble spore protein with DNA: protein binding is cooperative, stiffens the DNA, and induces negative supercoiling. *Proc Natl Acad Sci U S A* **91**: 8224-8228.

Guidi-Rontani, C., Pereira, Y., Ruffie, S., Sirard, J.C., Weber-Levy, M., and Mock, M. (1999a) Identification and characterization of a germination operon on the virulence plasmid pXO1 of Bacillus anthracis. *Mol Microbiol* **33**: 407-414.

Guidi-Rontani, C., Weber-Levy, M., Labruyere, E., and Mock, M. (1999b) Germination of Bacillus anthracis spores within alveolar macrophages. *Mol Microbiol* **31**: 9-17.

Guidi-Rontani, C. (2002) The alveolar macrophage: the Trojan horse of Bacillus anthracis. *Trends Microbiol* **10**: 405-409.

Guinebretiere, M.H., Thompson, F.L., Sorokin, A., Normand, P., Dawyndt, P., Ehling-Schulz, M., Svensson, B., Sanchis, V., Nguyen-The, C., Heyndrickx, M., and De Vos, P. (2008) Ecological diversification in the Bacillus cereus Group. *Environ Microbiol* **10**: 851-865.

Hachisuka, Y., and Kozuka, S. (1981) A new test of differentiation of Bacillus cereus and Bacillus anthracis based on the existence of spore appendages. *Microbiol Immunol* **25**: 1201-1207.

Hachisuka, Y., Kozuka, S., and Tsujikawa, M. (1984) Exosporia and appendages of spores of Bacillus species. *Microbiol Immunol* **28**: 619-624.

Hanna, P.C., and Ireland, J.A. (1999) Understanding Bacillus anthracis pathogenesis. *Trends Microbiol* **7**: 180-182.

Heffron, J.D., Orsburn, B., and Popham, D.L. (2009) Roles of germination-specific lytic enzymes CwlJ and SleB in Bacillus anthracis. *J Bacteriol* **191**: 2237-2247.

Helgason, E., Caugant, D.A., Olsen, I., and Kolsto, A.B. (2000a) Genetic structure of population of Bacillus cereus and B. thuringiensis isolates associated with periodontitis and other human infections. *J Clin Microbiol* **38**: 1615-1622.

Helgason, E., Okstad, O.A., Caugant, D.A., Johansen, H.A., Fouet, A., Mock, M., Hegna, I., and Kolsto, A.B. (2000b) Bacillus anthracis, Bacillus cereus, and Bacillus thuringiensis--one species on the basis of genetic evidence. *Appl Environ Microbiol* **66**: 2627-2630.

Helgason, E., Tourasse, N.J., Meisal, R., Caugant, D.A., and Kolsto, A.B. (2004) Multilocus sequence typing scheme for bacteria of the Bacillus cereus group. *Appl Environ Microbiol* **70**: 191-201.

Henriques, A.O., Beall, B.W., Roland, K., and Moran, C.P., Jr. (1995) Characterization of cotJ, a sigma E-controlled operon affecting the polypeptide composition of the coat of Bacillus subtilis spores. *J Bacteriol* **177**: 3394-3406.

Henriques, A.O., and Moran, C.P., Jr. (2000) Structure and assembly of the bacterial endospore coat. *Methods* **20**: 95-110.

Henriques, A.O., and Moran, C.P., Jr. (2007) Structure, assembly, and function of the spore surface layers. *Annu Rev Microbiol* **61**: 555-588.

Hill, K.K., Ticknor, L.O., Okinaka, R.T., Asay, M., Blair, H., Bliss, K.A., Laker, M., Pardington, P.E., Richardson, A.P., Tonks, M., Beecher, D.J., Kemp, J.D., Kolsto, A.B., Wong, A.C., Keim, P., and Jackson, P.J. (2004) Fluorescent amplified fragment length polymorphism analysis of Bacillus anthracis, Bacillus cereus, and Bacillus thuringiensis isolates. *Appl Environ Microbiol* **70**: 1068-1080.

Hoffmaster, A.R., Ravel, J., Rasko, D.A., Chapman, G.D., Chute, M.D., Marston, C.K., De, B.K., Sacchi, C.T., Fitzgerald, C., Mayer, L.W., Maiden, M.C., Priest, F.G., Barker, M., Jiang, L., Cer, R.Z., Rilstone, J., Peterson, S.N., Weyant, R.S., Galloway, D.R., Read, T.D., Popovic, T., and Fraser, C.M. (2004) Identification of anthrax toxin genes in a Bacillus cereus associated with an illness resembling inhalation anthrax. *Proc Natl Acad Sci U S A* **101**: 8449-8454.

Hoffmaster, A.R., Hill, K.K., Gee, J.E., Marston, C.K., De, B.K., Popovic, T., Sue, D., Wilkins, P.P., Avashia, S.B., Drumgoole, R., Helma, C.H., Ticknor, L.O., Okinaka, R.T., and Jackson, P.J. (2006) Characterization of Bacillus cereus isolates associated with fatal pneumonias: strains are closely related to Bacillus anthracis and harbor B. anthracis virulence genes. *J Clin Microbiol* **44**: 3352-3360.

Hofmeister, A. (1998) Activation of the proprotein transcription factor pro-sigmaE is associated with its progression through three patterns of subcellular localization during sporulation in Bacillus subtilis. *J Bacteriol* **180**: 2426-2433.

Holt, S.C., Gauther, J.J., and Tipper, D.J. (1975) Ultrastructural studies of sporulation in Bacillus sphaericus. *J Bacteriol* **122**: 1322-1338.

Hong, B.X., Jiang, L.F., Hu, Y.S., Fang, D.Y., and Guo, H.Y. (2004) Application of oligonucleotide array technology for the rapid detection of pathogenic bacteria of foodborne infections. *J Microbiol Methods* **58**: 403-411.

Hornstra, L.M., de Vries, Y.P., Wells-Bennik, M.H., de Vos, W.M., and Abee, T. (2006) Characterization of germination receptors of Bacillus cereus ATCC 14579. *Appl Environ Microbiol* **72**: 44-53.

Hornstra, L.M., van der Voort, M., Wijnands, L.M., Roubos-van den Hil, P.J., and Abee, T. (2009) Role of germinant receptors in Caco-2 cell-initiated germination of Bacillus cereus ATCC 14579 endospores. *Appl Environ Microbiol* **75**: 1201-1203.

Hyvonen, M. (2003) CHRD, a novel domain in the BMP inhibitor chordin, is also found in microbial proteins. *Trends Biochem Sci* **28**: 470-473.

Illing, N., and Errington, J. (1991) The spoIIIA operon of Bacillus subtilis defines a new temporal class of mother-cell-specific sporulation genes under the control of the sigma E form of RNA polymerase. *Mol Microbiol* **5**: 1927-1940.

Ireland, J.A., and Hanna, P.C. (2002) Amino acid- and purine ribonucleoside-induced germination of Bacillus anthracis DeltaSterne endospores: gerS mediates responses to aromatic ring structures. *J Bacteriol* **184**: 1296-1303.

Ivanova, N., Sorokin, A., Anderson, I., Galleron, N., Candelon, B., Kapatral, V., Bhattacharyya, A., Reznik, G., Mikhailova, N., Lapidus, A., Chu, L., Mazur, M., Goltsman, E., Larsen, N., D'Souza, M., Walunas, T., Grechkin, Y., Pusch, G., Haselkorn, R., Fonstein, M., Ehrlich, S.D., Overbeek, R., and Kyrpides, N. (2003) Genome sequence of Bacillus cereus and comparative analysis with Bacillus anthracis. *Nature* **423**: 87-91.

Jackson, S.G., Goodbrand, R.B., Ahmed, R., and Kasatiya, S. (1995) Bacillus cereus and Bacillus thuringiensis isolated in a gastroenteritis outbreak investigation. *Lett Appl Microbiol* **21**: 103-105.

Jensen, G.B., Hansen, B.M., Eilenberg, J., and Mahillon, J. (2003) The hidden lifestyles of Bacillus cereus and relatives. *Environ Microbiol* **5**: 631-640.

Jiang, M., Shao, W., Perego, M., and Hoch, J.A. (2000) Multiple histidine kinases regulate entry into stationary phase and sporulation in Bacillus subtilis. *Mol Microbiol* **38**: 535-542.

Johnson, D.A., Aulicino, P.L., and Newby, J.G. (1984) Bacillus cereus-induced myonecrosis. *J Trauma* **24**: 267-270.

Johnson, M.J., Todd, S.J., Ball, D.A., Shepherd, A.M., Sylvestre, P., and Moir, A. (2006) ExsY and CotY are required for the correct assembly of the exosporium and spore coat of Bacillus cereus. *J Bacteriol* **188**: 7905-7913.

Ju, J., Luo, T., and Haldenwang, W.G. (1997) Bacillus subtilis Pro-sigmaE fusion protein localizes to the forespore septum and fails to be processed when synthesized in the forespore. *J Bacteriol* **179**: 4888-4893.

Kadokura, H., Katzen, F., and Beckwith, J. (2003) Protein disulfide bond formation in prokaryotes. *Annu Rev Biochem* **72**: 111-135.

Karmazyn-Campelli, C., Rhayat, L., Carballido-Lopez, R., Duperrier, S., Frandsen, N., and Stragier, P. (2008) How the early sporulation sigma factor sigmaF delays the switch to late development in Bacillus subtilis. *Mol Microbiol* **67**: 1169-1180.

Karow, M.L., Glaser, P., and Piggot, P.J. (1995) Identification of a gene, spoIIR, that links the activation of sigma E to the transcriptional activity of sigma F during sporulation in Bacillus subtilis. *Proc Natl Acad Sci U S A* **92**: 2012-2016.

Kau, J.H., Sun, D.S., Tsai, W.J., Shyu, H.F., Huang, H.H., Lin, H.C., and Chang, H.H. (2005) Antiplatelet activities of anthrax lethal toxin are associated with suppressed p42/44 and p38 mitogen-activated protein kinase pathways in the platelets. *J Infect Dis* **192**: 1465-1474.

Keynan, A. (1969) The outgrowing bacterial endospore as a system for the study of cellular differentiation. *Curr Top Dev Biol* **4**: 1-36.

Kim, H., Hahn, M., Grabowski, P., McPherson, D.C., Otte, M.M., Wang, R., Ferguson, C.C., Eichenberger, P., and Driks, A. (2006) The Bacillus subtilis spore coat protein interaction network. *Mol Microbiol* **59**: 487-502.

Kim, H.S., Sherman, D., Johnson, F., and Aronson, A.I. (2004) Characterization of a major Bacillus anthracis spore coat protein and its role in spore inactivation. *J Bacteriol* **186**: 2413-2417.

Klobutcher, L.A., Ragkousi, K., and Setlow, P. (2006) The Bacillus subtilis spore coat provides "eat resistance" during phagocytic predation by the protozoan Tetrahymena thermophila. *Proc Natl Acad Sci U S A* **103**: 165-170.

Kolsto, A.B., Tourasse, N.J., and Okstad, O.A. (2009) What sets Bacillus anthracis apart from other Bacillus species? *Annu Rev Microbiol* **63**: 451-476.

Koshikawa, T., Yamazaki, M., Yoshimi, M., Ogawa, S., Yamada, A., Watabe, K., and Torii, M. (1989) Surface hydrophobicity of spores of Bacillus spp. *J Gen Microbiol* **135**: 2717-2722.

Kotiranta, A., Lounatmaa, K., and Haapasalo, M. (2000) Epidemiology and pathogenesis of Bacillus cereus infections. *Microbes Infect* **2**: 189-198.

Kozuka, S., and Tochikubo, K. (1985) Properties and origin of filamentous appendages on spores of Bacillus cereus. *Microbiol Immunol* **29**: 21-37.

Kroos, L., Kunkel, B., and Losick, R. (1989) Switch protein alters specificity of RNA polymerase containing a compartment-specific sigma factor. *Science* **243**: 526-529.

Kunkel, B., Losick, R., and Stragier, P. (1990) The Bacillus subtilis gene for the development transcription factor sigma K is generated by excision of a dispensable DNA element containing a sporulation recombinase gene. *Genes Dev* **4**: 525-535.

Kyriakis, S.C., Tsiloyiannis, V.K., Vlemmas, J., Sarris, K., Tsinas, A.C., Alexopoulos, C., and Jansegers, L. (1999) The effect of probiotic LSP 122 on the control of post-weaning diarrhoea syndrome of piglets. *Res Vet Sci* **67**: 223-228.

LaBell, T.L., Trempy, J.E., and Haldenwang, W.G. (1987) Sporulation-specific sigma factor sigma 29 of Bacillus subtilis is synthesized from a precursor protein, P31. *Proc Natl Acad Sci U S A* **84**: 1784-1788.

Lai, E.M., Phadke, N.D., Kachman, M.T., Giorno, R., Vazquez, S., Vazquez, J.A., Maddock, J.R., and Driks, A. (2003) Proteomic analysis of the spore coats of Bacillus subtilis and Bacillus anthracis. *J Bacteriol* **185**: 1443-1454.

Leighton, T.J., and Doi, R.H. (1971) The stability of messenger ribonucleic acid during sporulation in Bacillus subtilis. *J Biol Chem* **246**: 3189-3195.

Leppla, S.H. (1982) Anthrax toxin edema factor: a bacterial adenylate cyclase that increases cyclic AMP concentrations of eukaryotic cells. *Proc Natl Acad Sci U S A* **79**: 3162-3166.

Leppla, S.H. (1984) Bacillus anthracis calmodulin-dependent adenylate cyclase: chemical and enzymatic properties and interactions with eucaryotic cells. *Adv Cyclic Nucleotide Protein Phosphorylation Res* **17**: 189-198.

Leski, T.A., Caswell, C.C., Pawlowski, M., Klinke, D.J., Bujnicki, J.M., Hart, S.J., and Lukomski, S. (2009) Identification and classification of bcl genes and proteins of

Bacillus cereus group organisms and their application in Bacillus anthracis detection and fingerprinting. *Appl Environ Microbiol* **75**: 7163-7172.

Liang, L., He, X., Liu, G., and Tan, H. (2008) The role of a purine-specific nucleoside hydrolase in spore germination of Bacillus thuringiensis. *Microbiology* **154**: 1333-1340.

Lindback, T., Okstad, O.A., Rishovd, A.L., and Kolsto, A.B. (1999) Insertional inactivation of hblC encoding the L2 component of Bacillus cereus ATCC 14579 haemolysin BL strongly reduces enterotoxigenic activity, but not the haemolytic activity against human erythrocytes. *Microbiology* **145 (Pt 11)**: 3139-3146.

Londono-Vallejo, J.A., Frehel, C., and Stragier, P. (1997) SpoIIQ, a forespore-expressed gene required for engulfment in Bacillus subtilis. *Mol Microbiol* **24**: 29-39.

Lorand, L., and Graham, R.M. (2003) Transglutaminases: crosslinking enzymes with pleiotropic functions. *Nat Rev Mol Cell Biol* **4**: 140-156.

Lund, T., De Buyser, M.L., and Granum, P.E. (2000) A new cytotoxin from Bacillus cereus that may cause necrotic enteritis. *Mol Microbiol* **38**: 254-261.

Magill, N.G., Cowan, A.E., Koppel, D.E., and Setlow, P. (1994) The internal pH of the forespore compartment of Bacillus megaterium decreases by about 1 pH unit during sporulation. *J Bacteriol* **176**: 2252-2258.

Magill, N.G., Cowan, A.E., Leyva-Vazquez, M.A., Brown, M., Koppel, D.E., and Setlow, P. (1996) Analysis of the relationship between the decrease in pH and accumulation of 3-phosphoglyceric acid in developing forespores of Bacillus species. *J Bacteriol* **178**: 2204-2210.

Mahler, H., Pasi, A., Kramer, J.M., Schulte, P., Scoging, A.C., Bar, W., and Krahenbuhl, S. (1997) Fulminant liver failure in association with the emetic toxin of Bacillus cereus. *N Engl J Med* **336**: 1142-1148.

Makino, S., Watarai, M., Cheun, H.I., Shirahata, T., and Uchida, I. (2002) Effect of the lower molecular capsule released from the cell surface of Bacillus anthracis on the pathogenesis of anthrax. *J Infect Dis* **186**: 227-233.

Margolin, W. (2002) Bacterial sporulation: FtsZ rings do the twist. *Curr Biol* **12**: R391-392.

Margolis, P.S., Driks, A., and Losick, R. (1993) Sporulation gene spoIIB from Bacillus subtilis. *J Bacteriol* **175**: 528-540.

Margulis, L., Jorgensen, J.Z., Dolan, S., Kolchinsky, R., Rainey, F.A., and Lo, S.C. (1998) The Arthromitus stage of Bacillus cereus: intestinal symbionts of animals. *Proc Natl Acad Sci U S A* **95**: 1236-1241.

Marston, C.K., Gee, J.E., Popovic, T., and Hoffmaster, A.R. (2006) Molecular approaches to identify and differentiate Bacillus anthracis from phenotypically similar Bacillus species isolates. *BMC Microbiol* **6**: 22.

Martins, L.O., Soares, C.M., Pereira, M.M., Teixeira, M., Costa, T., Jones, G.H., and Henriques, A.O. (2002) Molecular and biochemical characterization of a highly stable bacterial laccase that occurs as a structural component of the Bacillus subtilis endospore coat. *J Biol Chem* **277**: 18849-18859.

Matsuno, K., and Sonenshein, A.L. (1999) Role of SpoVG in asymmetric septation in Bacillus subtilis. *J Bacteriol* **181**: 3392-3401.

Matz, L.L., Beaman, T.C., and Gerhardt, P. (1970) Chemical composition of exosporium from spores of Bacillus cereus. *J Bacteriol* **101**: 196-201.

McIntyre, L., Bernard, K., Beniac, D., Isaac-Renton, J.L., and Naseby, D.C. (2008) Identification of Bacillus cereus group species associated with food poisoning outbreaks in British Columbia, Canada. *Appl Environ Microbiol* **74**: 7451-7453.

McPherson, D.C., Driks, A., and Popham, D.L. (2001) Two class A high-molecular-weight penicillin-binding proteins of Bacillus subtilis play redundant roles in sporulation. *J Bacteriol* **183**: 6046-6053.

Meador-Parton, J., and Popham, D.L. (2000) Structural analysis of Bacillus subtilis spore peptidoglycan during sporulation. *J Bacteriol* **182**: 4491-4499.

Meisner, J., Wang, X., Serrano, M., Henriques, A.O., and Moran, C.P., Jr. (2008) A channel connecting the mother cell and forespore during bacterial endospore formation. *Proc Natl Acad Sci U S A* **105**: 15100-15105.

Mignot, T., Mock, M., Robichon, D., Landier, A., Lereclus, D., and Fouet, A. (2001) The incompatibility between the PlcR- and AtxA-controlled regulons may have selected a nonsense mutation in Bacillus anthracis. *Mol Microbiol* **42**: 1189-1198.

Mikkola, R., Saris, N.E., Grigoriev, P.A., Andersson, M.A., and Salkinoja-Salonen, M.S. (1999) Ionophoretic properties and mitochondrial effects of cereulide: the emetic toxin of B. cereus. *Eur J Biochem* **263**: 112-117.

Min, K.T., Hilditch, C.M., Diederich, B., Errington, J., and Yudkin, M.D. (1993) Sigma F, the first compartment-specific transcription factor of B. subtilis, is regulated by an anti-sigma factor that is also a protein kinase. *Cell* **74**: 735-742.

Mock, M., and Fouet, A. (2001) Anthrax. *Annu Rev Microbiol* **55**: 647-671.

Moffitt, M.C., and Neilan, B.A. (2000) The expansion of mechanistic and organismic diversity associated with non-ribosomal peptides. *FEMS Microbiol Lett* **191**: 159-167.

Moir, A., Corfe, B.M., and Behravan, J. (2002) Spore germination. *Cell Mol Life Sci* **59**: 403-409.

Moody, K.L., Driks, A., Rother, G.L., Cote, C.K., Brueggemann, E.E., Hines, H.B., Friedlander, A.M., and Bozue, J. Processing, assembly and localization of a Bacillus anthracis spore protein. *Microbiology* **156**: 174-183.

Moravek, M., Dietrich, R., Buerk, C., Broussolle, V., Guinebretiere, M.H., Granum, P.E., Nguyen-The, C., and Martlbauer, E. (2006) Determination of the toxic potential of Bacillus cereus isolates by quantitative enterotoxin analyses. *FEMS Microbiol Lett* **257**: 293-298.

Morris, S.L., and Hansen, J.N. (1981) Inhibition of Bacillus cereus spore outgrowth by covalent modification of a sulfhydryl group by nitrosothiol and iodoacetate. *J Bacteriol* **148**: 465-471.

Nessi, C., Jedrzejas, M.J., and Setlow, P. (1998) Structure and mechanism of action of the protease that degrades small, acid-soluble spore proteins during germination of spores of Bacillus species. *J Bacteriol* **180**: 5077-5084.

Nicholson, W.L., and Setlow, P. (1990) Sporulation, Germination and Outgrowth. In *Molecular biological methods for Bacillus*. Harwood, C.R. and Cutting, S. (eds). West Sussex, England: John Wiley and Sons, Ltd.

Nicholson, W.L., Munakata, N., Horneck, G., Melosh, H.J., and Setlow, P. (2000) Resistance of Bacillus endospores to extreme terrestrial and extraterrestrial environments. *Microbiol Mol Biol Rev* **64**: 548-572.

Ohye, D.F., and Murrell, W.G. (1973) Exosporium and spore coat formation in Bacillus cereus T. *J Bacteriol* **115**: 1179-1190.

Oliva, C., Turnbough, C.L., Jr., and Kearney, J.F. (2009) CD14-Mac-1 interactions in Bacillus anthracis spore internalization by macrophages. *Proc Natl Acad Sci U S A* **106**: 13957-13962.

Paidhungat, M., Ragkousi, K., and Setlow, P. (2001) Genetic requirements for induction of germination of spores of Bacillus subtilis by Ca(2+)-dipicolinate. *J Bacteriol* **183**: 4886-4893.

Paidhungat, M.S.P. (2002) Spore Germination and Outgrowth. In *Bacillus subtilis and Its Closest Relatives: From genes to cells*. Sonenshein, A.L.H., J.A.; Losick, R. (ed). Washington D.C.: American Society for Microbiology.

Panessa-Warren, B.J., Tortora, G.T., and Warren, J.B. (1997) Exosporial membrane plasticity of Clostridium sporogenes and Clostridium difficile. *Tissue Cell* **29**: 449-461.

Panessa-Warren, B.J., Tortora, G.T., and Warren, J.B. (2007) High resolution FESEM and TEM reveal bacterial spore attachment. *Microsc Microanal* **13**: 251-266.

Partridge, S.R., and Errington, J. (1993) The importance of morphological events and intercellular interactions in the regulation of prespore-specific gene expression during sporulation in Bacillus subtilis. *Mol Microbiol* **8**: 945-955.

Peerschke, E.I., and Ghebrehiwet, B. (2007) The contribution of gC1qR/p33 in infection and inflammation. *Immunobiology* **212**: 333-342.

Perego, M., Hanstein, C., Welsh, K.M., Djavakhishvili, T., Glaser, P., and Hoch, J.A. (1994) Multiple protein-aspartate phosphatases provide a mechanism for the integration of diverse signals in the control of development in B. subtilis. *Cell* **79**: 1047-1055.

Perego, M. (2001) A new family of aspartyl phosphate phosphatases targeting the sporulation transcription factor Spo0A of Bacillus subtilis. *Mol Microbiol* **42**: 133-143.

Perego, M., and Brannigan, J.A. (2001) Pentapeptide regulation of aspartyl-phosphate phosphatases. *Peptides* **22**: 1541-1547.

Perez, A.R., Abanes-De Mello, A., and Pogliano, K. (2000) SpoIIB localizes to active sites of septal biogenesis and spatially regulates septal thinning during engulfment in bacillus subtilis. *J Bacteriol* **182**: 1096-1108.

Pezard, C., Berche, P., and Mock, M. (1991) Contribution of individual toxin components to virulence of Bacillus anthracis. *Infect Immun* **59**: 3472-3477.

Pezard, C., Duflot, E., and Mock, M. (1993) Construction of Bacillus anthracis mutant strains producing a single toxin component. *J Gen Microbiol* **139**: 2459-2463.

Plomp, M., Leighton, T.J., Wheeler, K.E., and Malkin, A.J. (2005a) Architecture and high-resolution structure of Bacillus thuringiensis and Bacillus cereus spore coat surfaces. *Langmuir* **21**: 7892-7898.

Plomp, M., Leighton, T.J., Wheeler, K.E., and Malkin, A.J. (2005b) The high-resolution architecture and structural dynamics of Bacillus spores. *Biophys J* **88**: 603-608.

Pogliano, J., Osborne, N., Sharp, M.D., Abanes-De Mello, A., Perez, A., Sun, Y.L., and Pogliano, K. (1999) A vital stain for studying membrane dynamics in bacteria: a novel mechanism controlling septation during Bacillus subtilis sporulation. *Mol Microbiol* **31**: 1149-1159.

Pogliano, K., Hofmeister, A.E., and Losick, R. (1997) Disappearance of the sigma E transcription factor from the forespore and the SpoIIE phosphatase from the mother cell contributes to establishment of cell-specific gene expression during sporulation in Bacillus subtilis. *J Bacteriol* **179**: 3331-3341.

Porwal, S., Lal, S., Cheema, S., and Kalia, V.C. (2009) Phylogeny in aid of the present and novel microbial lineages: diversity in Bacillus. *PLoS One* **4**: e4438.

Preisz, H. (1909) Experimentelle studies veber virulenz, empfaenglich keit und immunitaet beim milzbrand. *Zeitschr Immunitaet-Forsch* **5**: 341-452.

Priest, F.G., Barker, M., Baillie, L.W., Holmes, E.C., and Maiden, M.C. (2004) Population structure and evolution of the Bacillus cereus group. *J Bacteriol* **186**: 7959-7970.

Quinn, C.P., Dull, P.M., Semenova, V., Li, H., Crotty, S., Taylor, T.H., Steward-Clark, E., Stamey, K.L., Schmidt, D.S., Stinson, K.W., Freeman, A.E., Elie, C.M., Martin, S.K., Greene, C., Aubert, R.D., Glidewell, J., Perkins, B.A., Ahmed, R., and Stephens, D.S. (2004) Immune responses to Bacillus anthracis protective antigen in patients with bioterrorism-related cutaneous or inhalation anthrax. *J Infect Dis* **190**: 1228-1236.

Quisel, J.D., Lin, D.C., and Grossman, A.D. (1999) Control of development by altered localization of a transcription factor in B. subtilis. *Mol Cell* **4**: 665-672.

Ragkousi, K., and Setlow, P. (2004) Transglutaminase-mediated cross-linking of GerQ in the coats of Bacillus subtilis spores. *J Bacteriol* **186**: 5567-5575.

Ramarao, N., and Lereclus, D. (2005) The InhA1 metalloprotease allows spores of the B. cereus group to escape macrophages. *Cell Microbiol* **7**: 1357-1364.

Rasko, D.A., Ravel, J., Okstad, O.A., Helgason, E., Cer, R.Z., Jiang, L., Shores, K.A., Fouts, D.E., Tourasse, N.J., Angiuoli, S.V., Kolonay, J., Nelson, W.C., Kolsto, A.B., Fraser, C.M., and Read, T.D. (2004) The genome sequence of Bacillus cereus ATCC 10987 reveals metabolic adaptations and a large plasmid related to Bacillus anthracis pXO1. *Nucleic Acids Res* **32**: 977-988.

Rasko, D.A., Altherr, M.R., Han, C.S., and Ravel, J. (2005) Genomics of the Bacillus cereus group of organisms. *FEMS Microbiol Rev* **29**: 303-329.

Redmond, C., Baillie, L.W., Hibbs, S., Moir, A.J., and Moir, A. (2004) Identification of proteins in the exosporium of Bacillus anthracis. *Microbiology* **150**: 355-363.

Rety, S., Salamitou, S., Garcia-Verdugo, I., Hulmes, D.J., Le Hegarat, F., Chaby, R., and Lewit-Bentley, A. (2005) The crystal structure of the Bacillus anthracis spore surface protein BclA shows remarkable similarity to mammalian proteins. *J Biol Chem* **280**: 43073-43078.

Ricca, E., Cutting, S., and Losick, R. (1992) Characterization of bofA, a gene involved in intercompartmental regulation of pro-sigma K processing during sporulation in Bacillus subtilis. *J Bacteriol* **174**: 3177-3184.

Romero, D., Aguilar, C., Losick, R., and Kolter, R. Amyloid fibers provide structural integrity to Bacillus subtilis biofilms. *Proc Natl Acad Sci U S A* **107**: 2230-2234.

Rudner, D.Z., Fawcett, P., and Losick, R. (1999) A family of membrane-embedded metalloproteases involved in regulated proteolysis of membrane-associated transcription factors. *Proc Natl Acad Sci U S A* **96**: 14765-14770.

Saile, E., and Koehler, T.M. (2006) Bacillus anthracis multiplication, persistence, and genetic exchange in the rhizosphere of grass plants. *Appl Environ Microbiol* **72**: 3168-3174.

Schmidt, M.A., Riley, L.W., and Benz, I. (2003) Sweet new world: glycoproteins in bacterial pathogens. *Trends Microbiol* **11**: 554-561.

Schneerson, R., Kubler-Kielb, J., Liu, T.Y., Dai, Z.D., Leppla, S.H., Yergey, A., Backlund, P., Shiloach, J., Majadly, F., and Robbins, J.B. (2003) Poly(gamma-D-glutamic acid) protein conjugates induce IgG antibodies in mice to the capsule of Bacillus anthracis: a potential addition to the anthrax vaccine. *Proc Natl Acad Sci U S A* **100**: 8945-8950.

Schuch, R., Nelson, D., and Fischetti, V.A. (2002) A bacteriolytic agent that detects and kills Bacillus anthracis. *Nature* **418**: 884-889.

Schuch, R., and Fischetti, V.A. (2009) The secret life of the anthrax agent Bacillus anthracis: bacteriophage-mediated ecological adaptations. *PLoS One* **4**: e6532.

Schwartz, M. (2009) Dr. Jekyll and Mr. Hyde: a short history of anthrax. *Mol Aspects Med* **30**: 347-355.

Setlow, B., Atluri, S., Kitchel, R., Koziol-Dube, K., and Setlow, P. (2006) Role of dipicolinic acid in resistance and stability of spores of Bacillus subtilis with or without DNA-protective alpha/beta-type small acid-soluble proteins. *J Bacteriol* **188**: 3740-3747.

Setlow, P., and Waites, W.M. (1976) Identification of several unique, low-molecular-weight basic proteins in dormant spores of clastridium bifermentans and their degradation during spore germination. *J Bacteriol* **127**: 1015-1017.

Setlow, P. (1995) Mechanisms for the prevention of damage to DNA in spores of Bacillus species. *Annu Rev Microbiol* **49**: 29-54.

Setlow, P. (2007) I will survive: DNA protection in bacterial spores. *Trends Microbiol* **15**: 172-180.

Severson, K.M., Mallozzi, M., Bozue, J., Welkos, S.L., Cote, C.K., Knight, K.L., and Driks, A. (2009) Roles of the Bacillus anthracis spore protein ExsK in exosporium maturation and germination. *J Bacteriol* **191**: 7587-7596.

Sharp, M.D., and Pogliano, K. (1999) An in vivo membrane fusion assay implicates SpoIIIE in the final stages of engulfment during Bacillus subtilis sporulation. *Proc Natl Acad Sci U S A* **96**: 14553-14558.

Shinagawa, K., Ueno, Y., Hu, D., Ueda, S., and Sugii, S. (1996) Mouse lethal activity of a HEp-2 vacuolation factor, cereulide, produced by Bacillus cereus isolated from vomiting-type food poisoning. *J Vet Med Sci* **58**: 1027-1029.

Sirard, J.C., Mock, M., and Fouet, A. (1994) The three Bacillus anthracis toxin genes are coordinately regulated by bicarbonate and temperature. *J Bacteriol* **176**: 5188-5192.

Slamti, L., Perchat, S., Gominet, M., Vilas-Boas, G., Fouet, A., Mock, M., Sanchis, V., Chaufaux, J., Gohar, M., and Lereclus, D. (2004) Distinct mutations in PlcR explain why some strains of the Bacillus cereus group are nonhemolytic. *J Bacteriol* **186**: 3531-3538.

Soderling, E., and Paunio, K.U. (1981) Conditions of production and properties of the collagenolytic enzymes by two Bacillus strains from dental plaque. *J Periodontal Res* **16**: 513-523.

Sonenshein, A.L. (2000) Control of sporulation initiation in Bacillus subtilis. *Curr Opin Microbiol* **3**: 561-566.

Southworth, T.W., Guffanti, A.A., Moir, A., and Krulwich, T.A. (2001) GerN, an endospore germination protein of Bacillus cereus, is an Na(+)/H(+)-K(+) antiporter. *J Bacteriol* **183**: 5896-5903.

Stachelhaus, T., and Marahiel, M.A. (1995) Modular structure of genes encoding multifunctional peptide synthetases required for non-ribosomal peptide synthesis. *FEMS Microbiol Lett* **125**: 3-14.

Steichen, C., Chen, P., Kearney, J.F., and Turnbough, C.L., Jr. (2003) Identification of the immunodominant protein and other proteins of the Bacillus anthracis exosporium. *J Bacteriol* **185**: 1903-1910.

Steichen, C.T., Kearney, J.F., and Turnbough, C.L., Jr. (2005) Characterization of the exosporium basal layer protein BxpB of Bacillus anthracis. *J Bacteriol* **187**: 5868-5876.

Steichen, C.T., Kearney, J.F., and Turnbough, C.L., Jr. (2007) Non-uniform assembly of the Bacillus anthracis exosporium and a bottle cap model for spore germination and outgrowth. *Mol Microbiol* **64**: 359-367.

Stenfors Arnesen, L.P., Fagerlund, A., and Granum, P.E. (2008) From soil to gut: Bacillus cereus and its food poisoning toxins. *FEMS Microbiol Rev* **32**: 579-606.

Stephenson, K., and Lewis, R.J. (2005) Molecular insights into the initiation of sporulation in Gram-positive bacteria: new technologies for an old phenomenon. *FEMS Microbiol Rev* **29**: 281-301.

Stock, A.M., Robinson, V.L., and Goudreau, P.N. (2000) Two-component signal transduction. *Annu Rev Biochem* **69**: 183-215.

Stragier, P., Bonamy, C., and Karmazyn-Campelli, C. (1988) Processing of a sporulation sigma factor in Bacillus subtilis: how morphological structure could control gene expression. *Cell* **52**: 697-704.

Stragier, P., Kunkel, B., Kroos, L., and Losick, R. (1989) Chromosomal rearrangement generating a composite gene for a developmental transcription factor. *Science* **243**: 507-512.

Sun, Y.L., Sharp, M.D., and Pogliano, K. (2000) A dispensable role for forespore-specific gene expression in engulfment of the forespore during sporulation of Bacillus subtilis. *J Bacteriol* **182**: 2919-2927.

Swiecicka, I., and Mahillon, J. (2006) Diversity of commensal Bacillus cereus sensu lato isolated from the common sow bug (Porcellio scaber, Isopoda). *FEMS Microbiol Ecol* **56**: 132-140.

Sylvestre, P., Couture-Tosi, E., and Mock, M. (2002) A collagen-like surface glycoprotein is a structural component of the Bacillus anthracis exosporium. *Mol Microbiol* **45**: 169-178.

Sylvestre, P., Couture-Tosi, E., and Mock, M. (2003) Polymorphism in the collagen-like region of the Bacillus anthracis BclA protein leads to variation in exosporium filament length. *J Bacteriol* **185**: 1555-1563.

Sylvestre, P., Couture-Tosi, E., and Mock, M. (2005) Contribution of ExsFA and ExsFB proteins to the localization of BclA on the spore surface and to the stability of the bacillus anthracis exosporium. *J Bacteriol* **187**: 5122-5128.

Taras, D., Vahjen, W., Macha, M., and Simon, O. (2005) Response of performance characteristics and fecal consistency to long-lasting dietary supplementation with the probiotic strain Bacillus cereus var. toyoi to sows and piglets. *Arch Anim Nutr* **59**: 405-417.

Tauveron, G., Slomianny, C., Henry, C., and Faille, C. (2006) Variability among Bacillus cereus strains in spore surface properties and influence on their ability to contaminate food surface equipment. *Int J Food Microbiol* **110**: 254-262.

Thompson, B.M., Waller, L.N., Fox, K.F., Fox, A., and Stewart, G.C. (2007) The BclB glycoprotein of Bacillus anthracis is involved in exosporium integrity. *J Bacteriol* **189**: 6704-6713.

Thompson, B.M., and Stewart, G.C. (2008) Targeting of the BclA and BclB proteins to the Bacillus anthracis spore surface. *Mol Microbiol* **70**: 421-434.

Tipper, D.J., and Linnett, P.E. (1976) Distribution of peptidoglycan synthetase activities between sporangia and forespores in sporulating cells of Bacillus sphaericus. *J Bacteriol* **126**: 213-221.

Tipper, D.J.G., J.J. (1972) Structure of the bacterial endospore. In *Spore V*. Halverson, H.O.H., R.; Cambell, L.L. (ed). Washington D.C.: America Society of Microbiology.

Todd, S.J., Moir, A.J., Johnson, M.J., and Moir, A. (2003) Genes of Bacillus cereus and Bacillus anthracis encoding proteins of the exosporium. *J Bacteriol* **185**: 3373-3378.

Tournier, J.N., Quesnel-Hellmann, A., Mathieu, J., Montecucco, C., Tang, W.J., Mock, M., Vidal, D.R., and Goossens, P.L. (2005) Anthrax edema toxin cooperates with lethal toxin to impair cytokine secretion during infection of dendritic cells. *J Immunol* **174**: 4934-4941.

Tournier, J.N., Quesnel-Hellmann, A., Cleret, A., and Vidal, D.R. (2007) Contribution of toxins to the pathogenesis of inhalational anthrax. *Cell Microbiol* **9**: 555-565.

Tournier, J.N., Rossi Paccani, S., Quesnel-Hellmann, A., and Baldari, C.T. (2009) Anthrax toxins: a weapon to systematically dismantle the host immune defenses. *Mol Aspects Med* **30**: 456-466.

Trempy, J.E., Bonamy, C., Szulmajster, J., and Haldenwang, W.G. (1985) Bacillus subtilis sigma factor sigma 29 is the product of the sporulation-essential gene spoIIG. *Proc Natl Acad Sci U S A* **82**: 4189-4192.

Turgeon, N., Laflamme, C., Ho, J., and Duchaine, C. (2006) Elaboration of an electroporation protocol for Bacillus cereus ATCC 14579. *J Microbiol Methods* **67**: 543-548.

Turnbull, P.C. (2002) Introduction: Anthrax History, Disease and Ecology. In *Anthrax*. Koehler, T.M. (ed). Berlin: Springer-Verlag.

Vassileva, M., Torii, K., Oshimoto, M., Okamoto, A., Agata, N., Yamada, K., Hasegawa, T., and Ohta, M. (2007) A new phylogenetic cluster of cereulide-producing Bacillus cereus strains. *J Clin Microbiol* **45**: 1274-1277.

Vasudevan, P., Weaver, A., Reichert, E.D., Linnstaedt, S.D., and Popham, D.L. (2007) Spore cortex formation in Bacillus subtilis is regulated by accumulation of peptidoglycan precursors under the control of sigma K. *Mol Microbiol* **65**: 1582-1594.

Vietri, N.J., Marrero, R., Hoover, T.A., and Welkos, S.L. (1995) Identification and characterization of a trans-activator involved in the regulation of encapsulation by Bacillus anthracis. *Gene* **152**: 1-9.

Walker, J.R., Gnanam, A.J., Blinkova, A.L., Hermandson, M.J., Karymov, M.A., Lyubchenko, Y.L., Graves, P.R., Haystead, T.A., and Linse, K.D. (2007) Clostridium taeniosporum spore ribbon-like appendage structure, composition and genes. *Mol Microbiol* **63**: 629-643.

Wallace, A.J., Stillman, T.J., Atkins, A., Jamieson, S.J., Bullough, P.A., Green, J., and Artymiuk, P.J. (2000) E. coli hemolysin E (HlyE, ClyA, SheA): X-ray crystal structure of the toxin and observation of membrane pores by electron microscopy. *Cell* **100**: 265-276.

Waller, L.N., Fox, N., Fox, K.F., Fox, A., and Price, R.L. (2004) Ruthenium red staining for ultrastructural visualization of a glycoprotein layer surrounding the spore of Bacillus anthracis and Bacillus subtilis. *J Microbiol Methods* **58**: 23-30.

Wang, L., Grau, R., Perego, M., and Hoch, J.A. (1997) A novel histidine kinase inhibitor regulating development in Bacillus subtilis. *Genes Dev* **11**: 2569-2579.

Wang, S.T., Setlow, B., Conlon, E.M., Lyon, J.L., Imamura, D., Sato, T., Setlow, P., Losick, R., and Eichenberger, P. (2006) The forespore line of gene expression in Bacillus subtilis. *J Mol Biol* **358**: 16-37.

Warfel, J.M., Steele, A.D., and D'Agnillo, F. (2005) Anthrax lethal toxin induces endothelial barrier dysfunction. *Am J Pathol* **166**: 1871-1881.

Warren, S.C., and Gould, G.W. (1968) Bacillus cereus spore germination:absolute requirement for an amine acid. *Biochim Biophys Acta* **170**: 341-350.

Weaver, J., Kang, T.J., Raines, K.W., Cao, G.L., Hibbs, S., Tsai, P., Baillie, L., Rosen, G.M., and Cross, A.S. (2007) Protective role of Bacillus anthracis exosporium in macrophage-mediated killing by nitric oxide. *Infect Immun* **75**: 3894-3901.

Webb, C.D., Decatur, A., Teleman, A., and Losick, R. (1995) Use of green fluorescent protein for visualization of cell-specific gene expression and subcellular protein localization during sporulation in Bacillus subtilis. *J Bacteriol* **177**: 5906-5911.

Welkos, S.L. (1991) Plasmid-associated virulence factors of non-toxigenic (pX01-) Bacillus anthracis. *Microb Pathog* **10**: 183-198.

Wenzel, M., Schonig, I., Berchtold, M., Kampfer, P., and Konig, H. (2002) Aerobic and facultatively anaerobic cellulolytic bacteria from the gut of the termite Zootermopsis angusticollis. *J Appl Microbiol* **92**: 32-40.

White, A.K., Hoch, J.A., Grynberg, M., Godzik, A., and Perego, M. (2006) Sensor domains encoded in Bacillus anthracis virulence plasmids prevent sporulation by hijacking a sporulation sensor histidine kinase. *J Bacteriol* **188**: 6354-6360.

Wu, L.J., and Errington, J. (1997) Septal localization of the SpoIIIE chromosome partitioning protein in Bacillus subtilis. *Embo J* **16**: 2161-2169.

Wu, L.J., and Errington, J. (2003) RacA and the Soj-Spo0J system combine to effect polar chromosome segregation in sporulating Bacillus subtilis. *Mol Microbiol* **49**: 1463-1475.

Yan, X., Gai, Y., Liang, L., Liu, G., and Tan, H. (2007) A gene encoding alanine racemase is involved in spore germination in Bacillus thuringiensis. *Arch Microbiol* **187**: 371-378.

Yu, K., Kang, K.H., Heine, P., Pyati, U., Srinivasan, S., Biehs, B., Kimelman, D., and Bier, E. (2004) Cysteine repeat domains and adjacent sequences determine distinct bone morphogenetic protein modulatory activities of the Drosophila Sog protein. *Genetics* **166**: 1323-1336.

Zhang, B., Hofmeister, A., and Kroos, L. (1998) The prosequence of pro-sigmaK promotes membrane association and inhibits RNA polymerase core binding. *J Bacteriol* **180**: 2434-2441.

Zheng, L.B., and Losick, R. (1990) Cascade regulation of spore coat gene expression in Bacillus subtilis. *J Mol Biol* **212**: 645-660.

Zilhao, R., Serrano, M., Isticato, R., Ricca, E., Moran, C.P., Jr., and Henriques, A.O. (2004) Interactions among CotB, CotG, and CotH during assembly of the Bacillus subtilis spore coat. *J Bacteriol* **186**: 1110-1119.